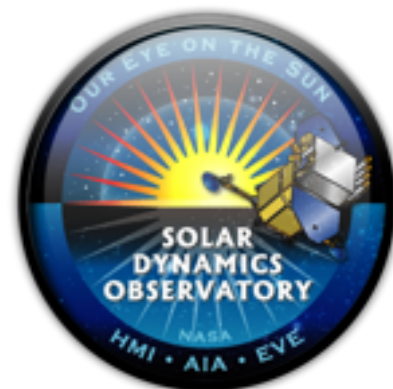
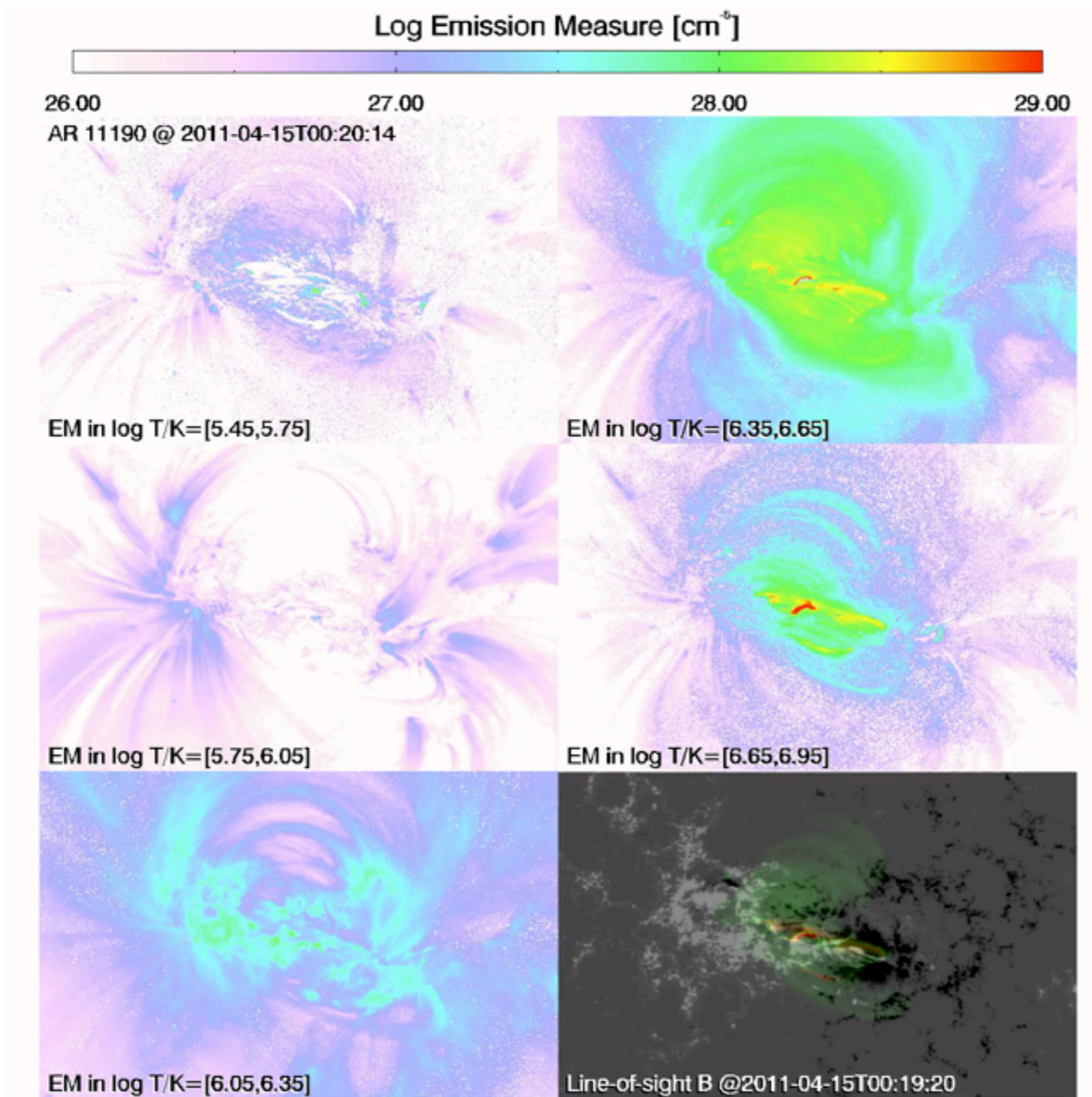


Using SDO/AIA to Probe the Thermal Structure of the Solar Corona

Mark Cheung, LMSAL
cheung@lmsal.com
<http://tinyurl.com/aiadem>



A taste of what we can do with AIA: Below is a differential emission measure inversion.



Useful links / documentation

SDO User Guide

<http://www.lmsal.com/sdouserguide.html>

(Does not yet include how to do DEMs)

AIA DEM package

<http://tinyurl.com/aiadem>

Documentation about AIA

<https://www.lmsal.com/sdodocs/>

- AIA Instrument Paper (Lemen et al. 2012)
- Initial Calibration of AIA (Boerner et al. 2012)

CHIANTI User Guide

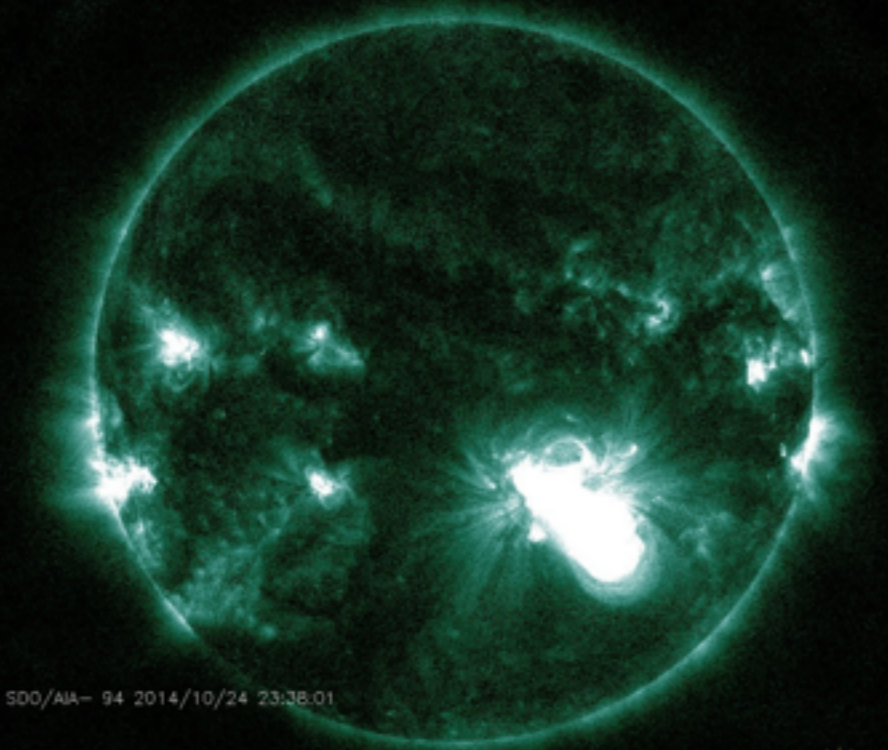
[\\$SSW/packages/chianti/doc/cug.pdf](#)


SDO User Guide

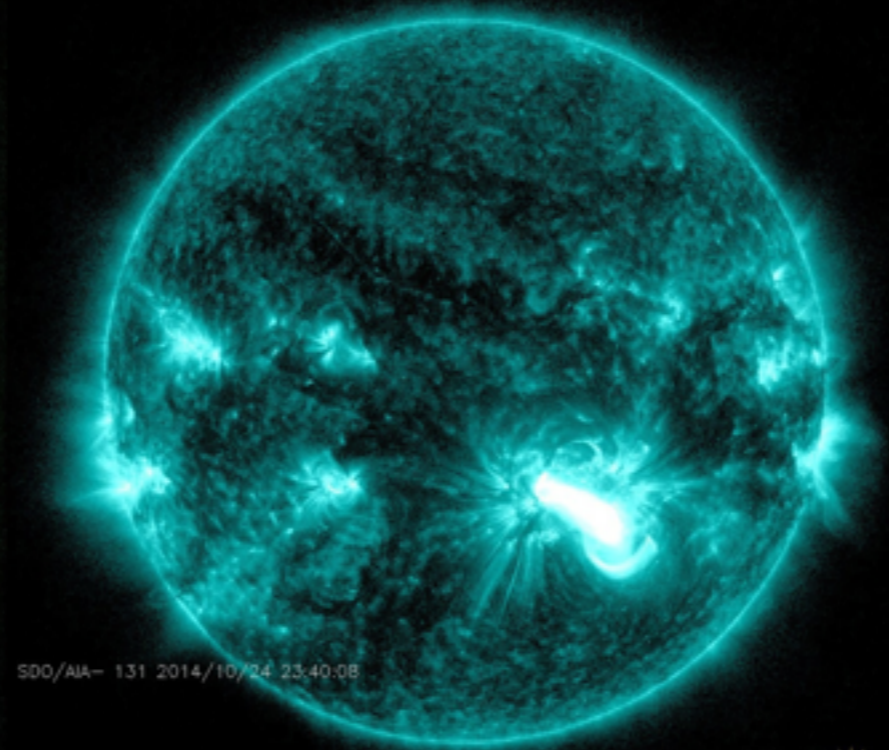
- 1 Introduction
 - 1.1 Synopsis of the SDO Mission
 - 1.2 About this Guide
 - 1.3 Data Products from AIA
 - 1.4 Data Products from EVE
 - 1.5 Data Products from HMI
 - 1.6 SDO Mission Data Policy
- 2 How to Browse SDO Data
 - 2.1 “The Sun Now”
 - 2.2 “Sun In Time”
 - 2.3 SolarMonitor
 - 2.4 The Helioviewer Project
- 3 How to Find SDO Data
 - 3.1 Heliophysics Events Knowledgebase
 - 3.2 iSolSearch
- 4 How to Get AIA and HMI Data
 - 4.1 How Data are Organized at the JSOC
 - 4.2 The lookdata Tool
 - 4.2.1 Getting Dataseries Names
 - 4.2.2 Selecting Records
 - 4.2.3 Exporting Data
 - 4.2.4 JSOC Image Timing Details
 - 4.3 The Cutout Service
 - 4.4 The Virtual Solar Observatory
 - 4.5 Synoptic Data
 - 4.6 Uncompressing the Data
 - 4.6.1 Compiling and Installing imcopy
- 5 How to Use SolarSoft with SDO Data
 - 5.1 Installing or Upgrading SolarSoft
 - 5.1.1 Doing a Clean Install
 - 5.1.2 Updating Packages for an Existing Installation
 - 5.1.3 Using a Proxy Server with SSW
 - 5.2 Querying the HER
 - 5.2.1 Basic Query Syntax
 - 5.2.2 Adding Filters to Queries
 - 5.3 Retrieving Data from the JSOC
 - 5.3.1 Getting Dataseries Names
 - 5.3.2 Selecting Records
 - 5.3.3 Exporting Data
 - 5.3.4 Exporting Specific Segments
 - 5.4 Requesting a Cutout Using SSW
 - 5.5 Using the SSW Interface to the VSO
 - 5.5.1 Querying the VSO
 - 5.5.2 Downloading Data from the VSO
 - 5.6 Uncompressing the Image Data
 - 5.6.1 Using read_sdo.pro
 - 5.6.2 Using read_sdo.pro with a Shared Library
- 6 How to Process AIA Data
 - 6.1 Using aia_prep.pro to Align and Derotate AIA Data
 - 6.1.1 Aligning Full-Disk Images
 - 6.1.2 Aligning Cropped Images and Cutouts
 - 6.2 Co-Aligning HMI Data with AIA Data
 - 6.3 Despiking and/or Respiking AIA Data
 - 6.4 Point Spread Function Deconvolution
 - 6.5 Getting AIA Filter Response Data
 - 6.6 Miscellaneous AIA Tasks
 - 6.6.1 Using AIA Standard Scaling and Colors
 - 6.6.2 Creating AIA Tri-Color Images
 - 6.6.3 Plotting an AIA Light Curve
 - 6.6.4 Interfacing with plot_map.pro
(Dom Zarro’s Mapping Software)
 - 6.6.5 Checking the QUALITY Keyword
- 7 Frequently Asked Questions
- 8 Lists of Useful Links
- 9 Version History of this Guide
- 10 Contributors to this Guide

<http://www.lmsal.com/sdouserguide.html>

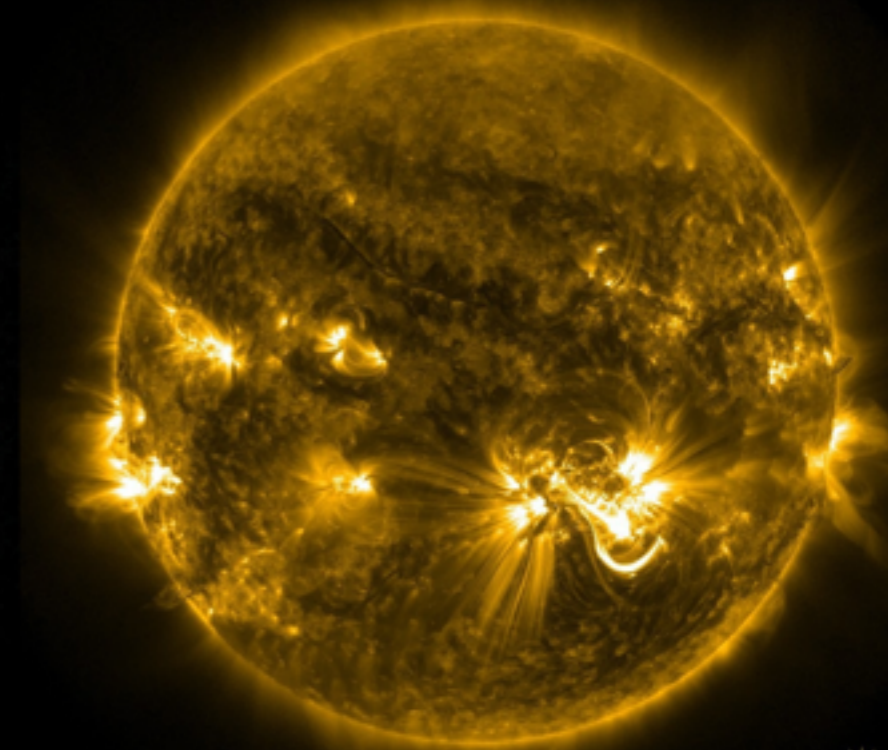
What do we see in AIA/EUV images?




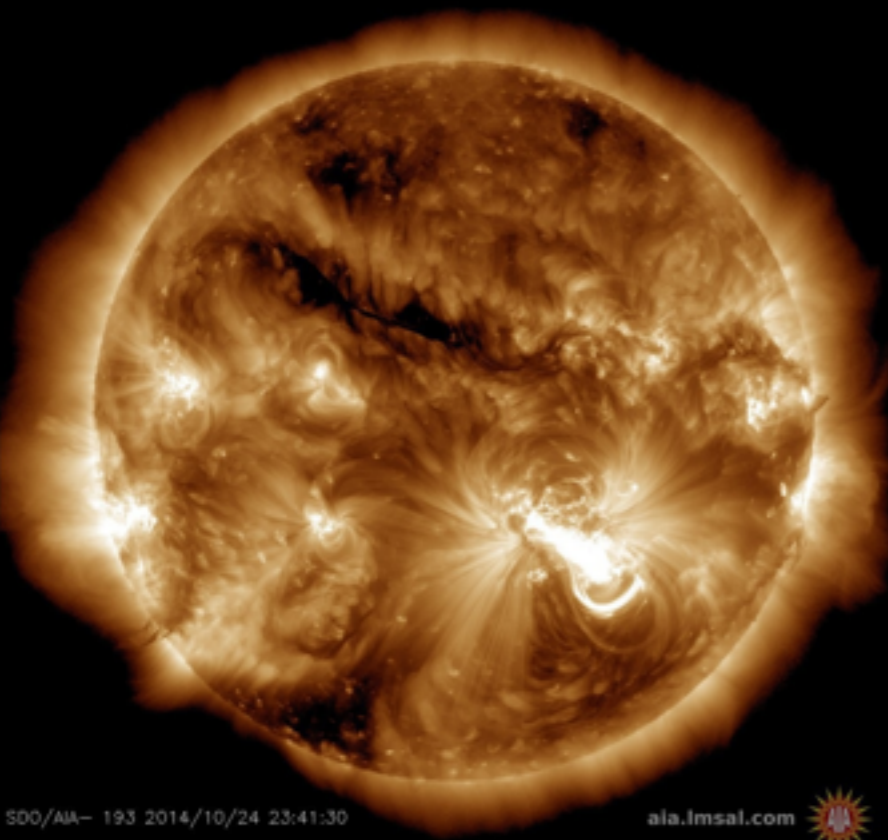
aia.lmsal.com 



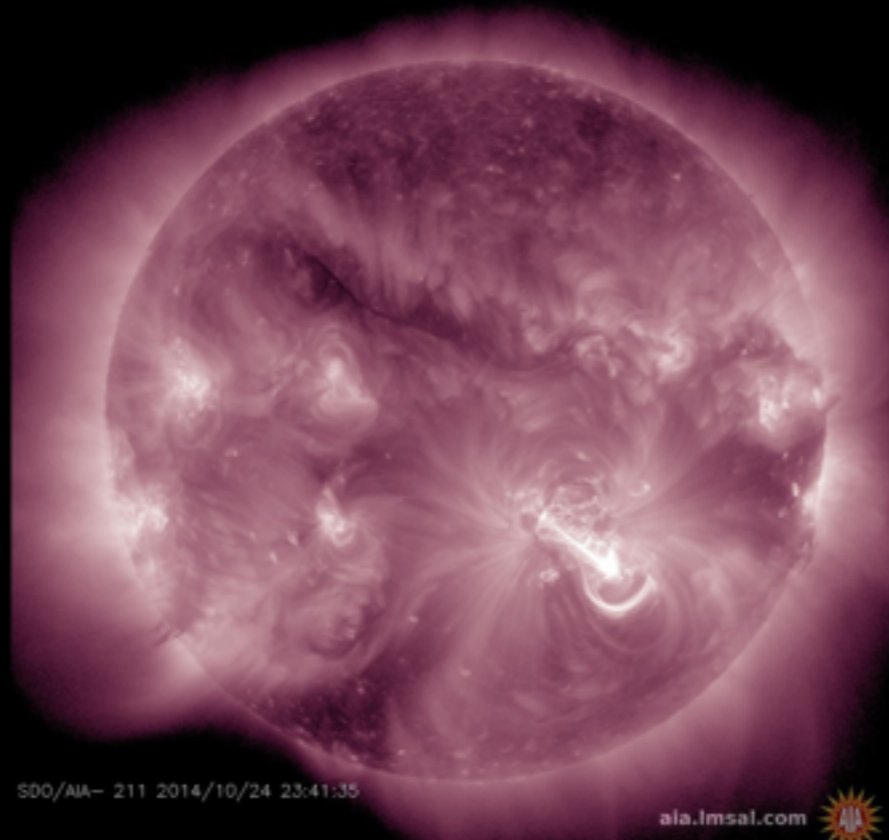
aia.lmsal.com 




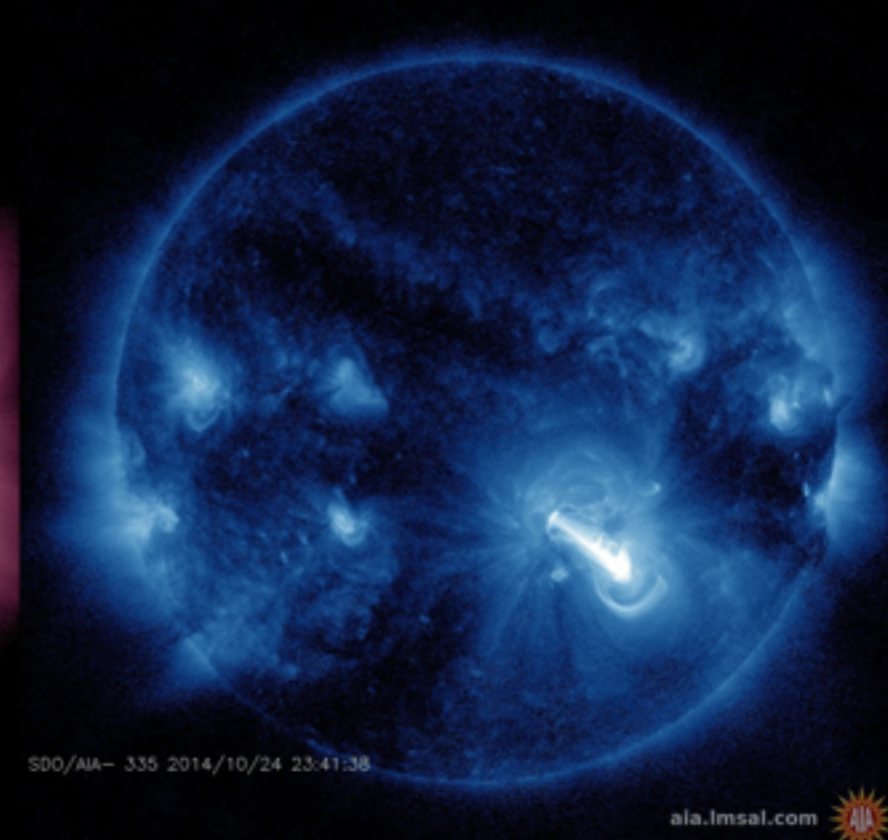
aia.lmsal.com 



aia.lmsal.com 



aia.lmsal.com 



aia.lmsal.com 

What do EUV images from SDO/AIA show?

Name: aia_get_response

Purpose: return SDO/AIA instrument response data structures

Input Parameters:

Output:

function returns AIA wavelength response, spectral model, or temperature response

Descriptions of the structures returned by this routine are available via:

<http://sohowww.nascom.nasa.gov/solarsoft/sdo/aia/response/README.txt>

Calling Examples:

IDL> effarea=aia_get_response(/area, /dn) ; return per wavelength effective area

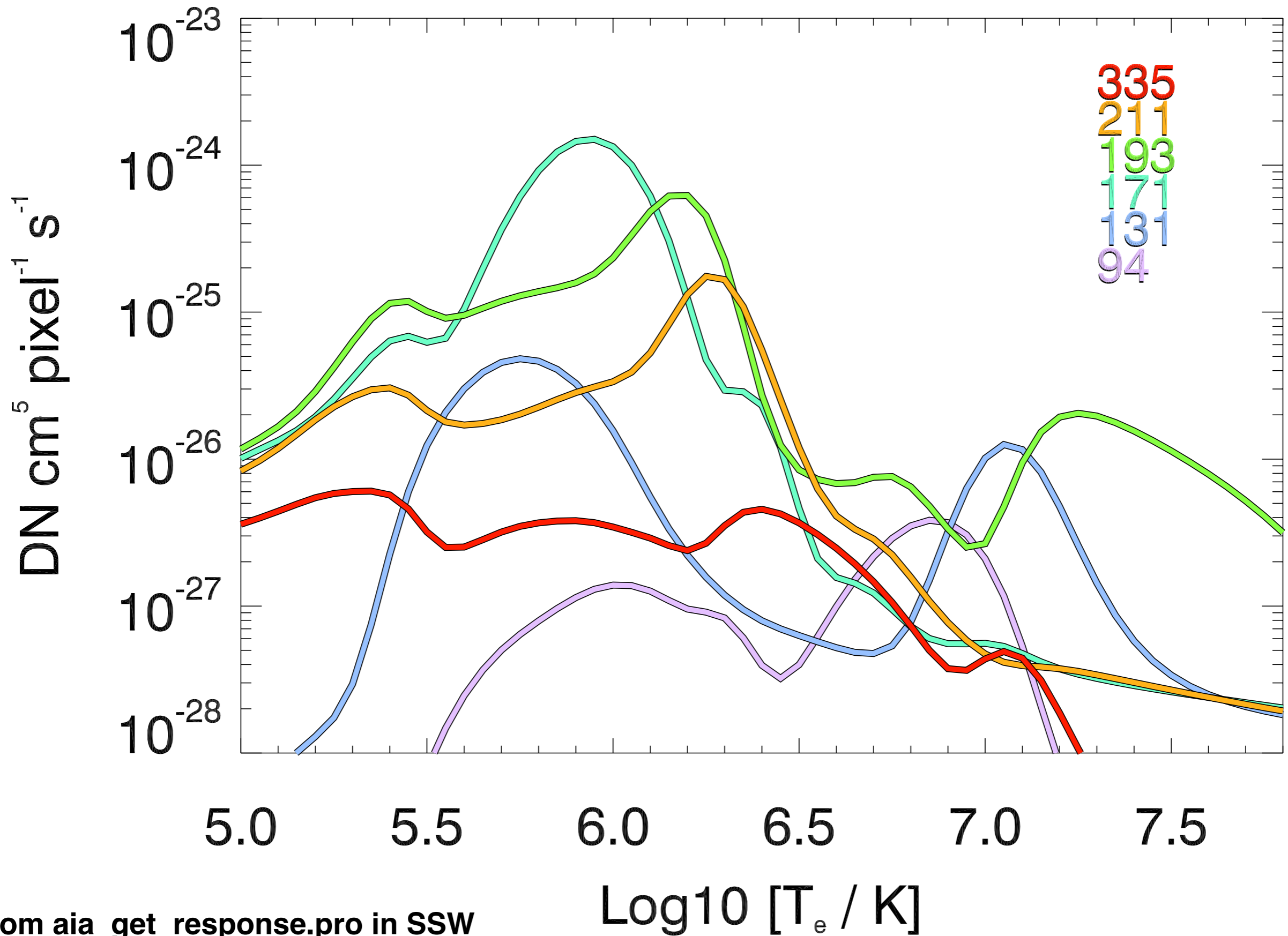
IDL> effarea=aia_get_response(/area,/full,/dn) ; same with component details (filter/ccd...)

IDL> emiss=aia_get_response(/emiss, /full) ; return default CHIANTI model with line list

**IDL> tresp=aia_get_response(/temp,/dn,/evenorm) ; return temperature response including
; constant scale factors to give good
; overall agreement with SDO/EVE**

See section 6.5 of SDO User Guide for extensive explanation.

AIA Temperature Response Functions



From aia_get_response.pro in SSW

Table 1. Predicted AIA count rates.

From O'Dwyer et al. 2010

	Ion	λ Å	T_p^a K	Fraction of total emission														
				CH	QS	AR	FL											
94 Å	Mg VIII	94.07	5.9	0.03	-	-	-											
	Fe XX	93.78	7.0	-	-	-	0.10											
	Fe XVIII	93.93	6.85	-	-	0.74	0.85											
	Fe X	94.01	6.05	0.63	0.72	0.05	-											
	Fe VIII	93.47	5.6	0.04	-	-	-											
	Fe VIII	93.62	5.6	0.05	-	-	-											
	Cont.				0.11	0.12	0.17	-										
131 Å	O VI	129.87	5.45	0.04	0.05	-	-											
	Fe XXIII	132.91	7.15	-	-	-	0.07											
	Fe XXI	128.75	7.05	-	-	-	0.83											
	Fe VIII	130.94	5.6	0.30	0.25	0.09	-											
	Fe VIII	131.24	5.6	0.39	0.33	0.13	-											
	Cont.				0.11	0.20	0.54	0.04										
171 Å	Ni XIV	171.37	6.35	-	-	0.04	-											
	Fe X	174.53	6.05	-	0.03	-	-											
	Fe IX	171.07	5.85	0.95	0.92	0.80	0.54											
	Cont.			-	-	-	0.23											
193 Å	O V	192.90	5.35	0.03	-	-	-											
	Ca XVII	192.85	6.75	-	-	-	0.08											
	Ca XIV	193.87	6.55	-	-	0.04	-											
	Fe XXIV	192.03	7.25	-	-	-	0.81											
	Fe XII	195.12	6.2	0.08	0.18	0.17	-											
	Fe XII	193.51	6.2	0.09	0.19	0.17	-											
	Fe XII	192.39	6.2	0.04	0.09	0.08	-											
	Fe XI	188.23	6.15	0.09	0.10	0.04	-											
	Fe XI	192.83	6.15	0.05	0.06	-	-											
	Fe XI	188.30	6.15	0.04	0.04	-	-											
	Fe X	190.04	6.05	0.06	0.04	-	-											
	Fe IX	189.94	5.85	0.06	-	-	-											
	Fe IX	188.50	5.85	0.07	-	-	-											
	Cont.				-	-	0.05	0.04										
	211 Å	Cr IX	210.61	5.95	0.07	-	-	-										
Ca XVI		208.60	6.7	-	-	-	0.09											
Fe XVII		204.67	6.6	-	-	-	0.07											
Fe XIV		211.32	6.3	-	-	0.13	0.39	0.12										
Fe XIII		202.04	6.25	-	-	0.05	-											
Fe XIII		203.83	6.25	-	-	-	0.07	-										
Fe XIII		209.62	6.25	-	-	0.05	0.05	-										
Fe XI		209.78	6.15	0.11	0.12	-	-											
Fe X	207.45	6.05	0.05	0.03	-	-												
Ni XI	207.92	6.1	0.03	-	-	-												
Cont.								0.08	0.04	0.07	0.41							
304 Å	He II	303.786	4.7	0.33	0.32	0.27	0.29											
	He II	303.781	4.7	0.66	0.65	0.54	0.58											
	Ca XVIII	302.19	6.85	-	-	-	0.05											
	Si XI	303.33	6.2	-	-	0.11	-											
	Cont.																	
335 Å	Al X	332.79	6.1	0.05	0.11	-	-											
	Mg VIII	335.23	5.9	0.11	0.06	-	-											
	Mg VIII	338.98	5.9	0.11	0.06	-	-											
	Si IX	341.95	6.05	0.03	0.03	-	-											
	Si VIII	319.84	5.95	0.04	-	-	-											
	Fe XVI	335.41	6.45	-	-	0.86	0.81											
	Fe XIV	334.18	6.3	-	0.04	0.04	-											
	Fe X	184.54	6.05	0.13	0.15	-	-											
	Cont.				0.08	0.05	-	0.06										

Statement of the Problem

The Atmospheric Imaging Assembly (AIA, [Lemen et al. 2012](#); [Boerner et al. 2012](#)) instrument onboard NASA's Solar Dynamics Observatory (SDO, [Pesnell et al. 2012](#)) is a suite of four normal-incidence reflecting telescopes that image the Sun in seven EUV channels, two UV channels and one visible wavelength channel.

The aim of this and many other studies is to extract thermal information about the Sun's optically thin corona using the EUV observations. The calibrated (i.e. dark-subtracted, flat-fielded and exposure time normalized) count rate y_i in the i -th EUV channel is related to the thermal distribution of coronal plasma by:

$$y_i = \int_0^{\infty} K_i(T) \text{DEM}(T) dT,$$

where $K_i(T)$ is the temperature response function (see next slide):

Statement of the Problem

and
$$\text{DEM}(T)dT = \int_0^\infty n_e^2(T)dz,$$

where $\text{DEM}(T)$ is the differential emission measure (in units of $\text{cm}^{-5} \text{K}^{-1}$) of plasma along the line-of-sight. $n_e(T)$ is the electron number density of plasma at temperature T . **The challenge is to solve for $\text{DEM}(T)$ given a set of EUV measurements y .**

Let the temperature range be divided into n neighboring bins, so that:

$$y_i = \sum_{j=1}^n \int_{T_j}^{T_j + \Delta T_j} K_i(T) \text{DEM}(T) dT,$$

where the j -th temperature bin has range $T \in [T_j, T_j + \Delta T_j)$. Assuming that $K_i(T)$ is piecewise constant in each temperature bin, we have:

$$y_i = \sum_{j=1}^n K_{ij} \text{EM}_j, \text{ where } \text{EM}_j = \int_{T_j}^{T_j + \Delta T_j} \text{DEM}(T) dT.$$

Statement of the Problem: $\mathbf{y} = \mathbf{K}\mathbf{x}$

$$y_i = \sum_{j=1}^n K_{ij} \text{EM}_j, \text{ where } \text{EM}_j = \int_{T_j}^{T_j + \Delta T_j} \text{DEM}(T) dT.$$

The above is a matrix equation of the form $\mathbf{y} = \mathbf{K}\mathbf{x}$, where

- \mathbf{K} is an $m \times n$ response matrix*, with each row corresponding to the temperature response function of one AIA channel
- \mathbf{y} is an m -tuple corresponding of AIA count (rates), and
- \mathbf{x} is an n -tuple with components EM_j .

The He II line in the 304 Å channel is not well-modeled by CHIANTI (Warren, 2005, ApJ 157, 147) so it is usually not used for DEM analysis. So $m = 6$ for AIA. Usually we want more than 6 temperature bins. **For $m < n$, the matrix equation $\mathbf{y} = \mathbf{K}\mathbf{x}$ represents an underdetermined system.**

*Matrix elements depends on basis functions used for computing the integral

Usual Approach: χ -squared Minimization

Function to minimize: $\|y - Kx\|^2$ or $\|(y - Kx)/\sigma\|^2$

Basically, minimize difference between observed and predicted counts. The benefits of a least-squares approach is that it leads to Euler-Lagrange equations that can be used to seek (global or local) minima.

For an overdetermined system, we know no single model will fit all the data. So χ -squared minimization is ideal. However, **for underdetermined systems such an approach can be subject to the perils of overfitting.**

Usual way to get around this:

Parameterization: e.g. Guennou et al (2012a,b), xrt_dem_iterative2.pro (M. Weber in SSW, see also Cheng et al 2012)

Regularization: e.g. Hannah & Kontar (2012), Plowman et al. (2013)

See Aschwanden et al. (2015, Sol Phys, 290, 2, 2733) for comparison between previously existing methods.

Cheung et al. 2015: The Sparse Solution

We address the inverse problem using an approach different than chi-squared minimization. The set of solutions satisfying the underdetermined matrix equation $\mathbf{y} = \mathbf{K}\mathbf{x}$ lies in an affine subspace of \mathbf{R}^n . We pick the solution $\mathbf{x}^\#$ within this subspace such that:

$$\text{minimize } \sum_j^n x_j \text{ subject to } \mathcal{K}\vec{x} = \vec{y}, \vec{x} \geq 0.$$

The linear program above finds a solution that minimizes the L1-norm of the solution vector (c.f. [Candes 2006](#)). This is not chi-squared minimization.

If \mathbf{K} is the response function sampled by Dirac Delta functions at specific temperatures, this is equivalent to minimizing the total EM. If other basis functions are used, there is no simple corresponding physical interpretation.

The Sparse Solution

We are unaware of physical principles pertaining to coronal plasma that motivate the optimization problem posed above. However, this choice has some important benefits:

- 1) It does not overfit (consistent with the principle of parsimony, i.e. Ockham's Razor).
- 2) It ensures positivity of the solution (if solutions exist).
- 3) It is an L1-norm minimization problem, so we can use standard techniques from compressed sensing (c.f. Candes & Tao 2006).
BTW the L1-norm of a vector $x = \sum |x_i|$
- 4) Speed: $O(10^4)$ solutions / sec with single IDL thread.

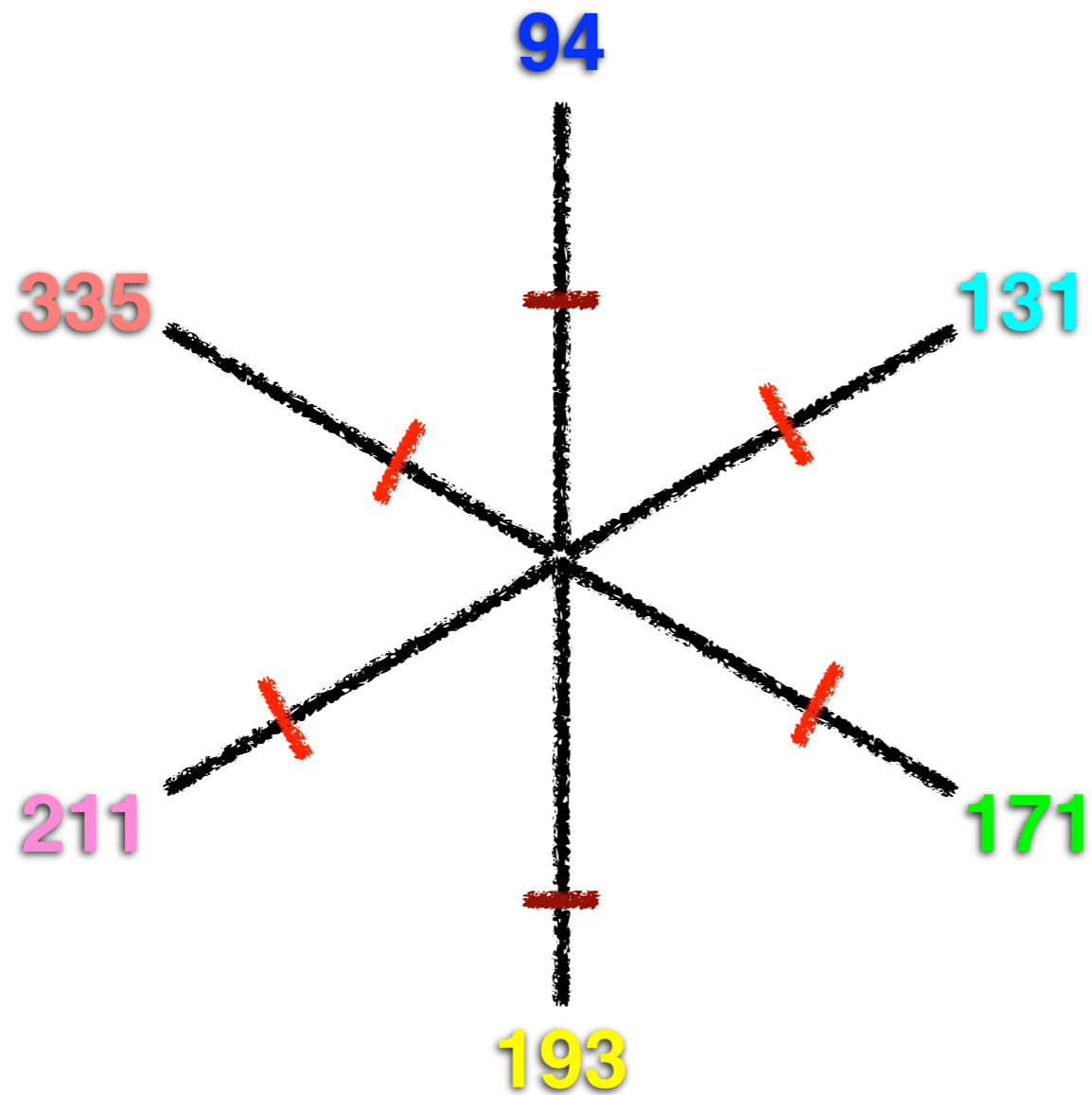
Handling noise

In practice, measurement uncertainties imply that the equality $\mathbf{y} = \mathbf{K}\mathbf{x}$ may not be satisfied. So our method solves the followed modified linear program:

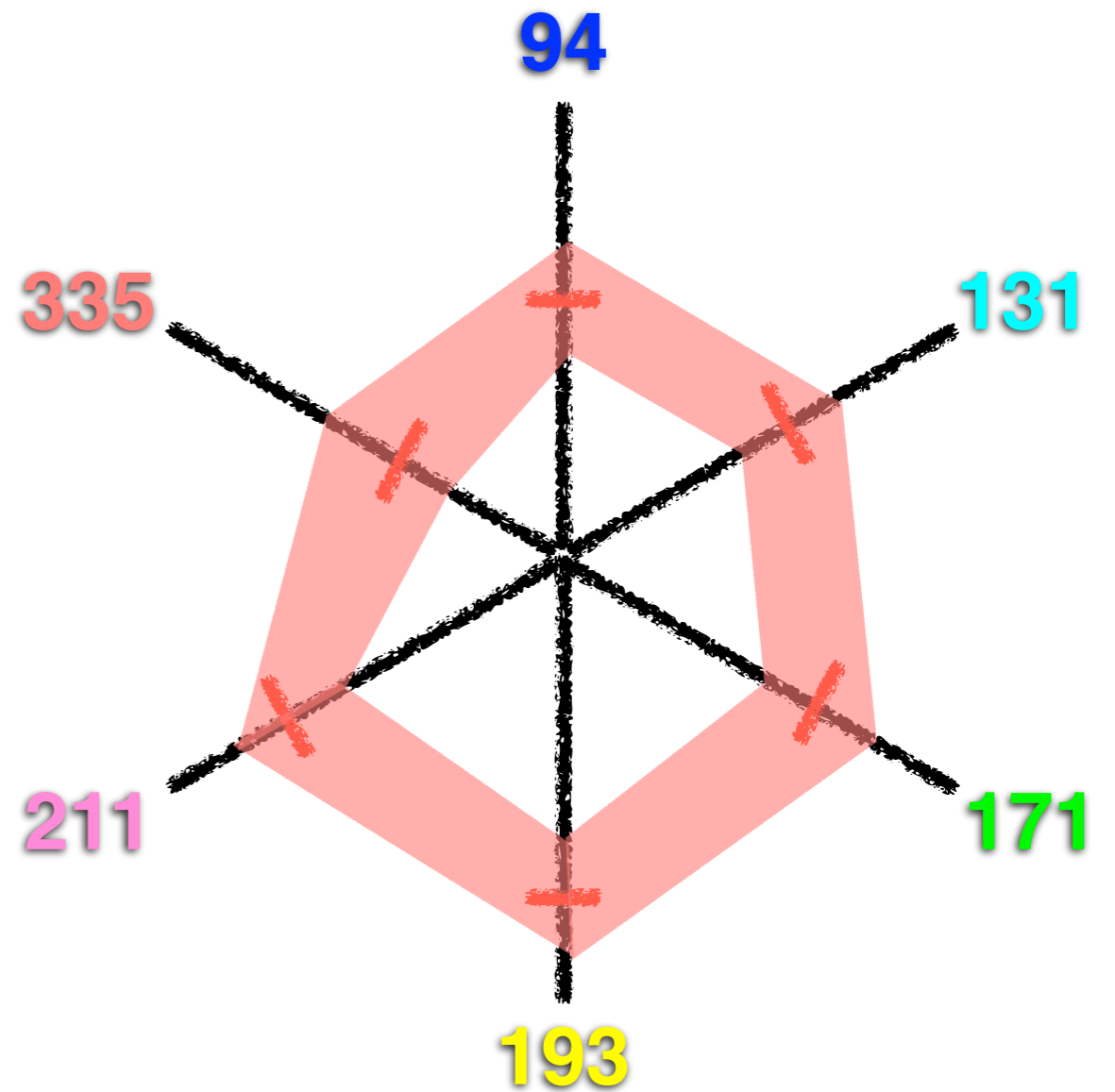
$$\begin{aligned} \text{minimize } & \sum_{j=1}^n x_j \text{ subject to } \mathcal{K}\vec{x} \leq \vec{y} + \vec{\eta}, \\ & \vec{x} \geq 0, \mathcal{K}\vec{x} \geq \max(\vec{y} - \vec{\eta}, 0). \end{aligned}$$

The vector $\boldsymbol{\eta}$ is a measure of the uncertainty in the count rate and provides tolerance for the predicted counts ($\mathbf{K}\mathbf{x}$) to deviate from the observed values (\mathbf{y}). To enforce positive counts the lower bound is set to $\max(\mathbf{y} - \boldsymbol{\eta}, 0)$.

χ -squared minimization



Sparse inversion



vs.

 Crossmarks are observed counts

Subspace of allowed solutions in our method

Basis Functions for DEM

Let $i = 1, 2, \dots, m$ denote the index over a set of wavelength band channels and/or line spectra. Let the DEM function be written in terms of a set of positive semidefinite basis functions $\{b_j(\log T) \geq 0 \mid k = 1, 2, \dots, l\}$, viz.

$$\text{DEM}(\log T) = \sum_{k=1}^l b_k(\log T) x_k, \quad (\text{A1})$$

with quadrature coefficients $x_k \geq 0$. Approximating the integrals in equation (1) as sums in $\log T$ space, we have

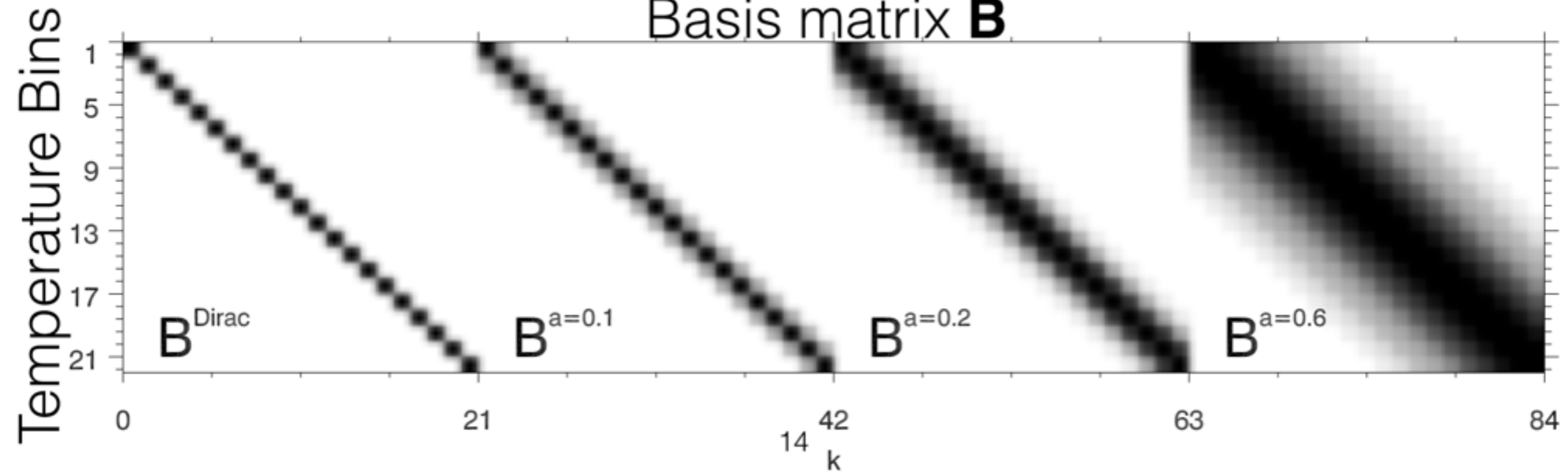
$$y_i = \sum_{j=1}^n \sum_{k=1}^l K_{ij} B_{jk} x_k \Delta \log T, \quad (\text{A2})$$

where $j = 1, 2, \dots, n$ is the index over temperature bins, $K_{ij} = K_i(\log T_j)$ and $B_{jk} = b_k(\log T_j)$. The response matrix $\mathbf{K} = (K_{ij})$ has dimensions $m \times n$. The basis matrix $\mathbf{B} = (B_{jk})$ has dimensions $n \times l$, with the k -th column vector corresponding to the k -th basis function $b_k(\log T_j)$. Defining the *dictionary matrix* $\mathbf{D} = \mathbf{KB}$ the set of integral equations (1) can be written in matrix form:

In practice we solve this $\rightarrow \mathbf{\bar{y}} = \mathbf{D}\vec{x},$ (A3)

where the sought-after solution vector \vec{x} is an l -tuple with components $x_k \Delta \log T$ ($k = 1, 2, \dots, l$). When the number of basis functions exceeds the number of image channels (i.e. $l > m$), the linear system Eq. (A3) is underdetermined.

Basis matrix \mathbf{B}



Geometrical Interpretation of Problem

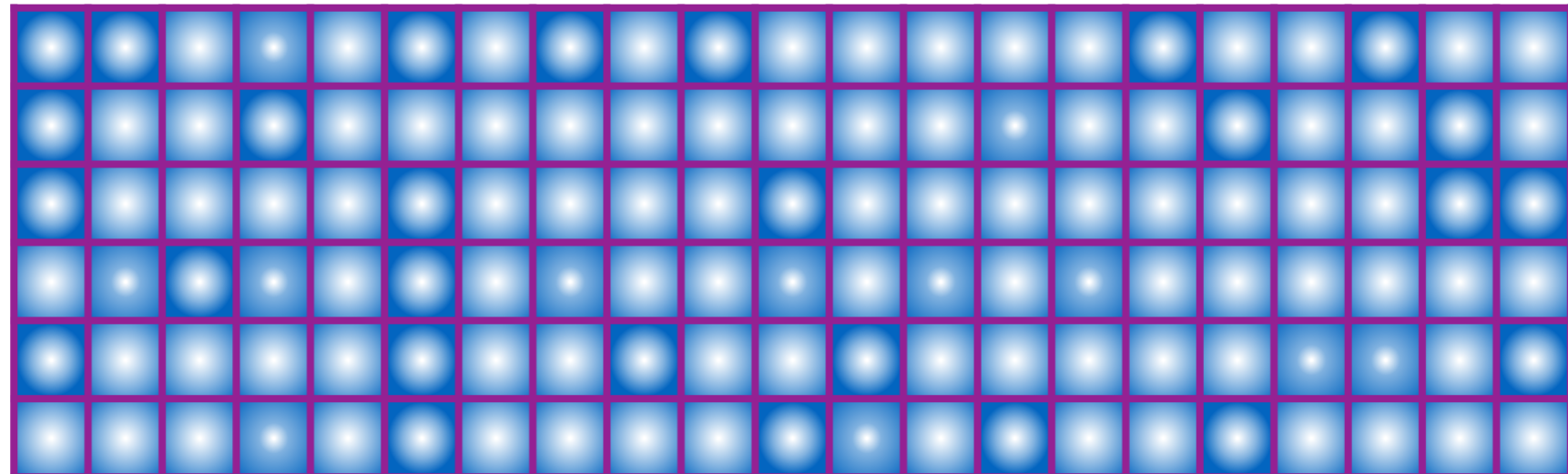
y

$$D = KB$$

x

94 DN/s
131 DN/s
171 DN/s
193 DN/s
211 DN/s
335 DN/s

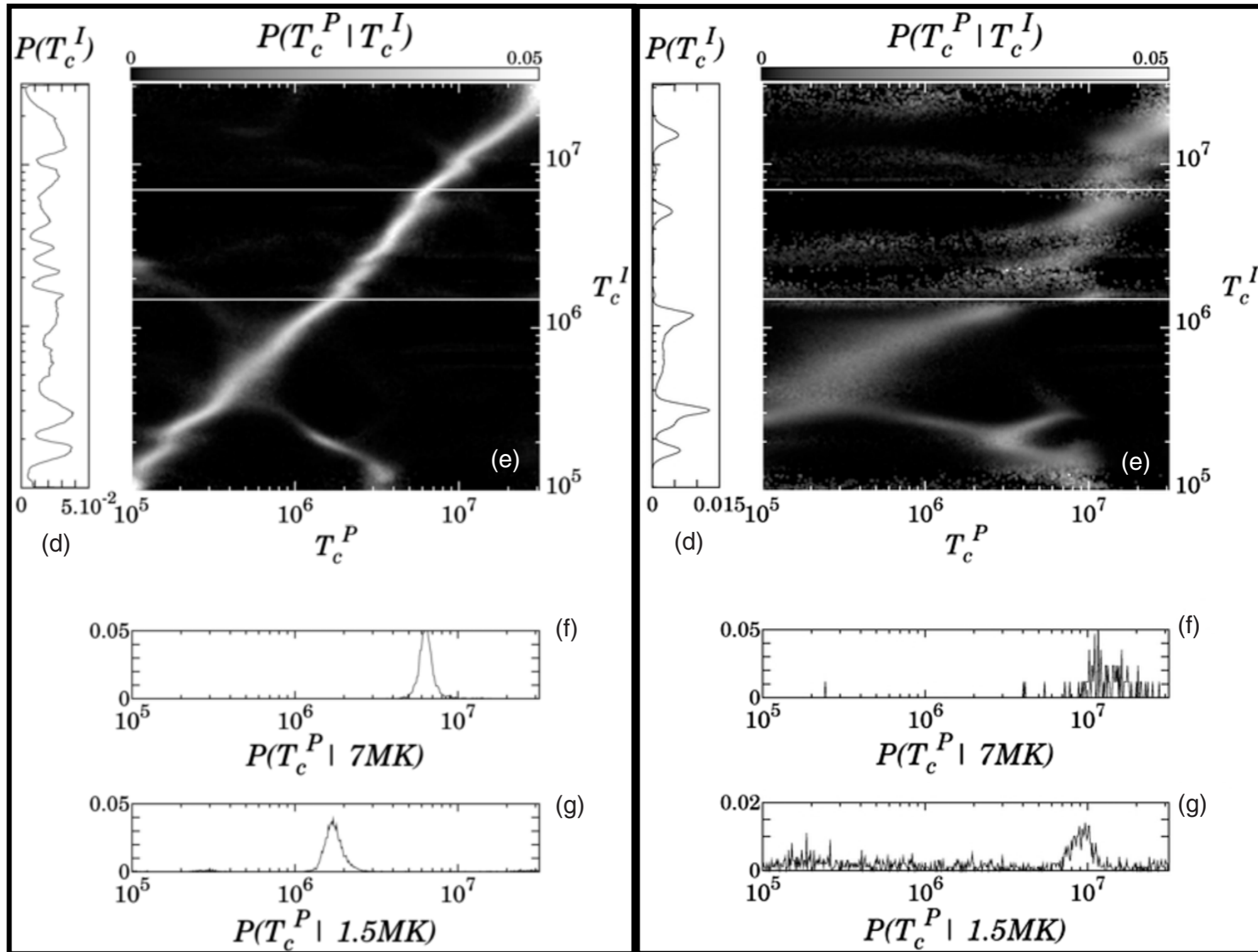
=



We seek to build a column vector **y** by linear combinations of columns of the matrix **D=KB**. x_j are the coefficients of the linear combination. More columns of **KB** from which to choose than components of **y** \Rightarrow **underdetermined problem**.

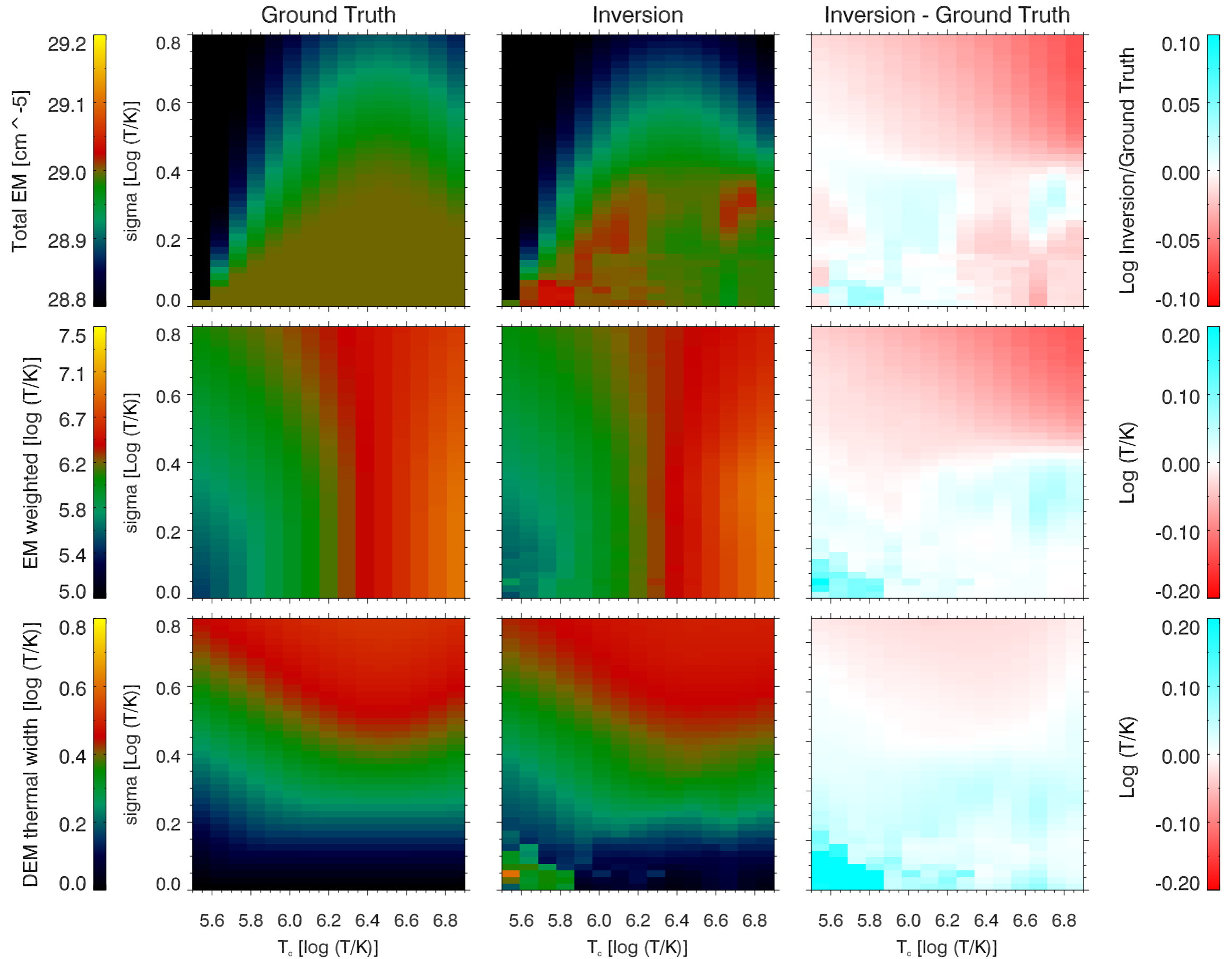
Do “**basis pursuit**” by minimizing **L1 norm** of **x**.

Validation Exercise 1: Gaussian DEMs



Guennou et al (2012) reported that when the input gaussian is moderately wide (0.3 log T_e , right panel), AIA 6-channel inversions yield spurious temperatures.

Test DEMs: $\xi(T, T_c, \sigma) = \frac{EM_0}{\sigma\sqrt{2\pi}} \exp\left[-\frac{(\log T - \log T_c)^2}{2\sigma^2}\right]$ $EM_0 = 10^{29} \text{ cm}^{-5}$



Validation Exercise 2: Quasi-steady loops in a NLFFF model of AR 11158

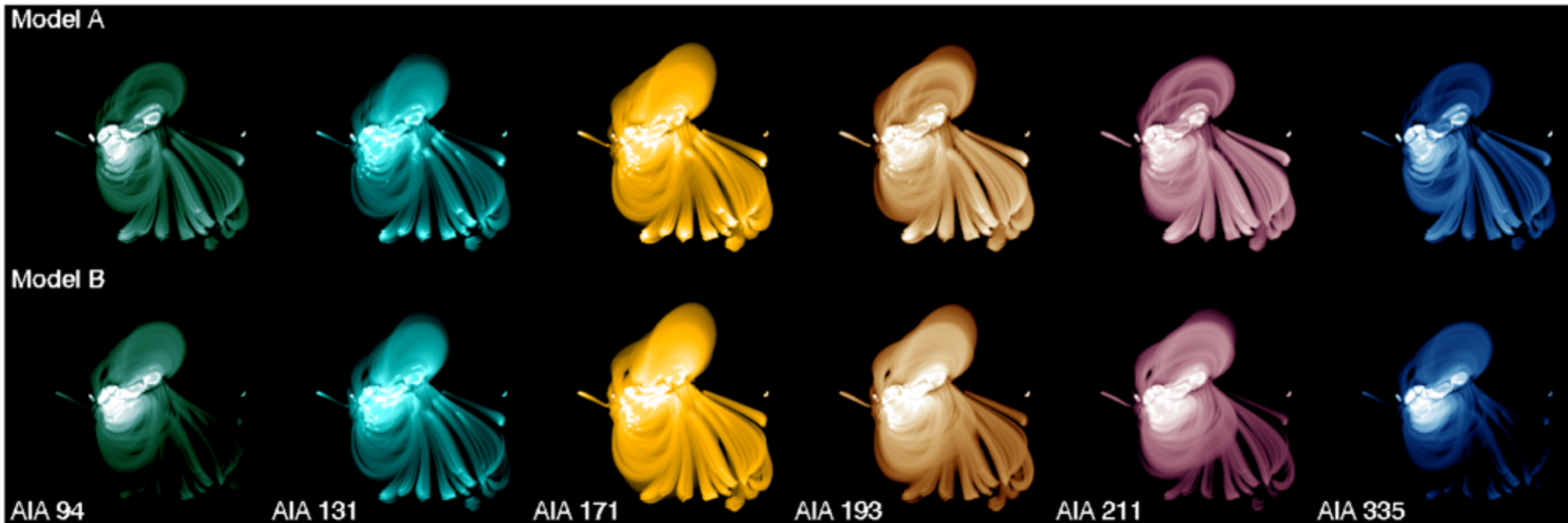
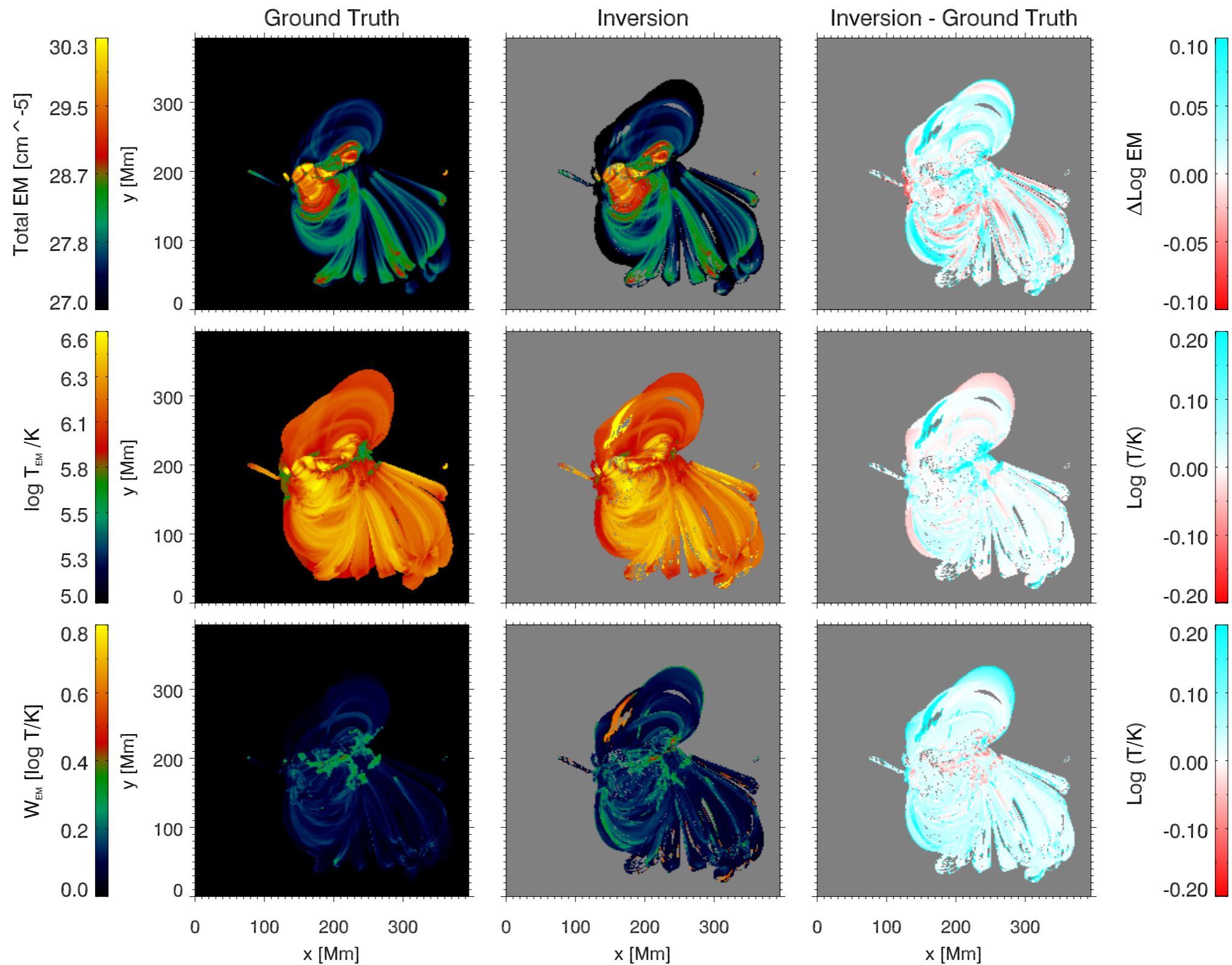


FIG. 5.— Synthetic AIA images (log-scaled) for the two thermal models (top and bottom rows) of NOAA AR 11158.

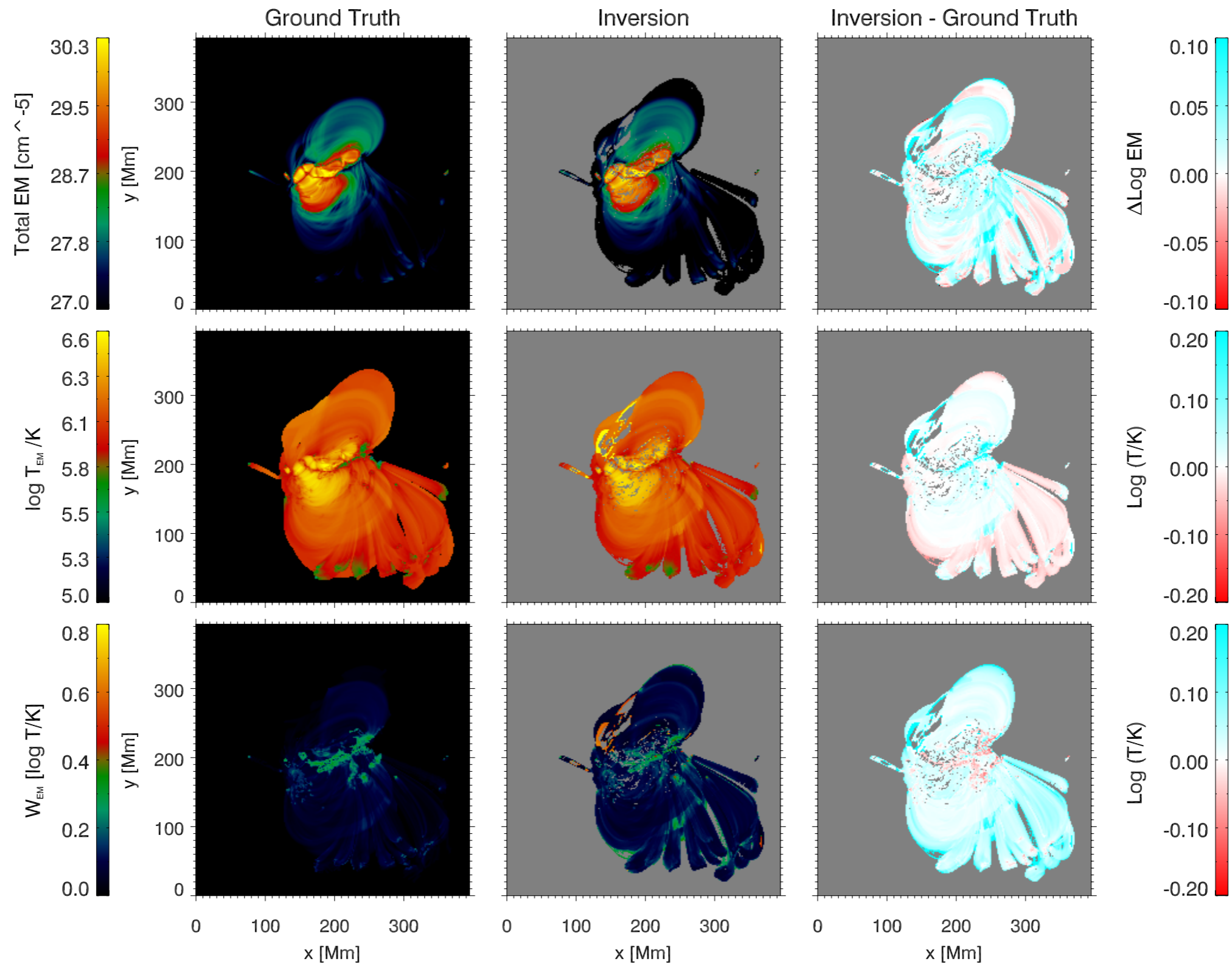
Magnetic Model: Quasi-Grad-Rubin Non-linear force-free Field reconstruction of AR 11158.

Thermal Model: Quasi-steady loops with different heating functions.

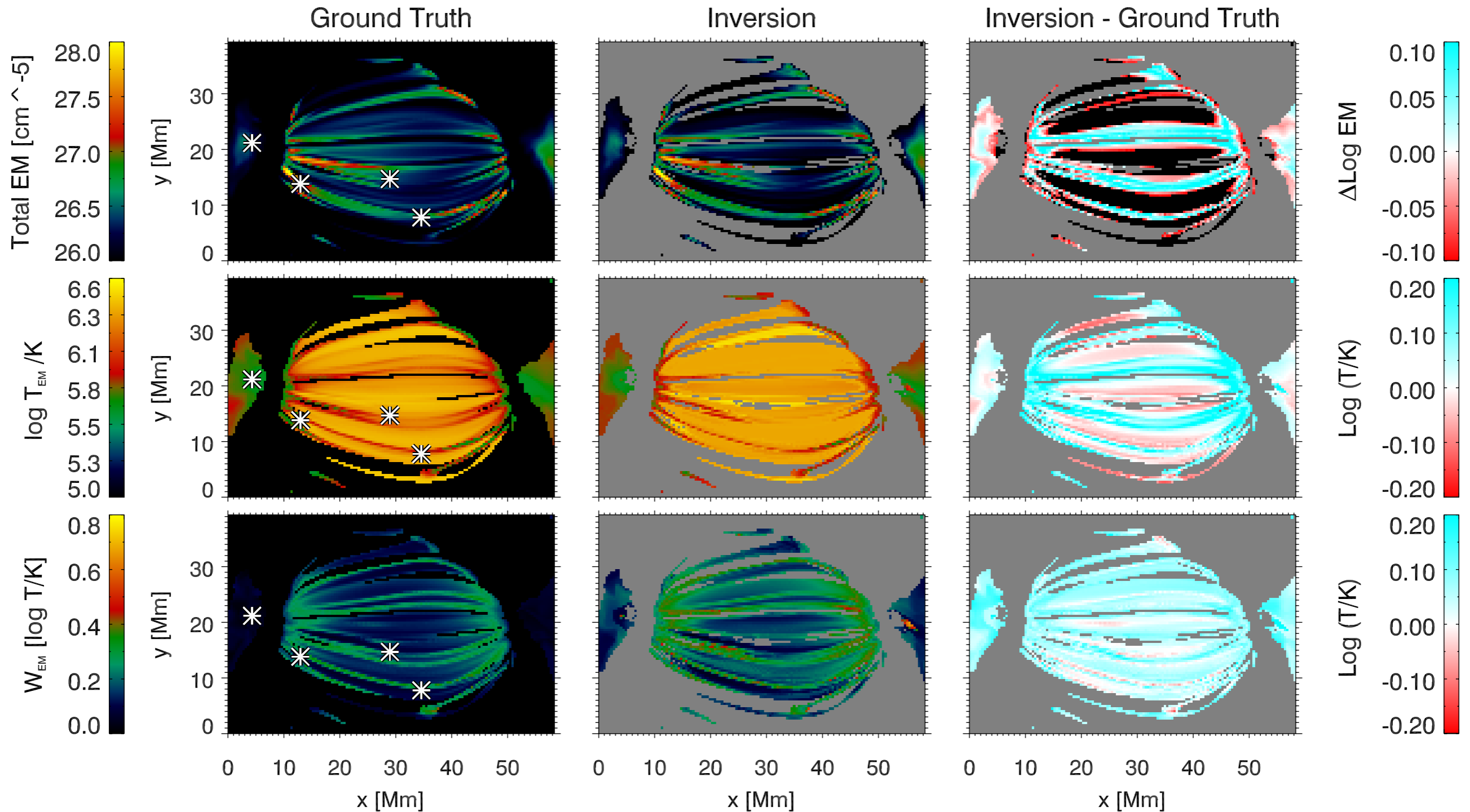
AR 11158 Model A



AR 11158 Model B

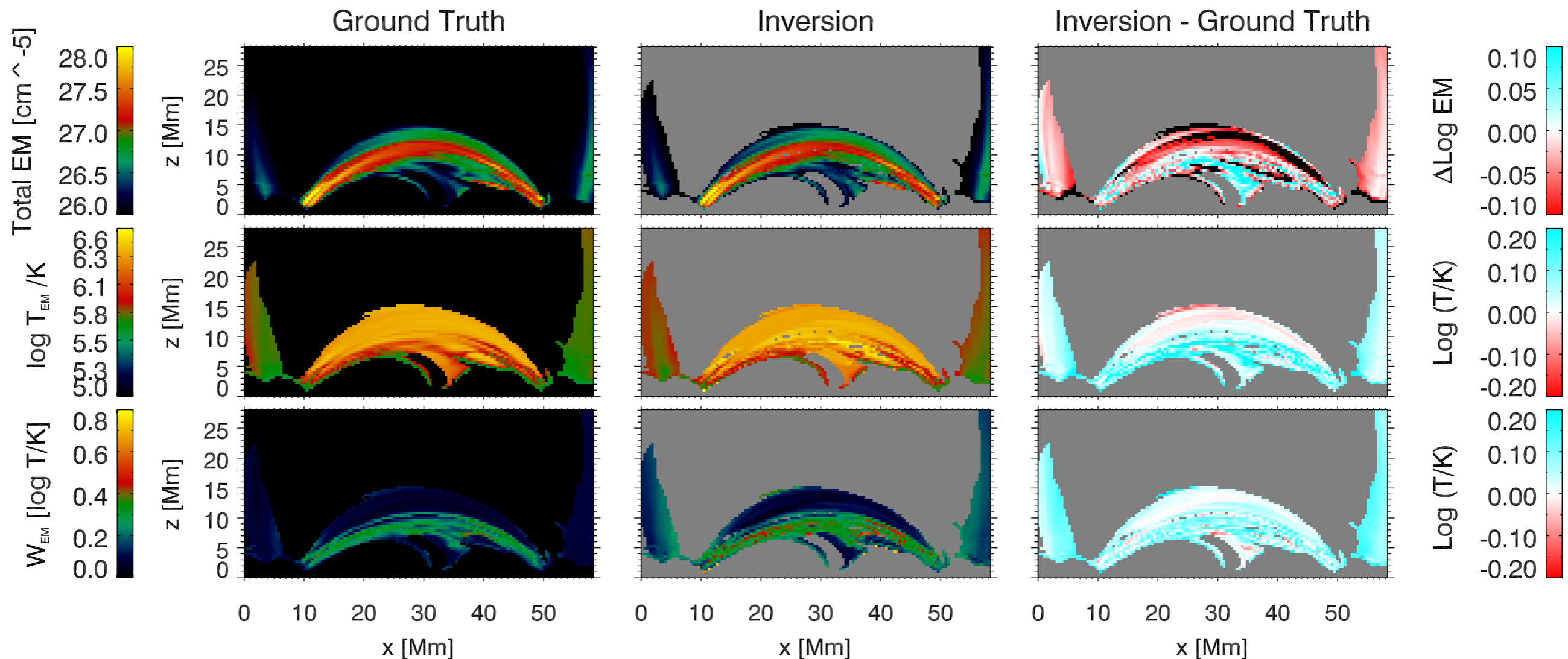


Validation Exercise 3: MHD Model



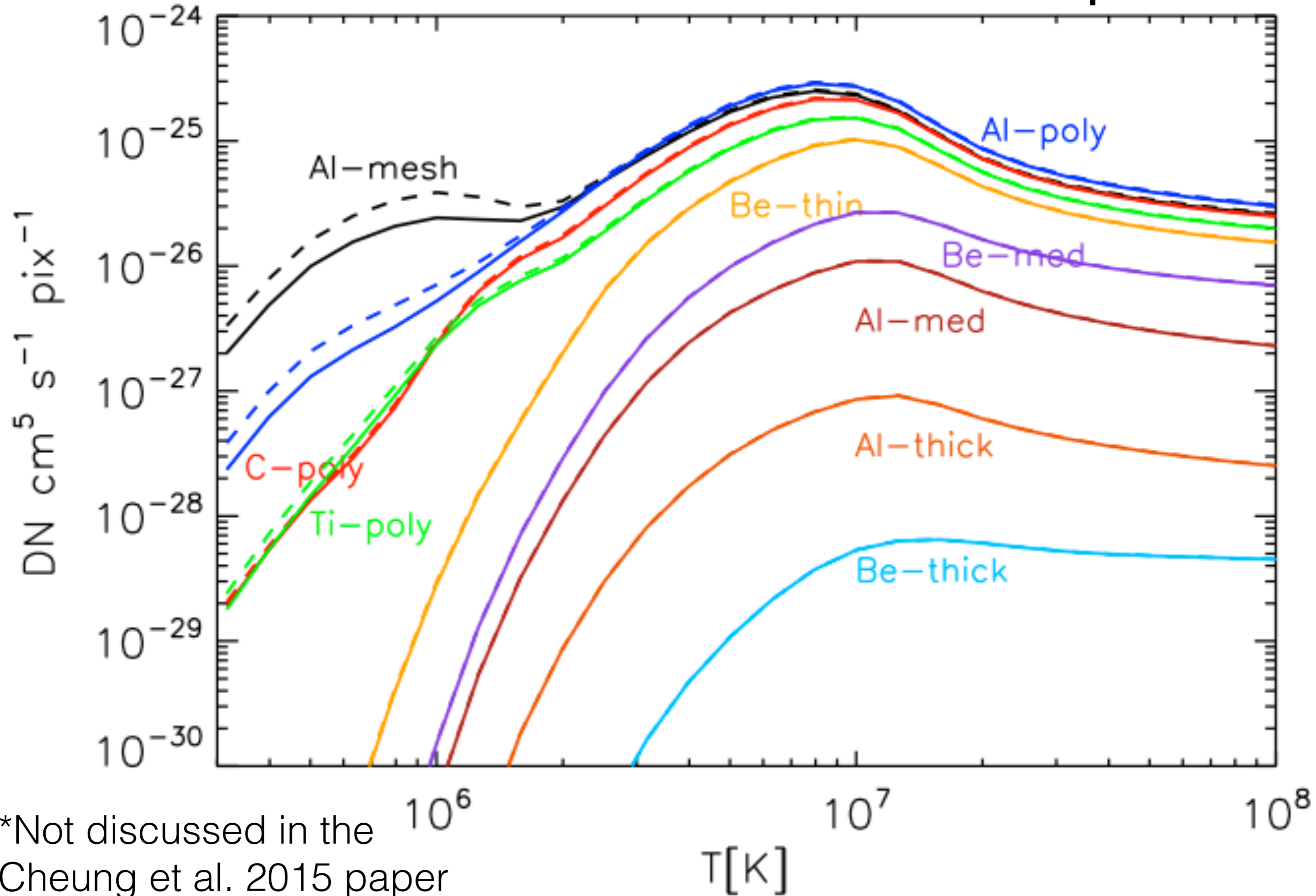
MHD model of AR formation (with thermal conduction) by
Chen et al. (2014A&A...564A..12C, 2015NatPh..11..492C)

Validation Exercise 3: MHD Model



MHD model of AR formation (with thermal conduction) by
Chen et al. (2014A&A...564A..12C, 2015NatPh..11..492C)

Validation Exercise: AIA-XRT Cross-Comparison

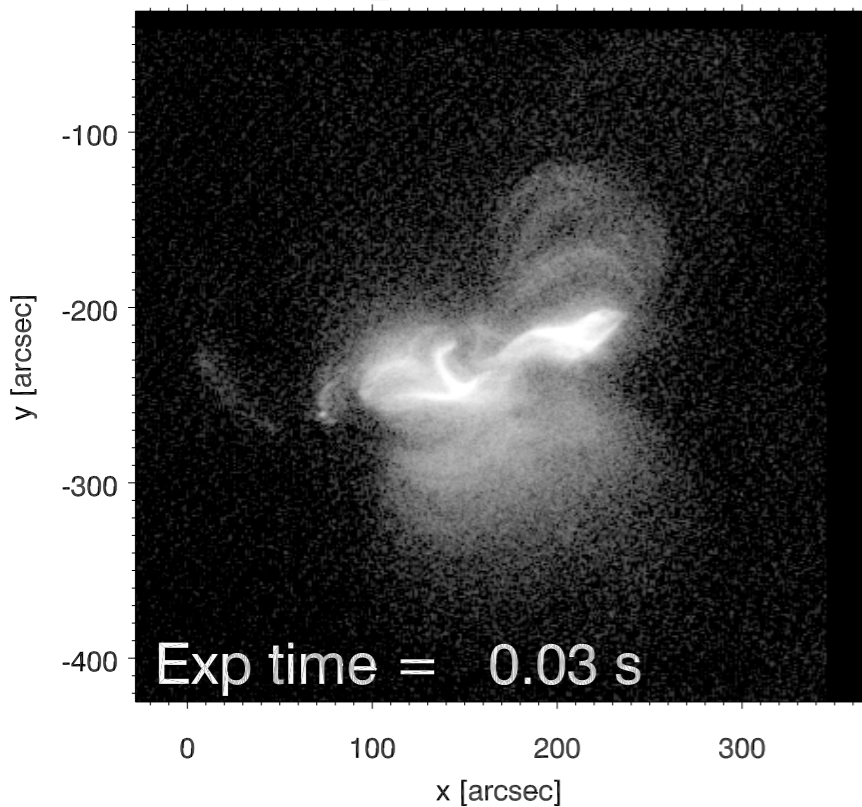


*Not discussed in the Cheung et al. 2015 paper

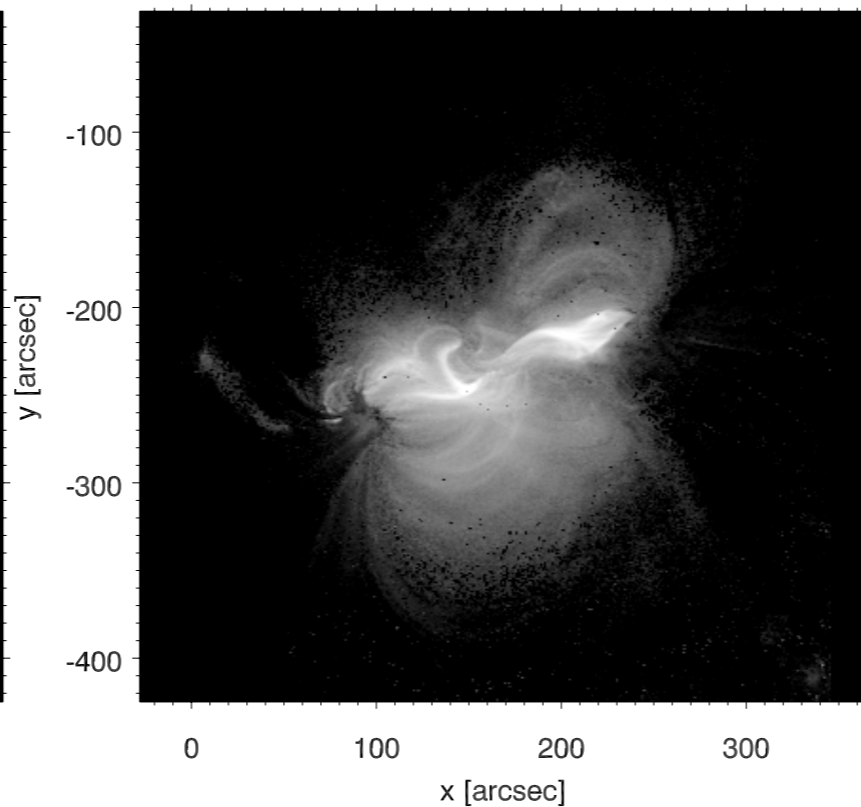
XRT

AIA DEM -> Mock XRT

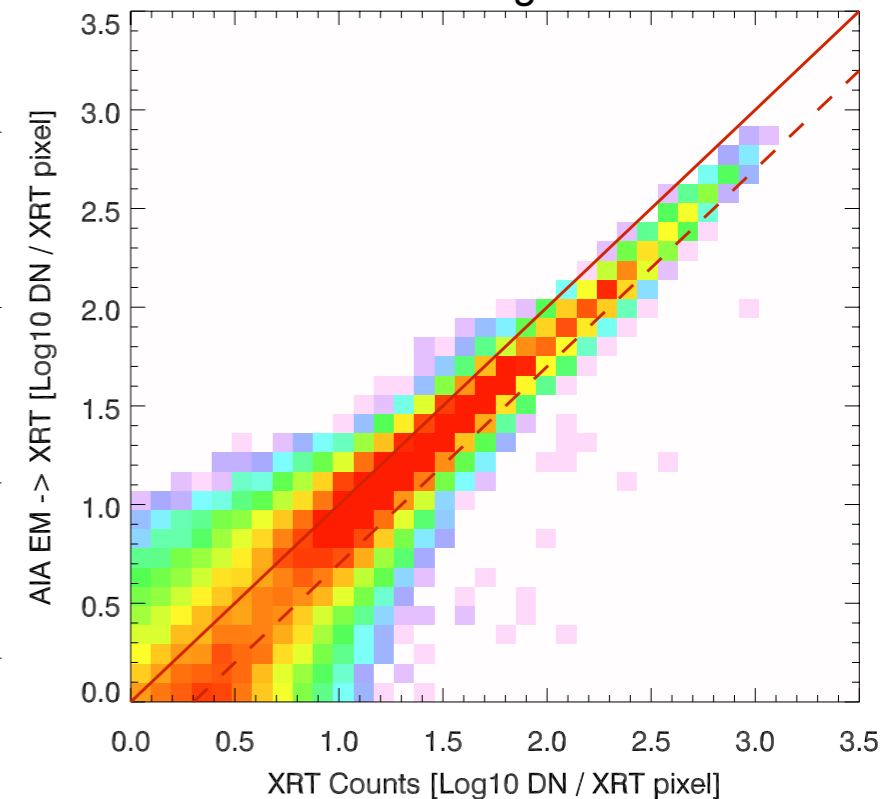
XRT Open/Ti_poly@2011-02-14T23:31:19



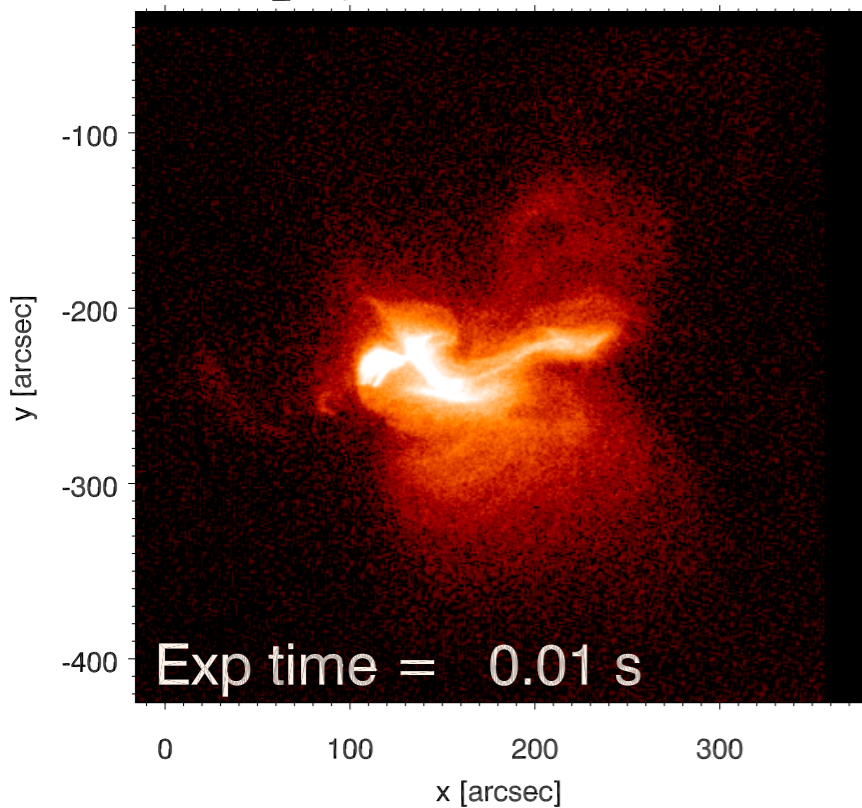
Synthesized from AIA 1x1 binned EM



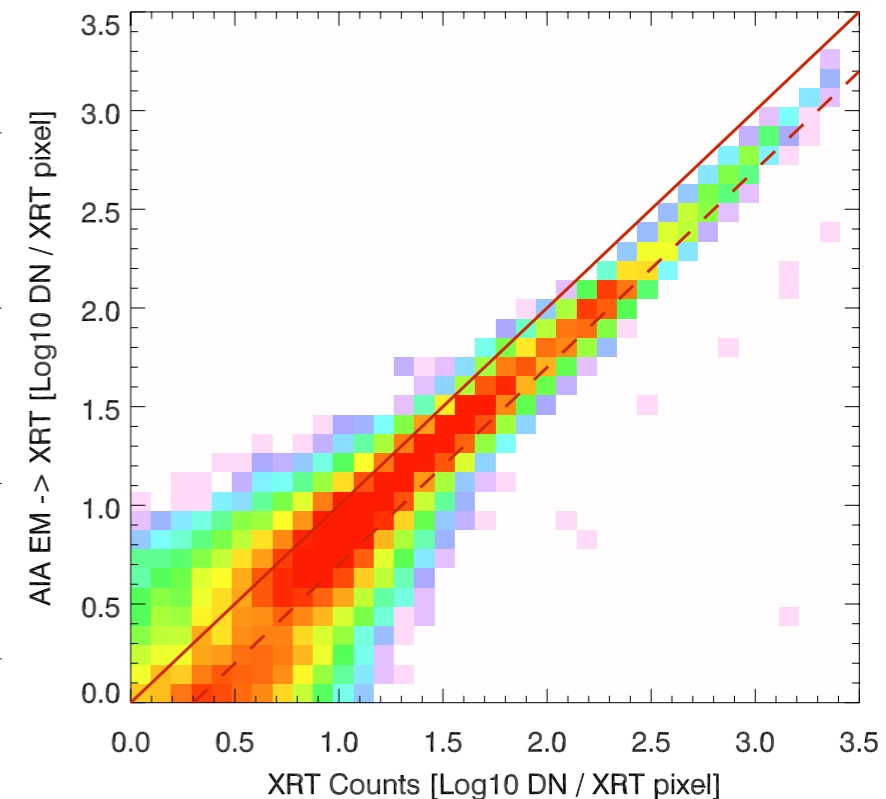
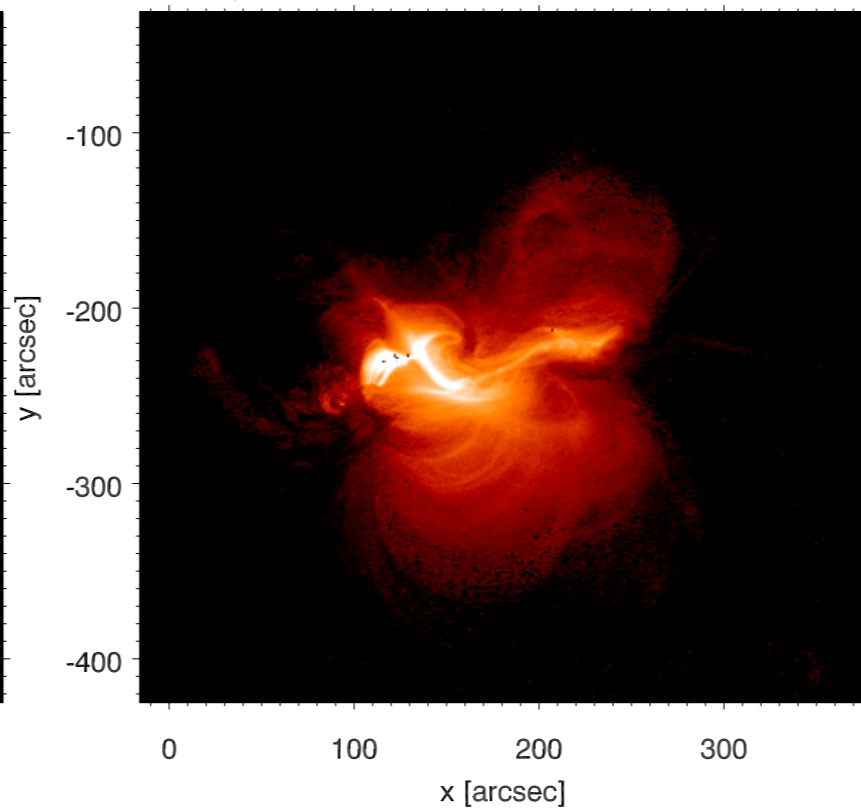
2D histograms



XRT AI_poly/Open@2011-02-15T00:56:07



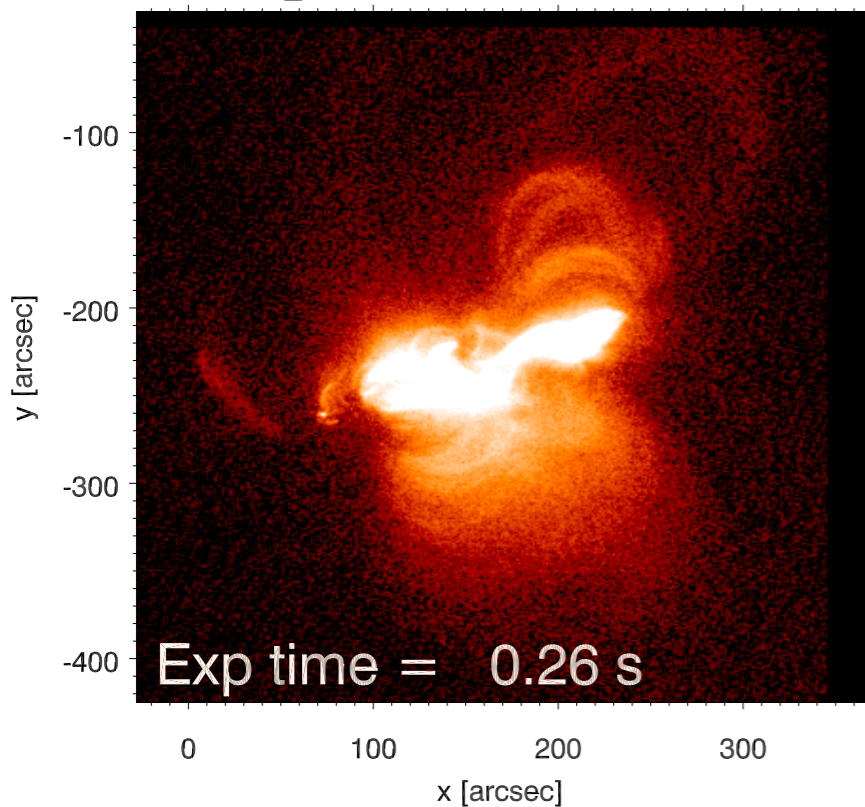
Synthesized from AIA 1x1 binned EM



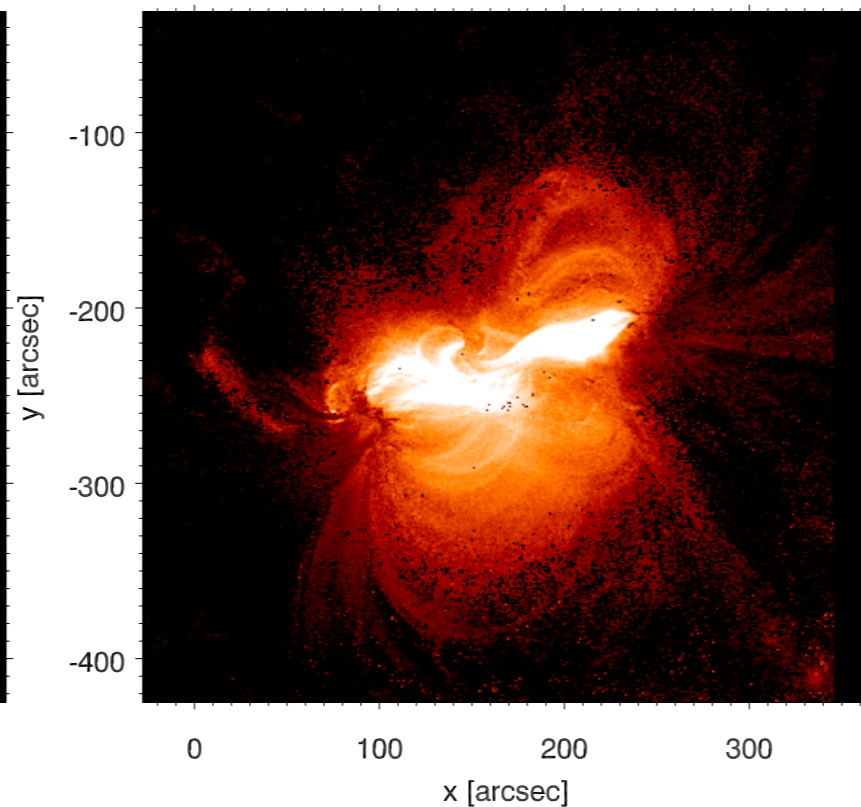
XRT

AIA DEM -> Mock XRT

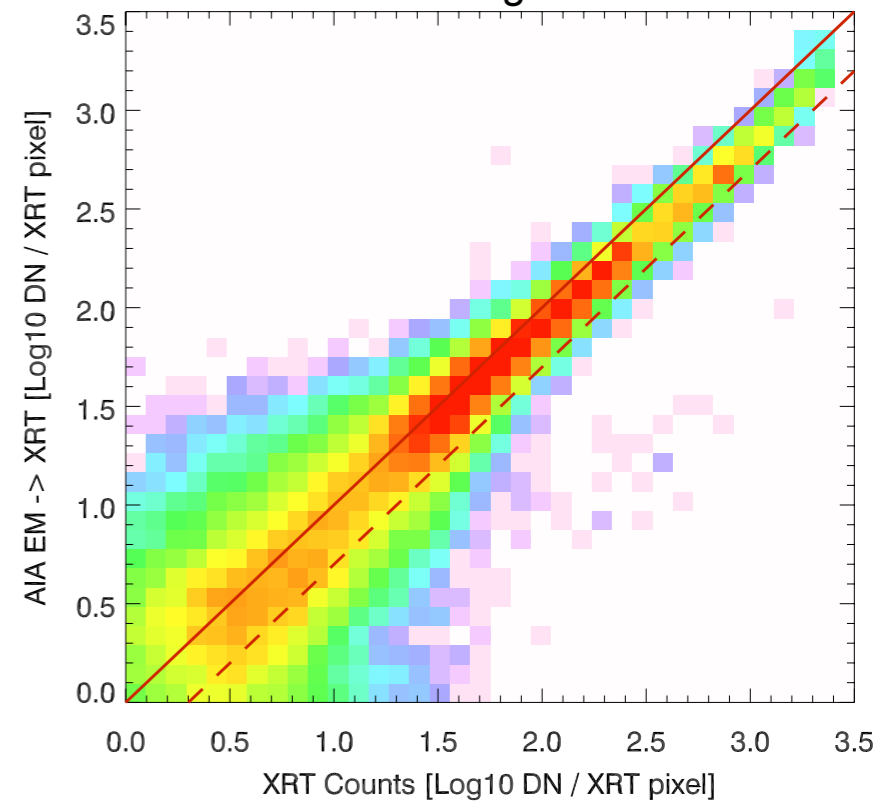
XRT Be_thin/Open@2011-02-14T23:31:10



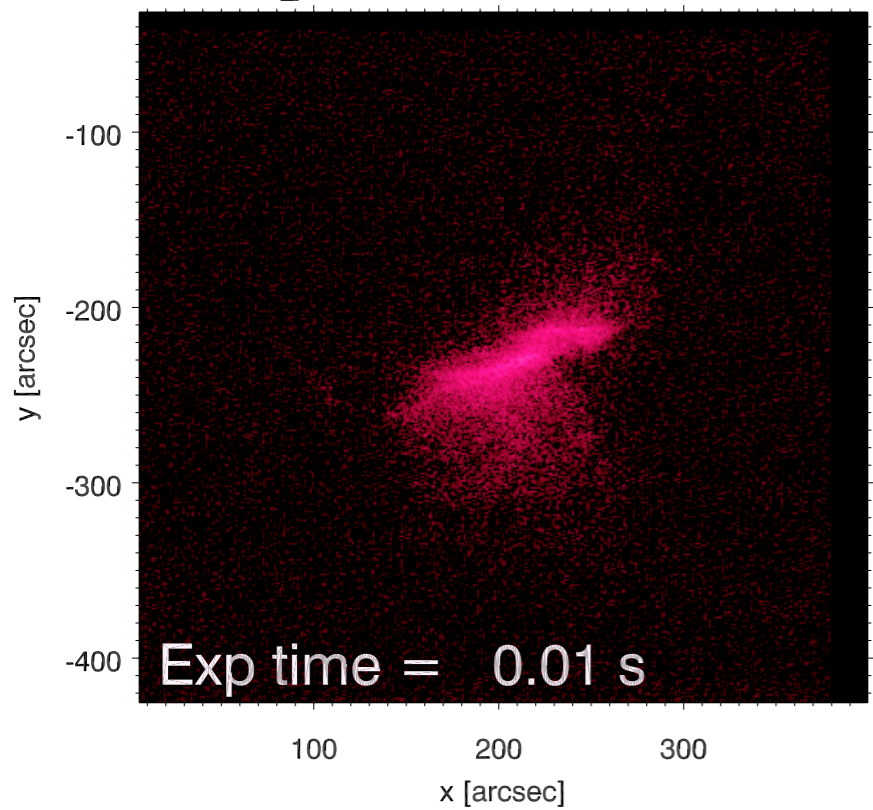
Synthesized from AIA 1x1 binned EM



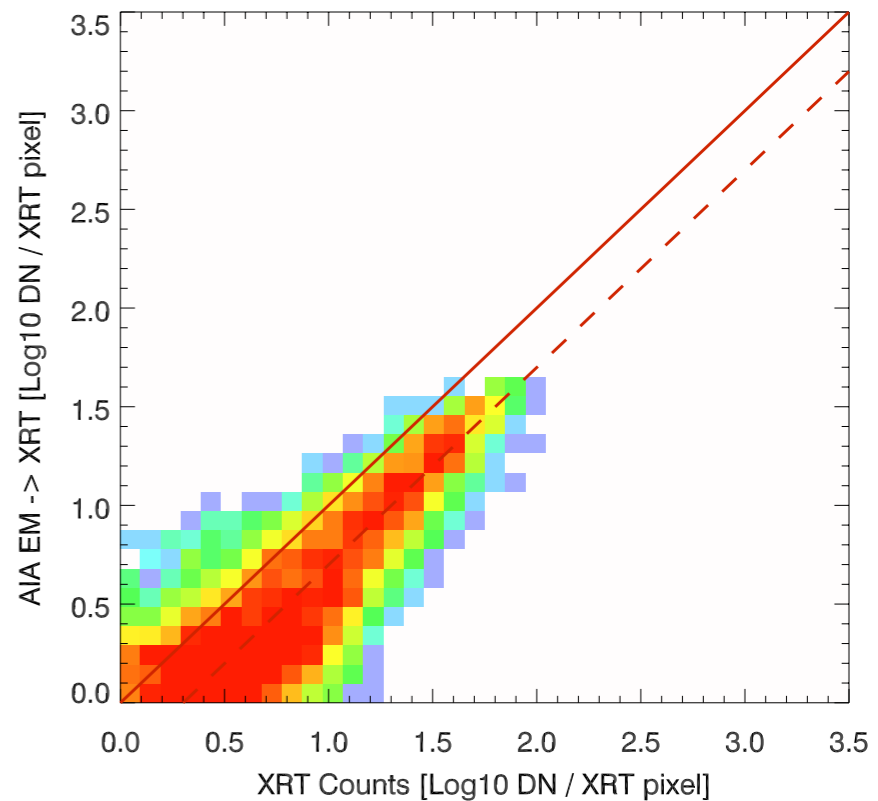
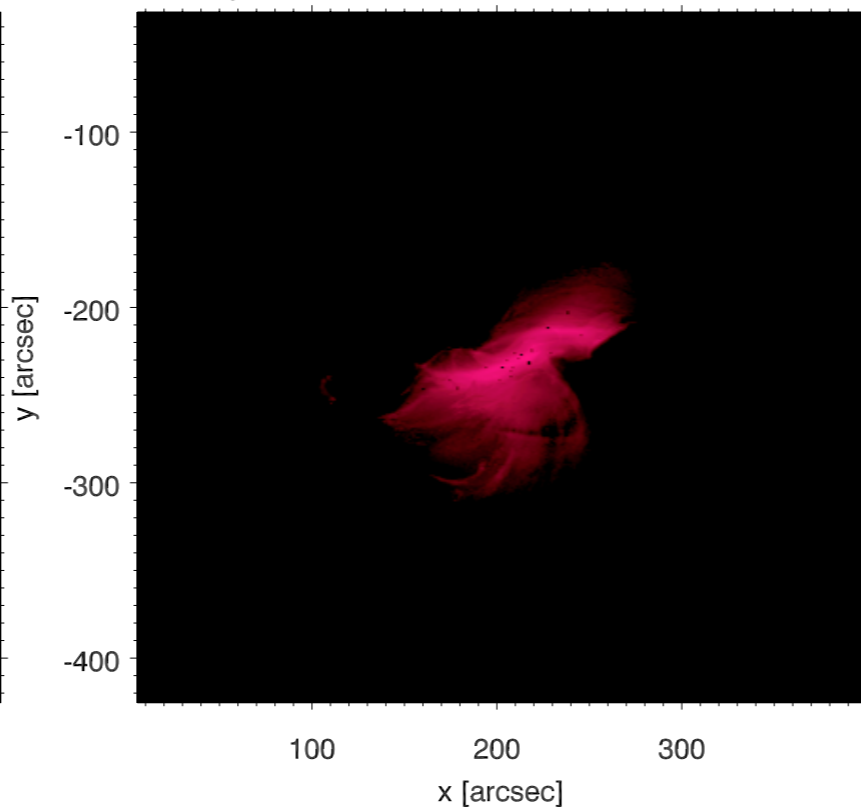
2D histograms



XRT Be_med/Open@2011-02-15T03:28:10



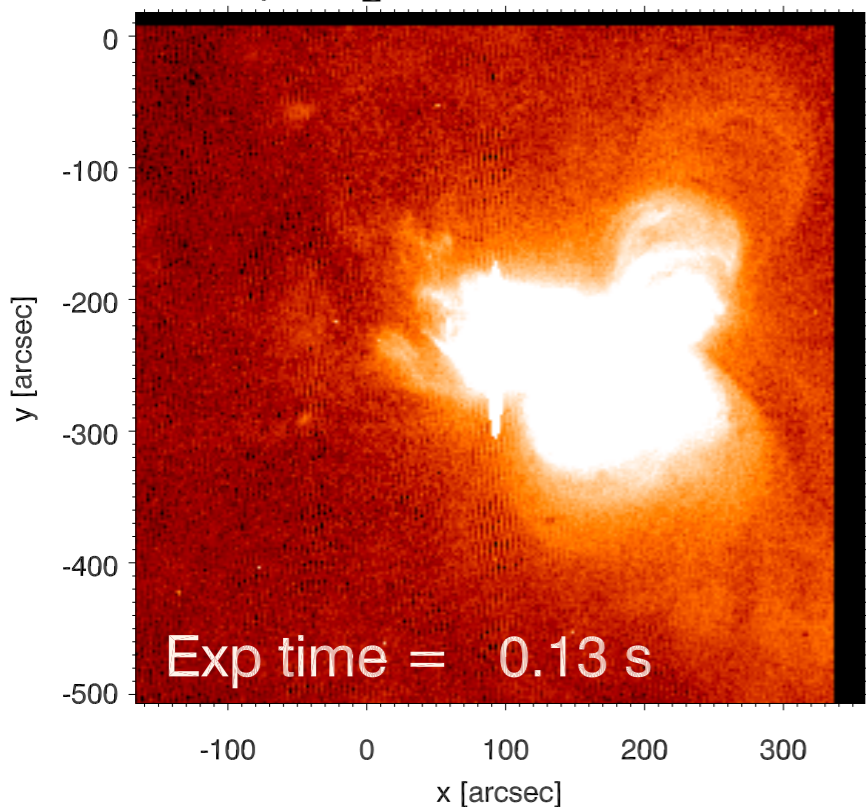
Synthesized from AIA 1x1 binned EM



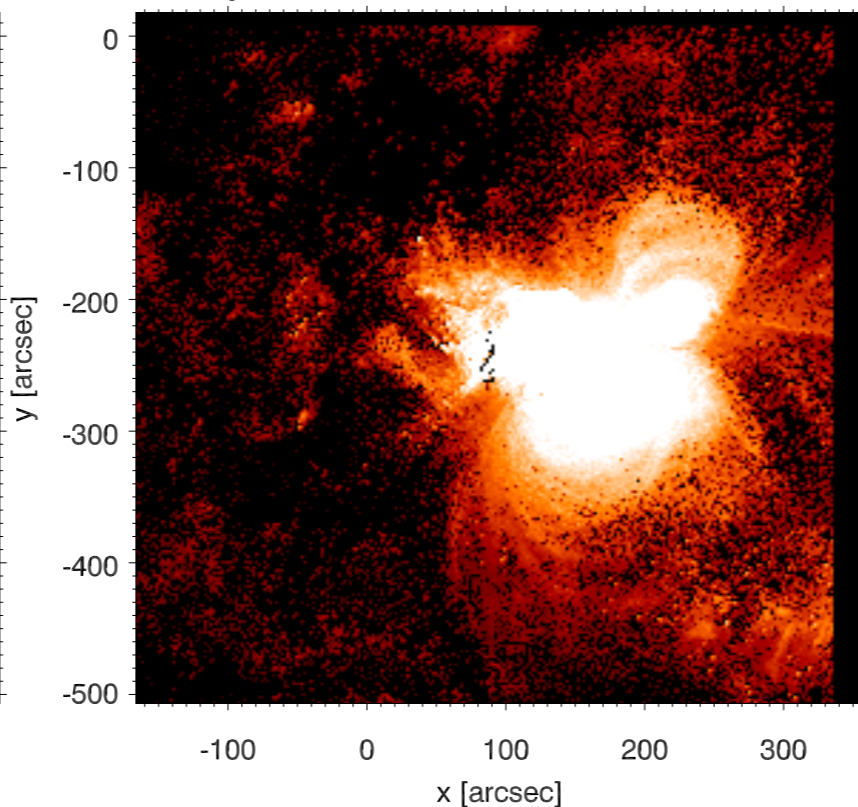
XRT

AIA DEM -> Mock XRT

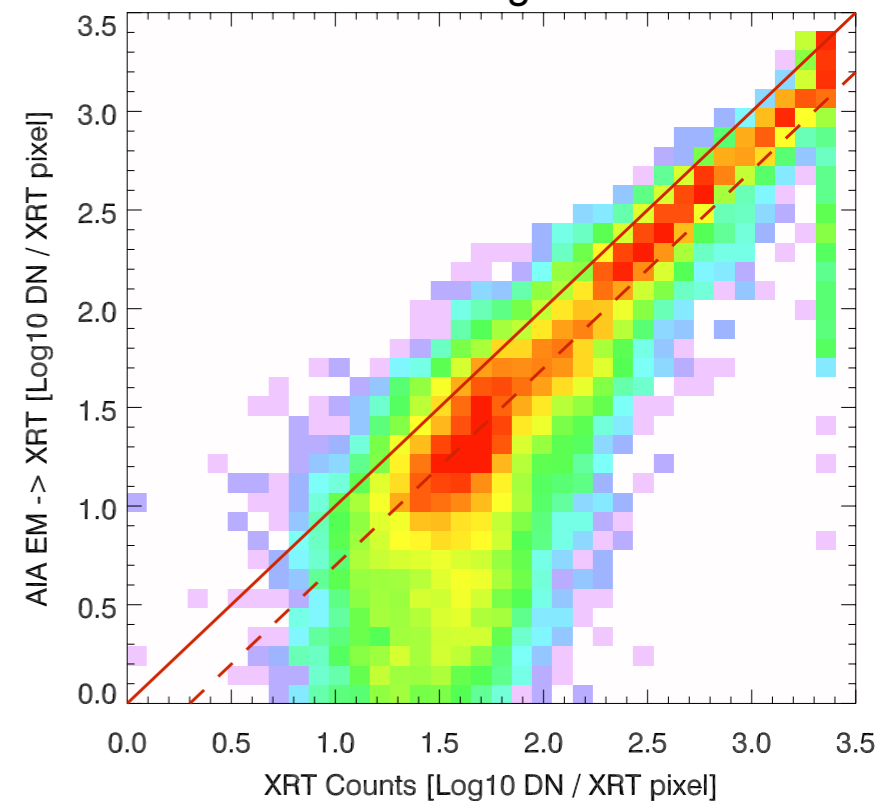
XRT Open/AI_mesh@2011-02-15T00:37:12



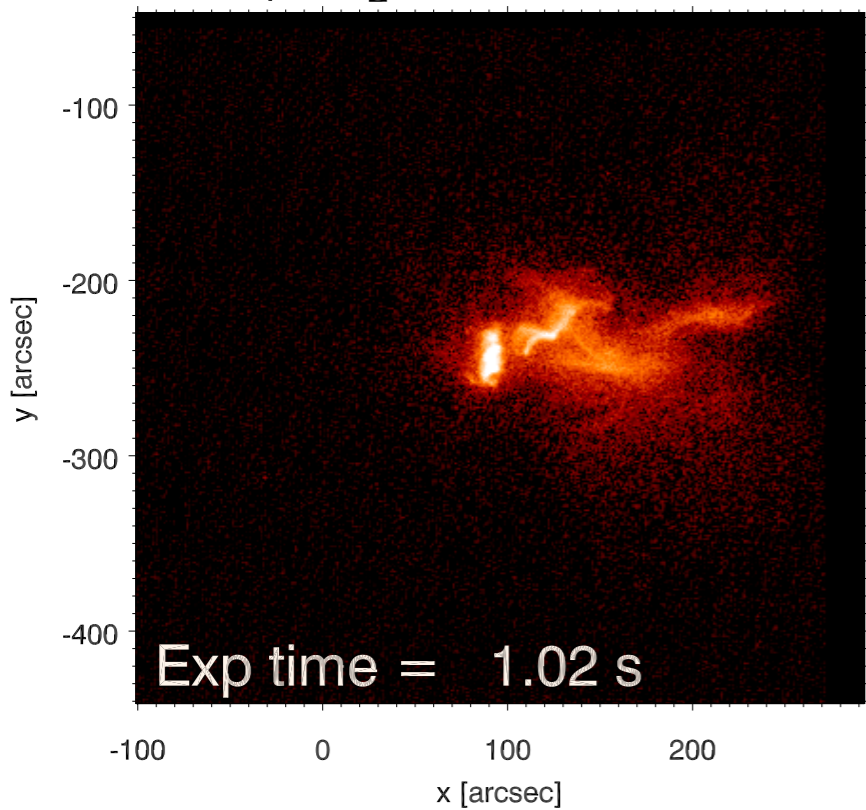
Synthesized from AIA 1x1 binned EM



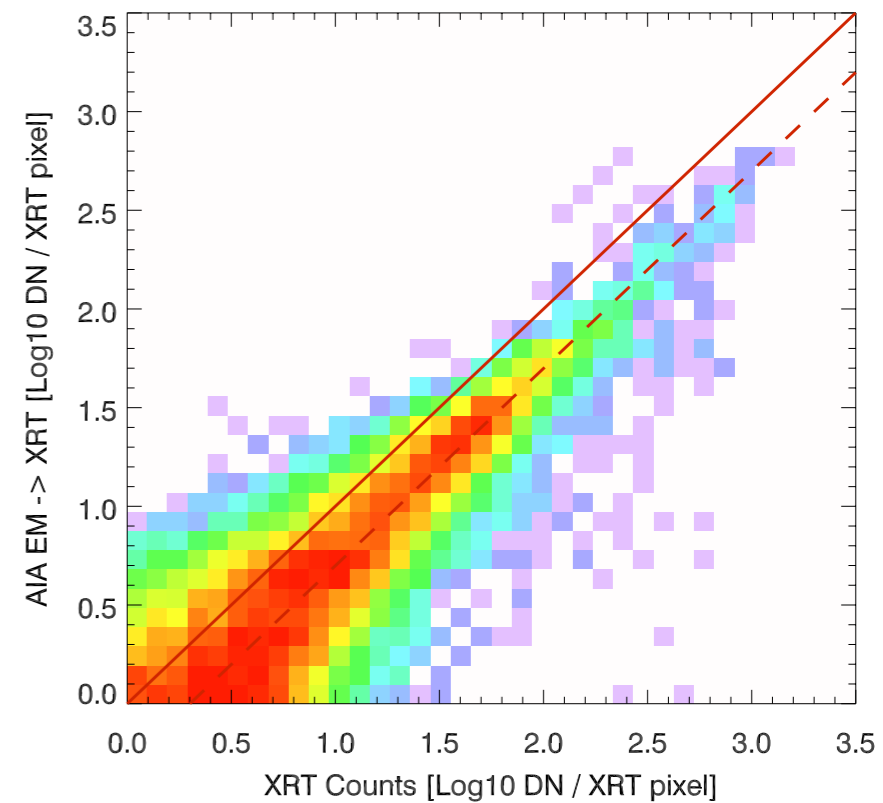
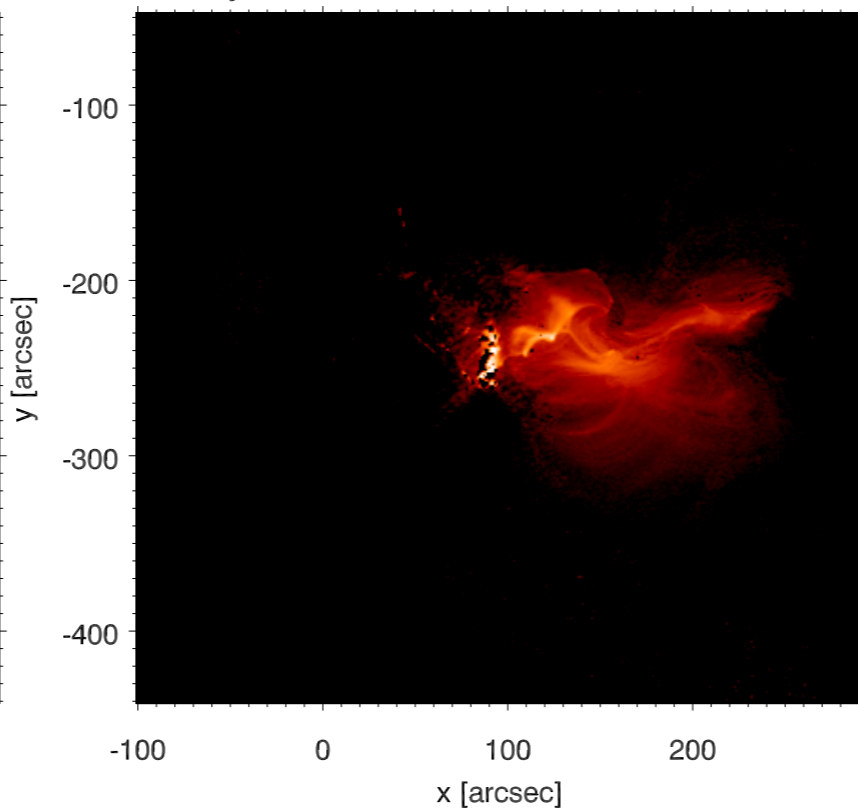
2D histograms



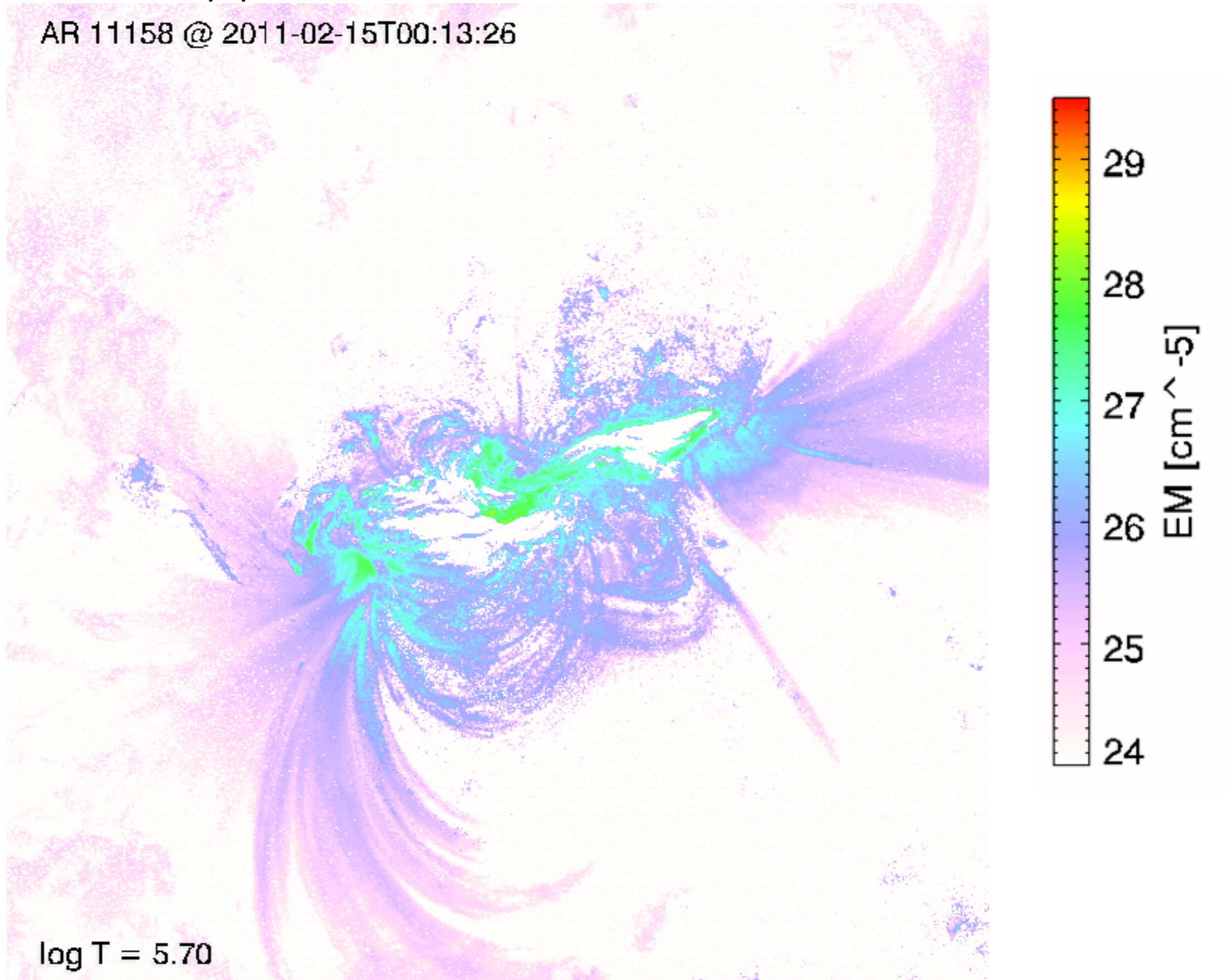
XRT Open/AI_thick@2011-02-15T00:36:59



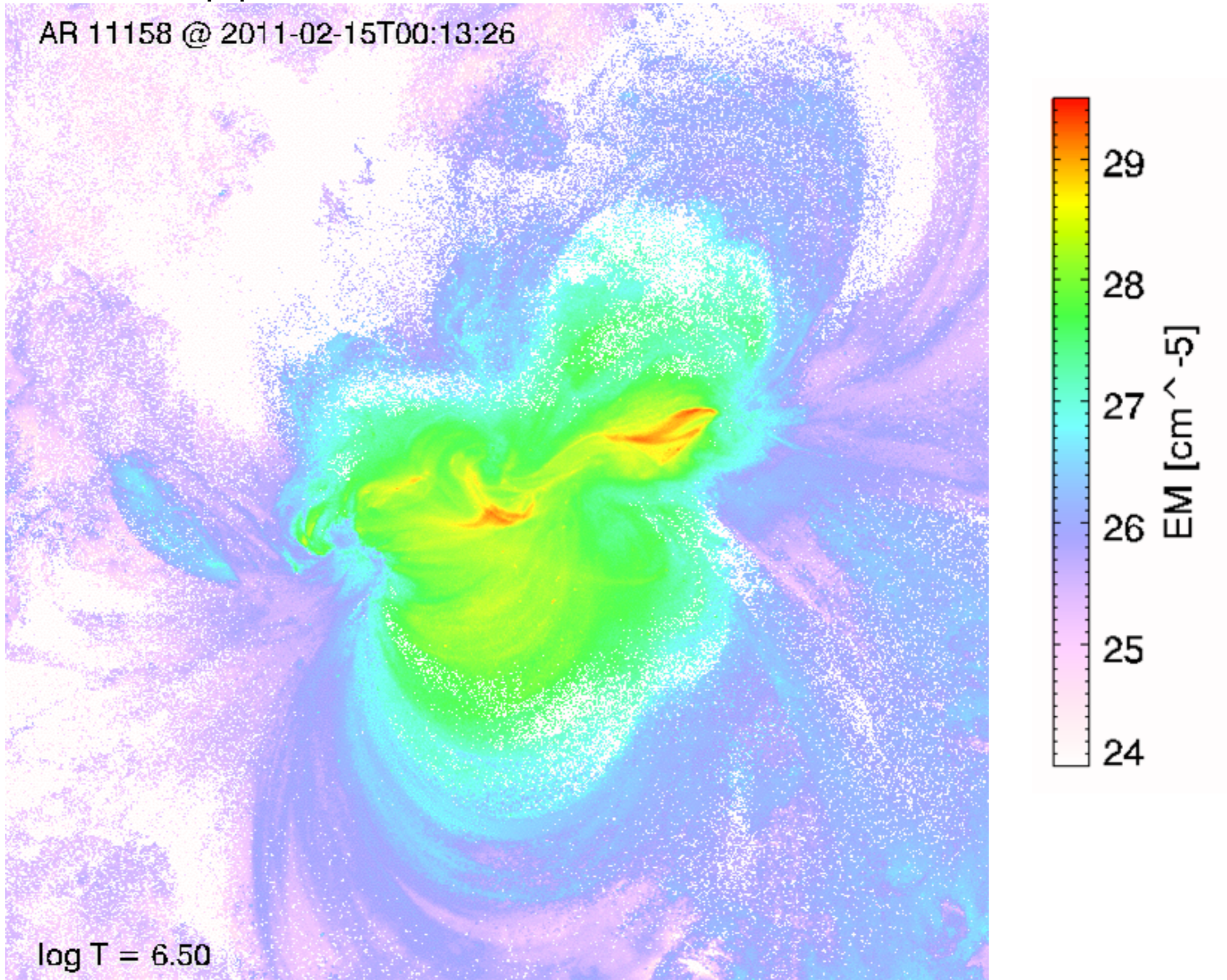
Synthesized from AIA 1x1 binned EM



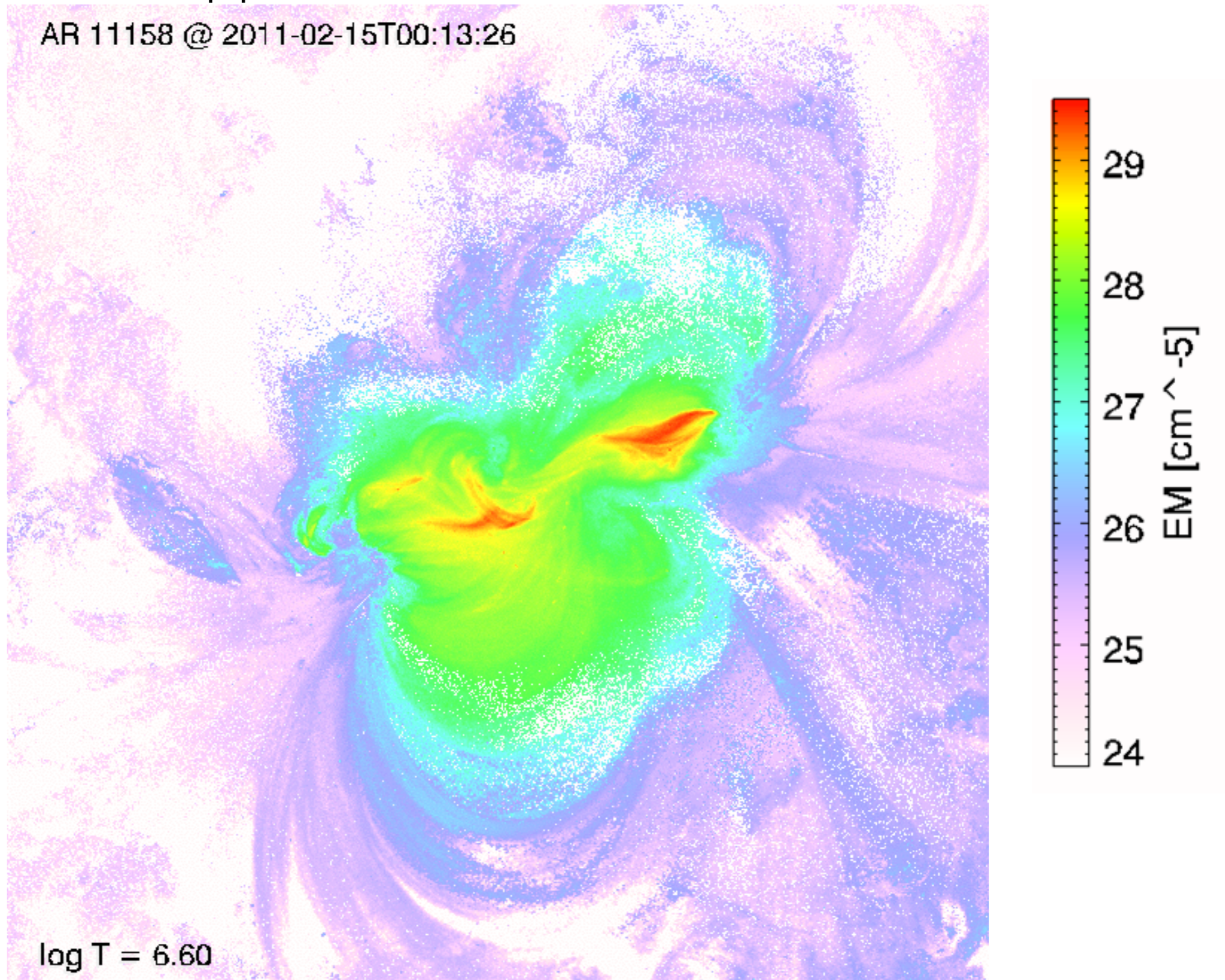
Application to real AIA data



Application to real AIA data

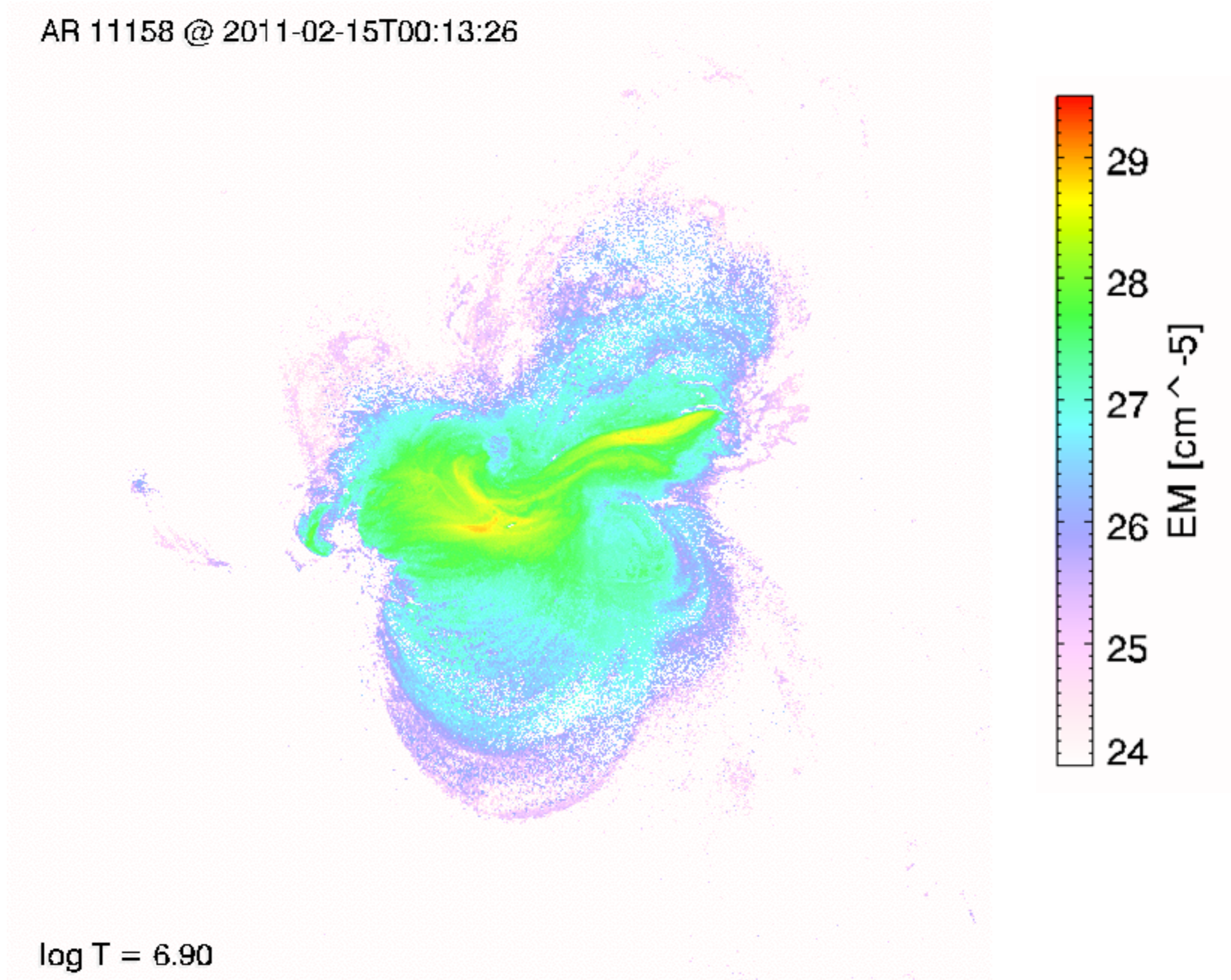


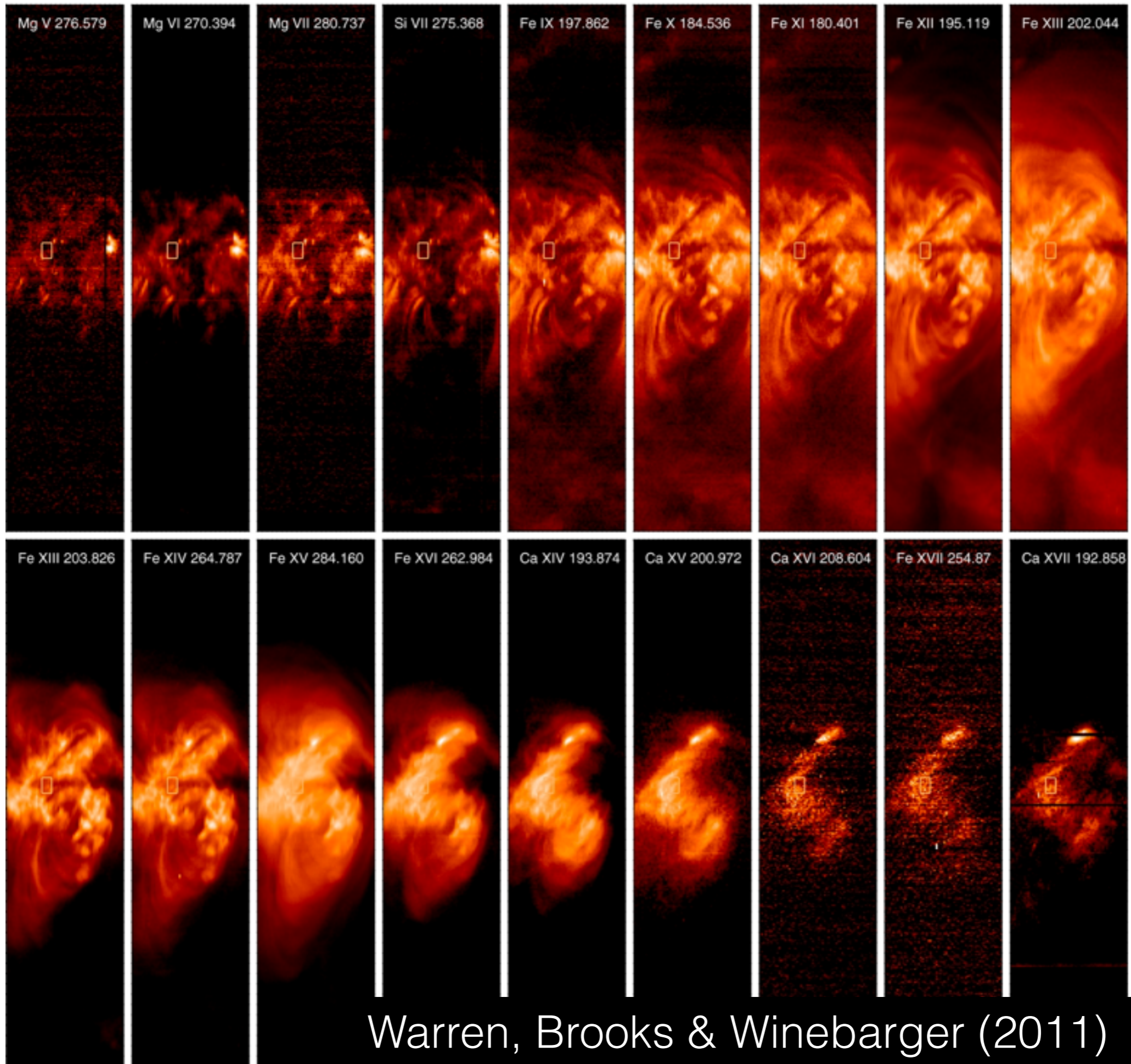
Application to real AIA data



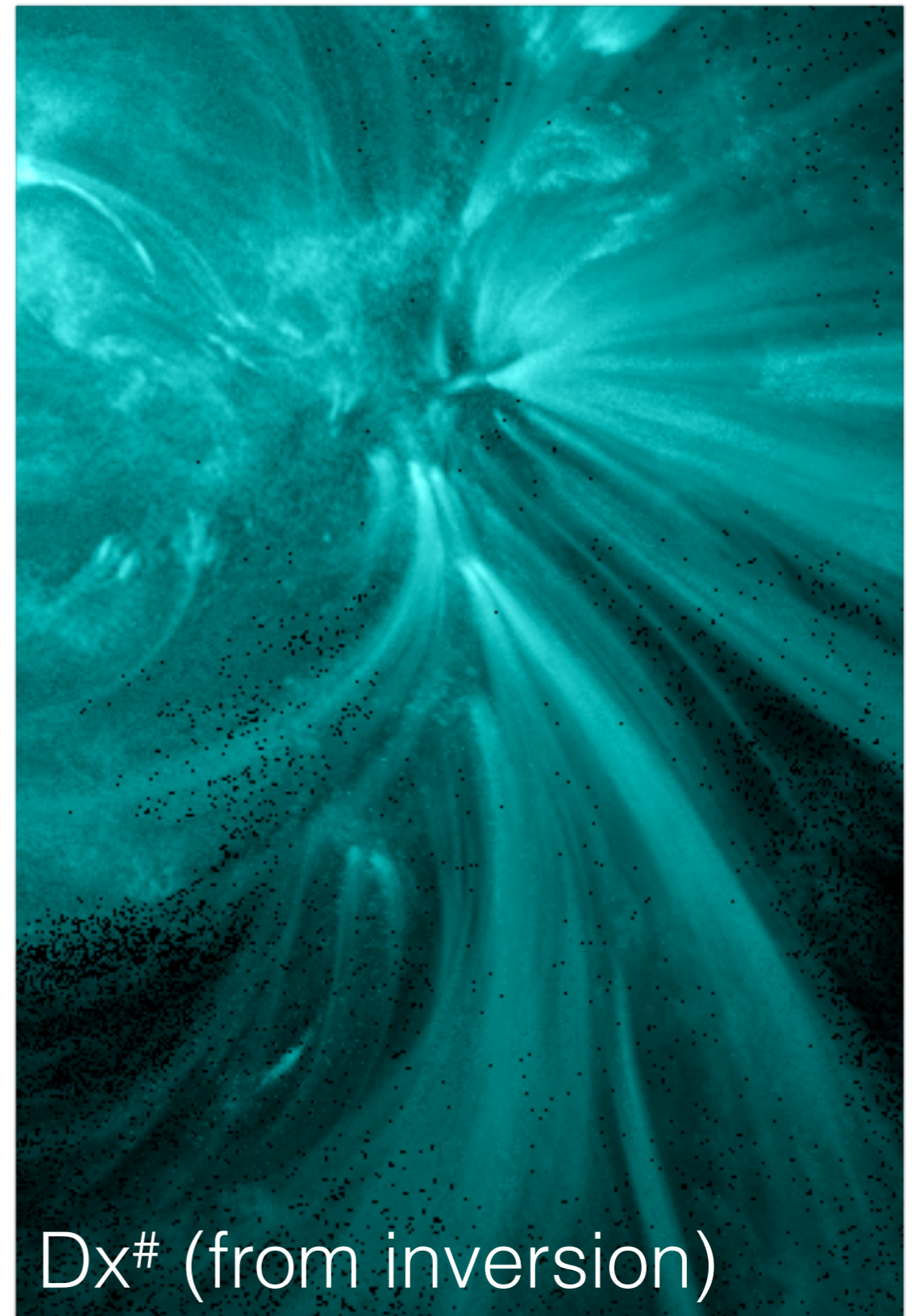
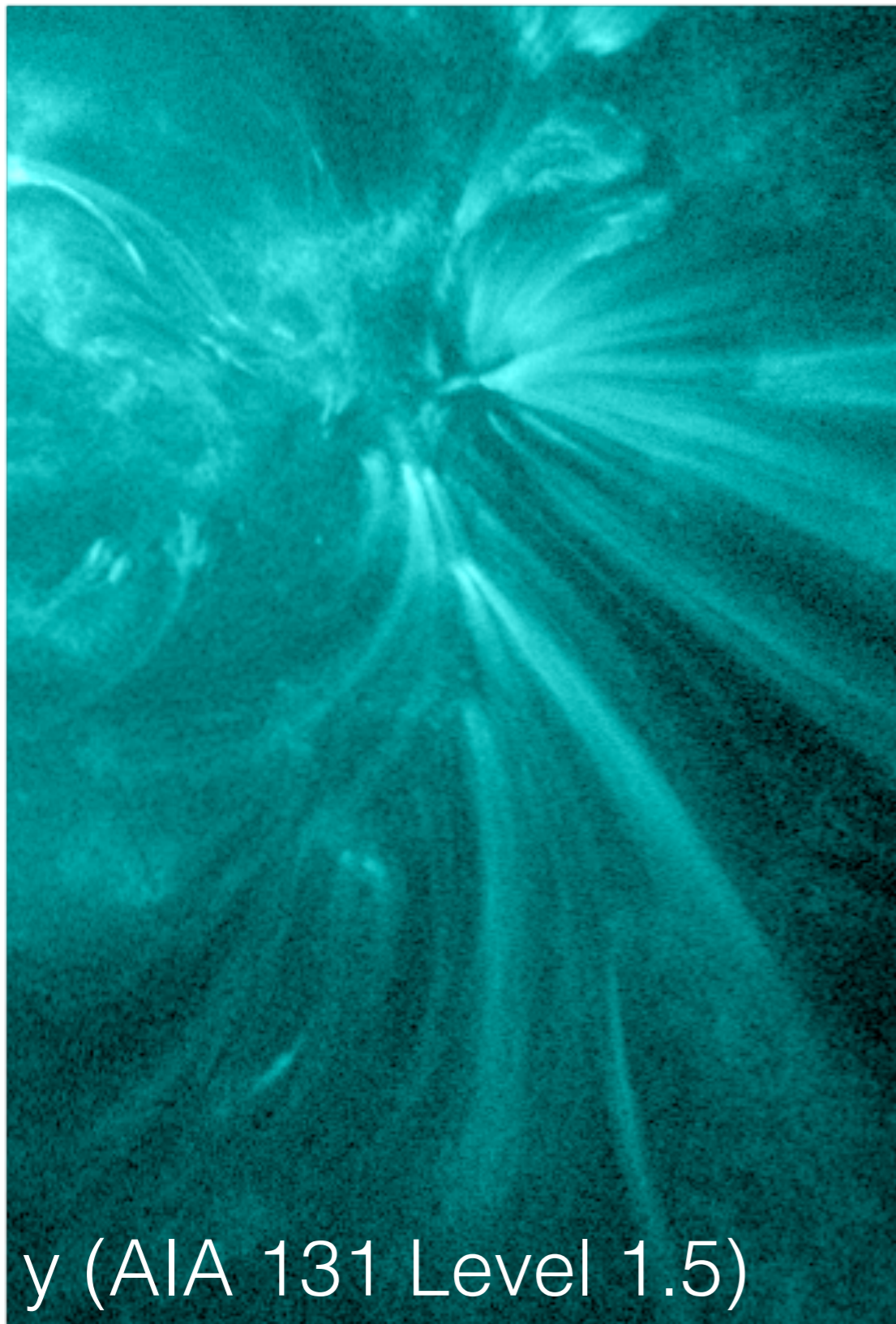
Application to real AIA data

AR 11158 @ 2011-02-15T00:13:26





Side benefit: Image Denoising



How to use the Sparse DEM code

<http://tinyurl.com/aiadem>

- Instructions in the readme file
- Download *genx files, which contain sample AIA 6-channel data.
- Download aia_sparse_em_init.pro & exercise1.pro
 - ➔ `.compile aia_sparse_em_init`
 - ➔ `.r exercise1` ; Example of DEM inversion
 - ➔ `.r exercise2` ; Example of DEM sensitivity to noise

```
; Author: Mark Cheung
; Purpose: Sample script for running sparse DEM inversion (see Cheung
; et al. 2015) for details.
; Revision history: 2015-10-20 First version
;                 2015-10-23 Added note about lgT axis
```

```
files = file_list('.', '*genx')
aiadatafile = files[0]
```

```
; Restore some prepared AIA level 1.5 data (i.e. already been aia_preped)
restgen, file=aiadatafile, struct=s
```

```
; Initialize solver.
; This step builds up the response functions (which are
; time-dependent) and the basis functions.
; If running inversions over a set of data spanning over a few hours
; or even days, it is not necessary to re-initialize
```

```
;IF (0) THEN BEGIN
```

```
; As discussed in the Appendix of Cheung et al. (2015), the inversion
; can push some EM into temperature bins if the lgT axis goes below
;  $\log T \sim 5.7$  (see Fig. 18). It is suggested the user check the
; dependence of the solution by varying lgTmin.
```

```
lgTmin = 5.7 ; minimum for lgT axis for inversion
```

```
dlgT = 0.1 ; width of lgT bin
```

```
nlgT = 21 ; number of lgT bins
```

```
aia_sparse_em_init, timedepend = s.oindex[0].date_obs, /evenorm, $  
use_lgtaxis=findgen(nlgT)*dlgT+lgTmin
```

```
lgtaxis = aia_sparse_em_lgtaxis()
```

```
; ENDIF
```

; We will use the data in s.img to invert. s.img is a stack of level
; 1.5, exposure time normalized AIA pixel values.

```
exptimestr = '['+strjoin(string(s.oindex.exptime,format='(F8.5)'),',')+']'
```

; This defines the tolerance function for the inversion.
; y denotes the values in DN/s/pixel (i.e. level 1.5, exposure time
; normalized)

; aia_bp_estimate_error gives the estimated uncertainty for a given
; DN / pixel for a given AIA channel. Since y contains DN/pixel/s,
; we have to multiply by exposure time first to pass
; aia_bp_estimate_error. Then we will divide the output of
; aia_bp_estimate_error by the exposure time again.
; If one wants to include uncertainties in atomic data, suggest to add
; the /temp keyword to aia_bp_estimate_error()

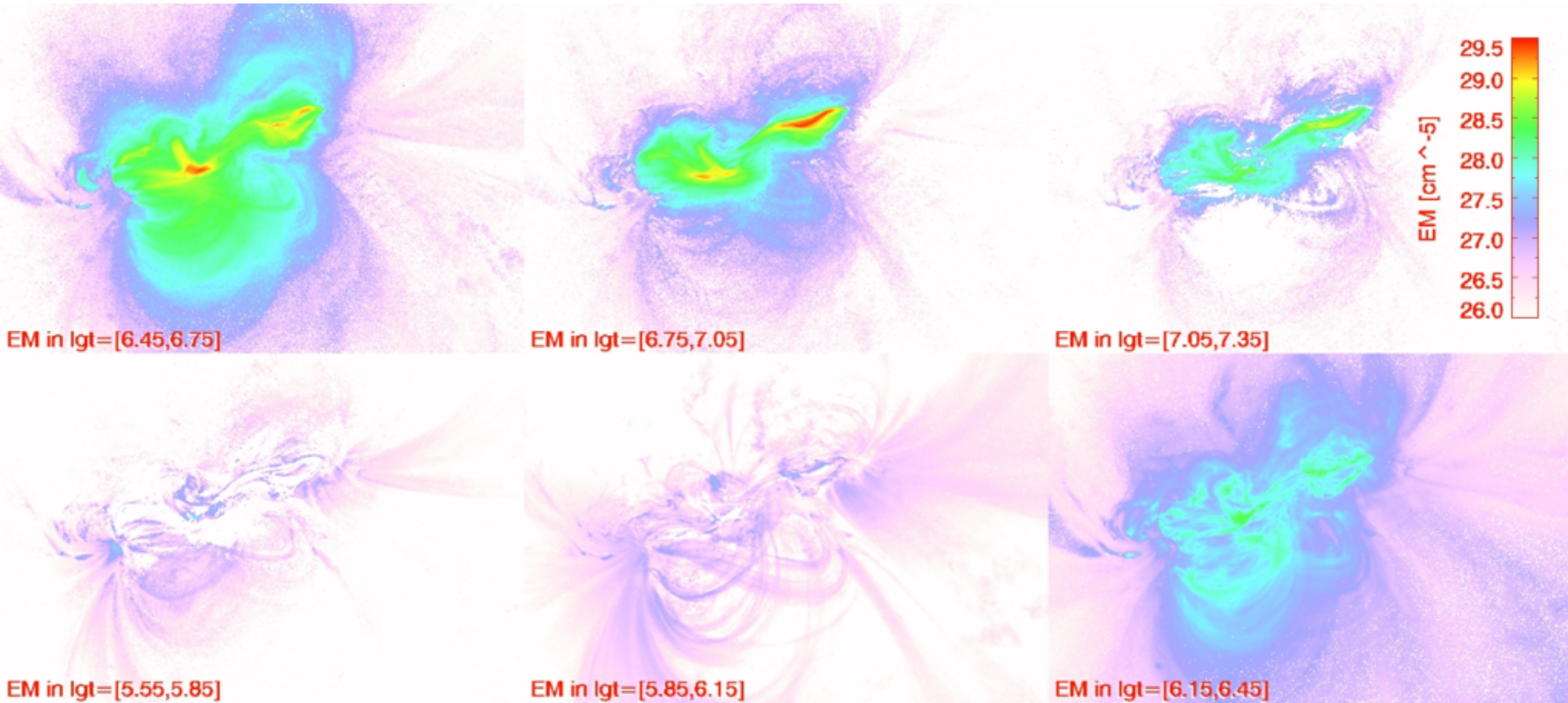
```
tolfunc = 'aia_bp_estimate_error(y*'+exptimestr+', [94,131,171,193,211,335], $  
num_images='+strtrim(string(s.binning^2,format='(I4)'),2)+'/' +exptimestr
```

; Do DEM solve.

; Note!!! The solver assumes the third dimension is arranged according to
[94,131,171,193,211,335]

```
aia_sparse_em_solve, s.img, tolfunc=tolfunc, tolfac=1.4, oem=emcube, status=status,  
coeff=coeff
```

Output of exercise1.pro



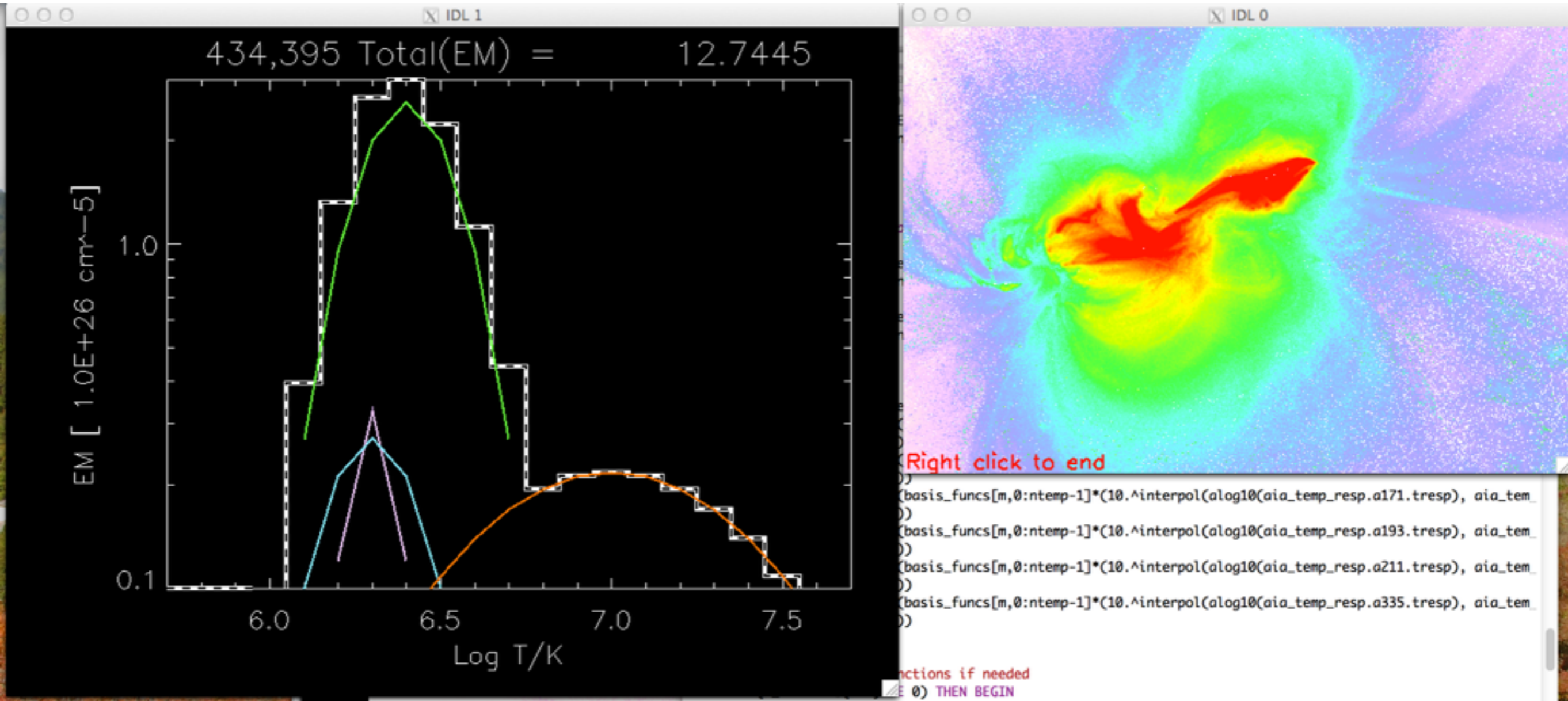
status[Nx, Ny] - Indicating where a DEM solution was found, 0 is yes

coeff[Nx, Ny, 84] - Coefficients of basis functions used to express DEM; i.e. the x in equation $y = \mathbf{KB}x$.

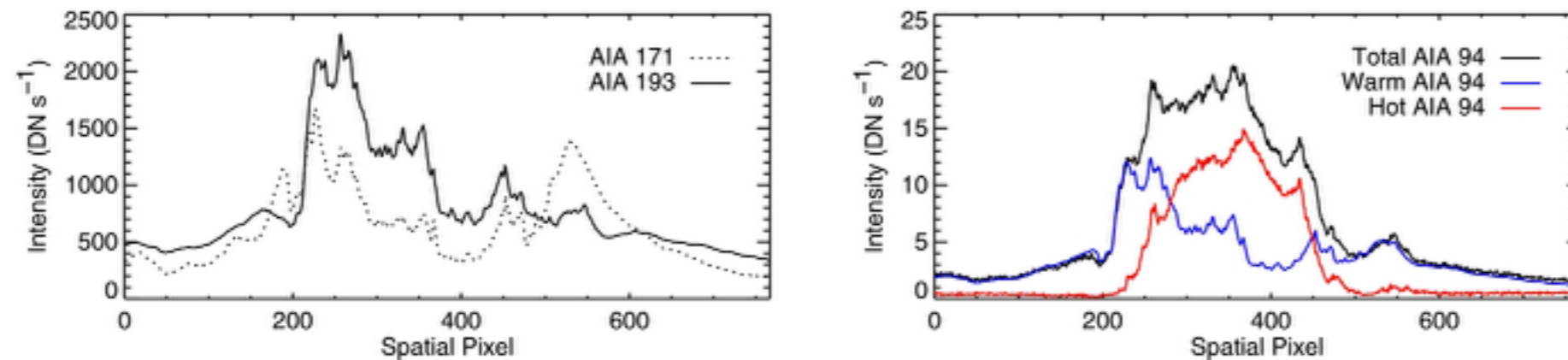
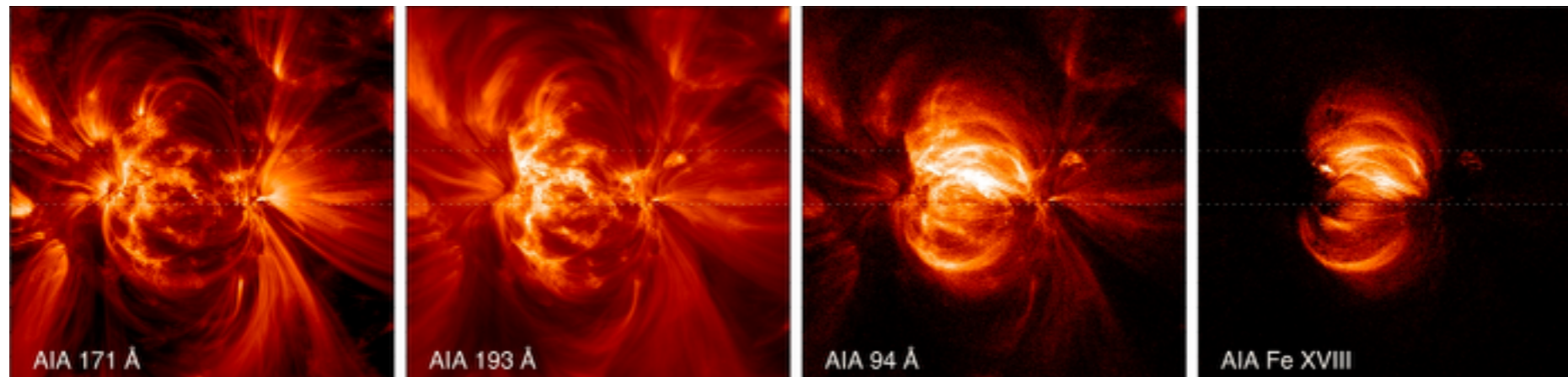
emcube[Nx, Ny, 21] - DEM solution. i.e. $\mathbf{B}x$.

Interactively inspect DEM profiles

- aia_sparse_dem_inspect, coeff, emcube, status, /ylog



Active Region Thermal Structure



Warren, Winebarger & Brooks (2012) devised a method to separate the ‘warm’ and ‘hot’ components of emission from the AIA 94 Å channel. They use this empirical fit:

$$I_{94\text{warm}} = 0.39 \sum_{i=1}^4 a_i \left[\frac{f I_{171} + (1 - f) I_{193}}{116.54} \right]^i$$

“for this value of f [$=0.3$], the coefficients to the polynomial fit are -7.31×10^{-2} , 9.75×10^{-1} , 9.90×10^{-2} , and -2.84×10^{-3} .”

Log Emission Measure [cm⁻⁵]



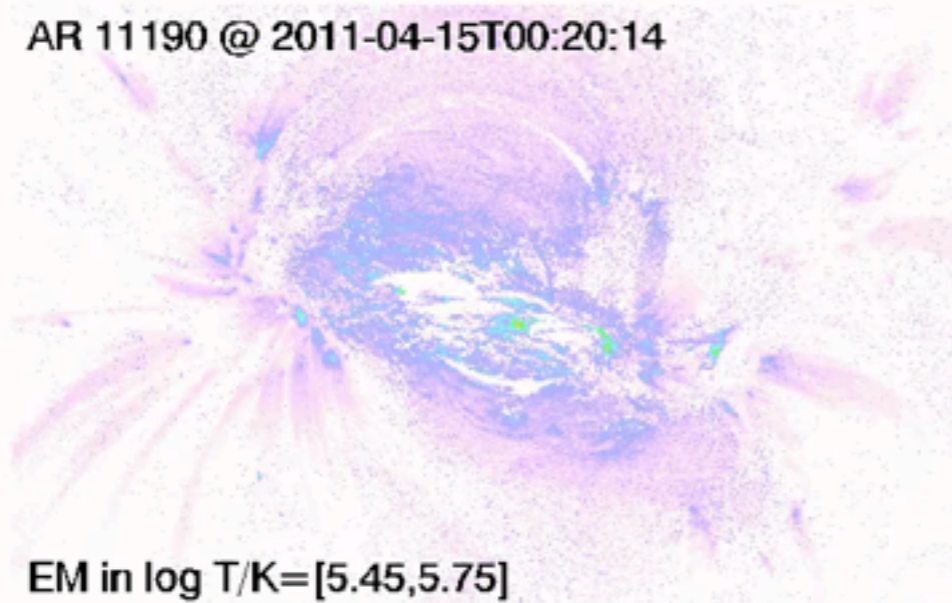
26.00

27.00

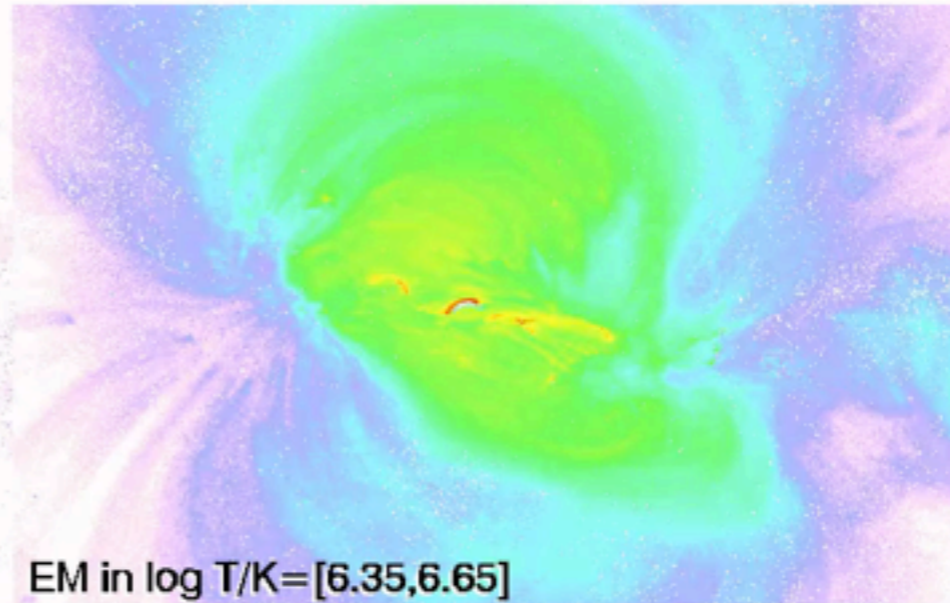
28.00

29.00

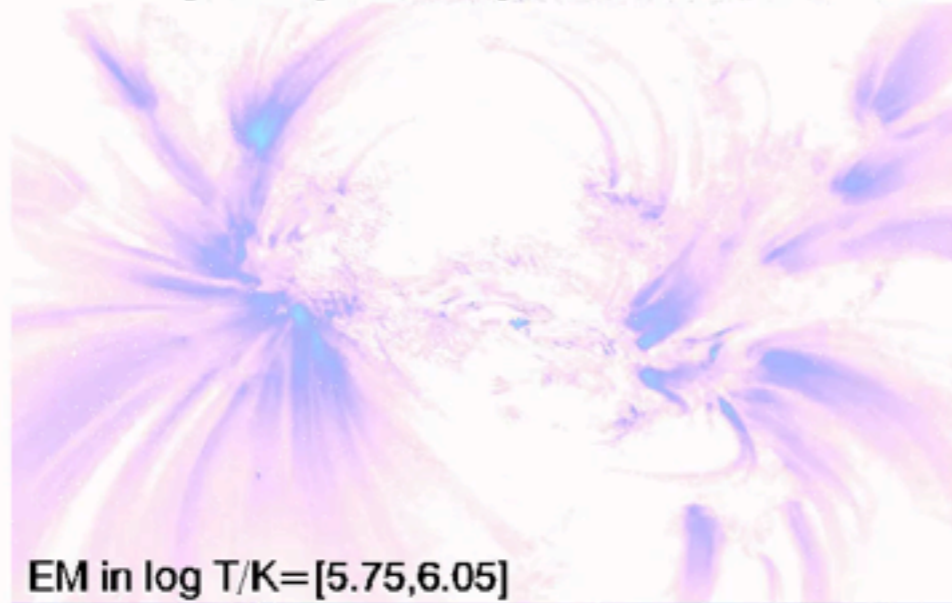
AR 11190 @ 2011-04-15T00:20:14



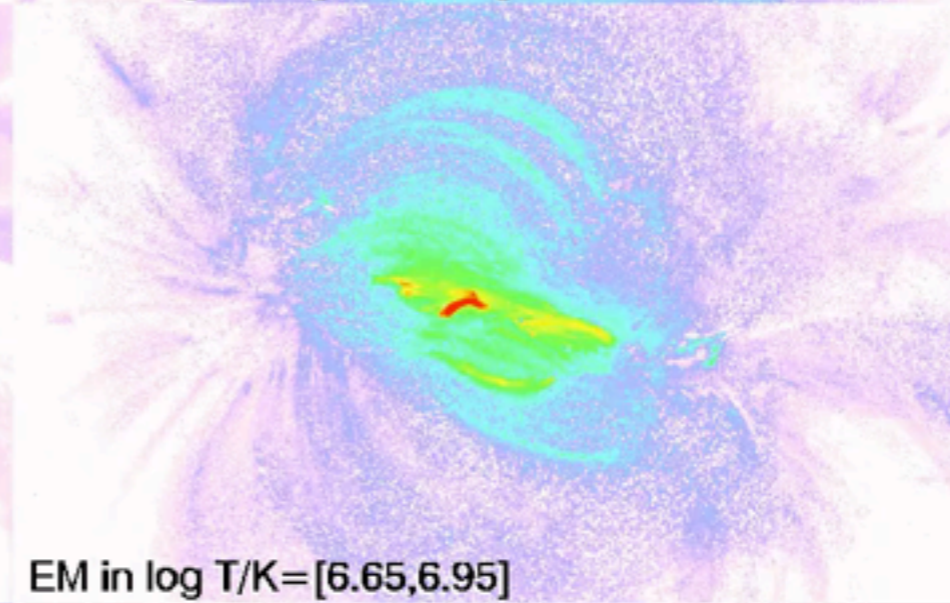
EM in log T/K=[5.45,5.75]



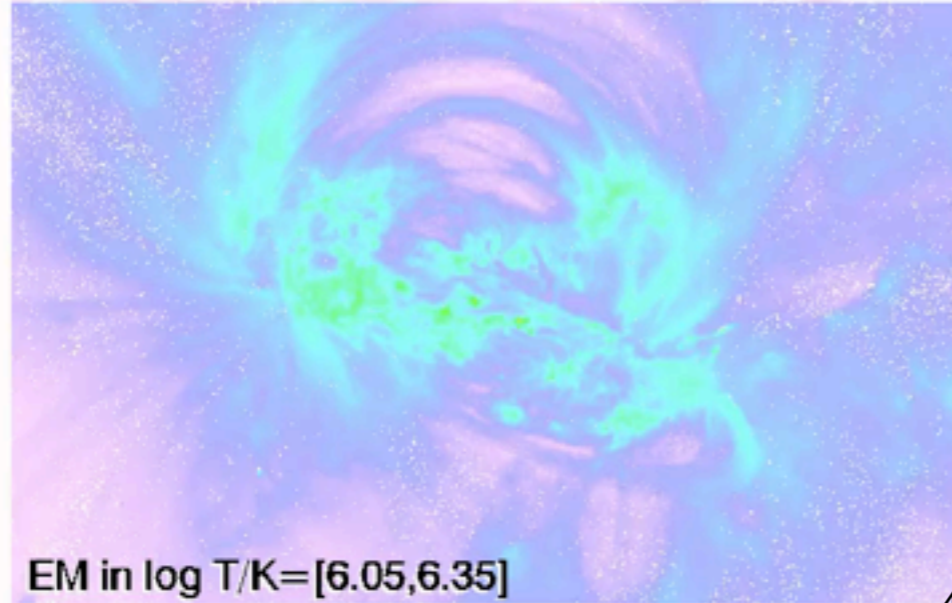
EM in log T/K=[6.35,6.65]



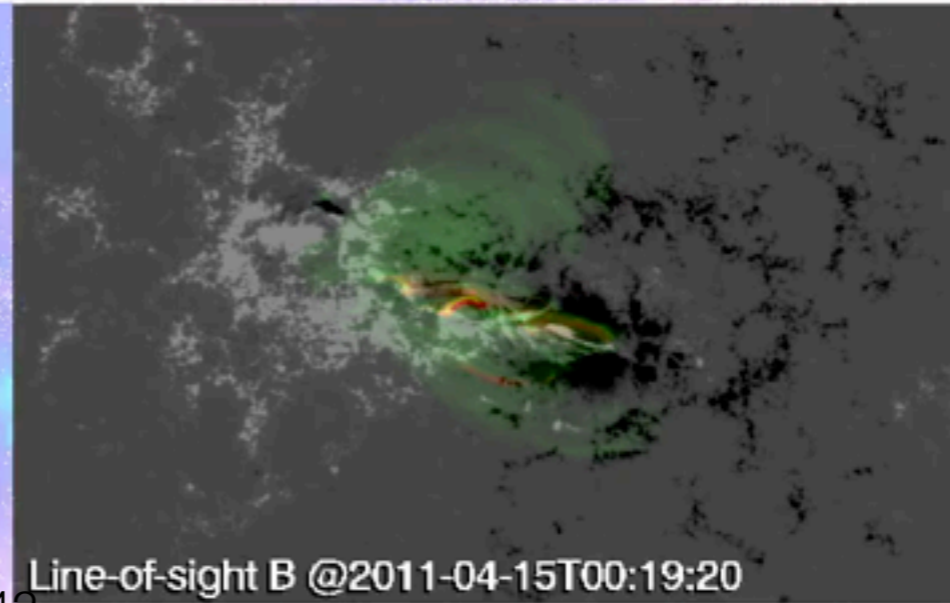
EM in log T/K=[5.75,6.05]



EM in log T/K=[6.65,6.95]



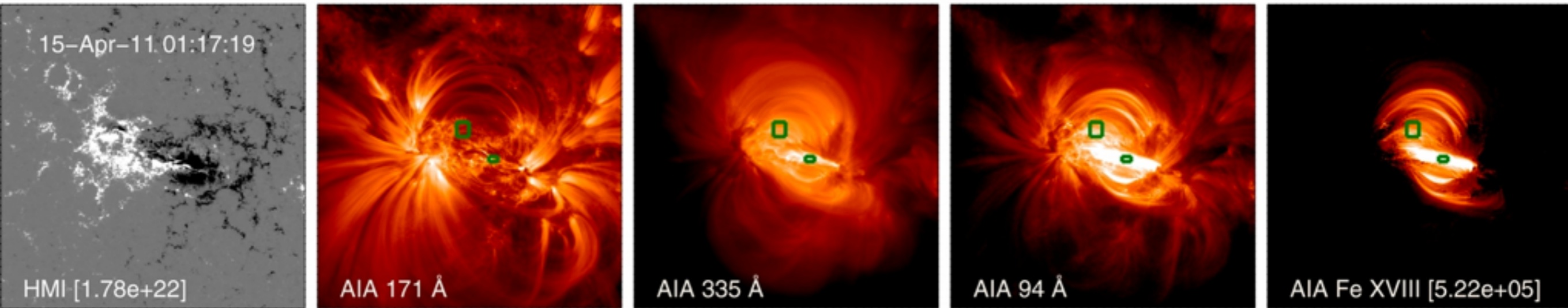
EM in log T/K=[6.05,6.35]



Line-of-sight B @2011-04-15T00:19:20

Workshop Practice Exercise 1:

AR 11190



From: Warren, Winebarger & Brooks (2012)

Go to <http://www.lmsal.com/~cheung/AIA/ar11190/>

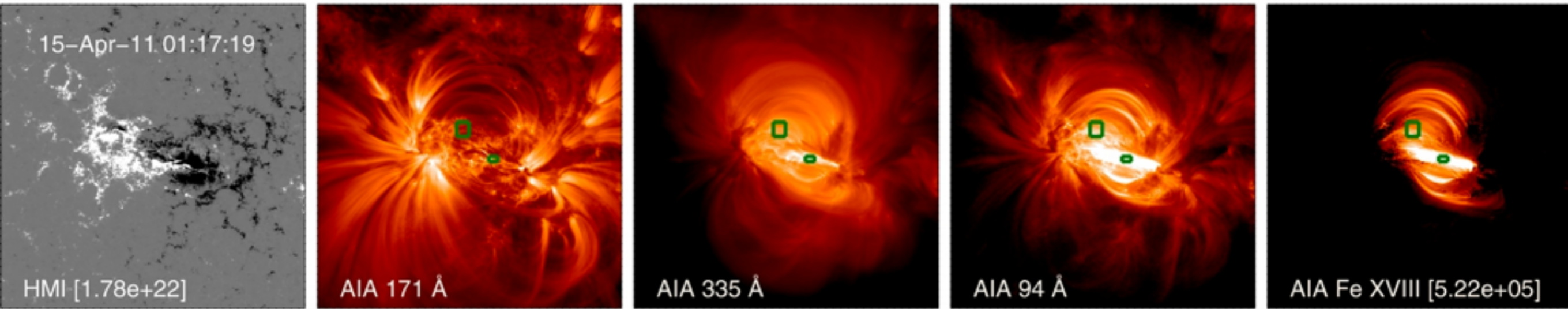
Download a genx file and plot the DEM distribution in regions marked by the green boxes.

How do the DEMs in these boxes evolve?

What about the DEM averaged over the AR? (Take care with pixels that have no DEM solutions).

Workshop Practice Exercise 2:

AR 11190



From: Warren, Winebarger & Brooks (2012)

<http://www.lmsal.com/~cheung/AIA/11190/>

Download a genx file

Starting from the DEM solution, generate AIA 94 images separately for the 'warm' and 'hot' components.

Hint: use

`PRO AIA_SPARSE_EM_EM2IMAGE, em, image=image,
status=status`

Workshop Practice Exercise 3:

Examine impact of choice of basis functions

- By default, `aia_sparse_em_init` uses 4 sets of basis functions (Dirac + 3 sets of truncated gaussians).
- Default keyword is `bases_sigmas = [0,0.1,0.2,0.6]`
- Test how choosing other basis sets changes DEM results. e.g.
 - Only Dirac Delta functions `bases_sigmas = [0]`
 - Dirac + Gaussians of width 0.1 `bases_sigmas = [0,0.1]`
 - Dirac + Gaussians of width 0.1, 0.2 and 0.3 `bases_sigmas = [0,0.1,0.2,0.3]`

Workshop Practice Exercise 4: AIA + XRT DEM inversions

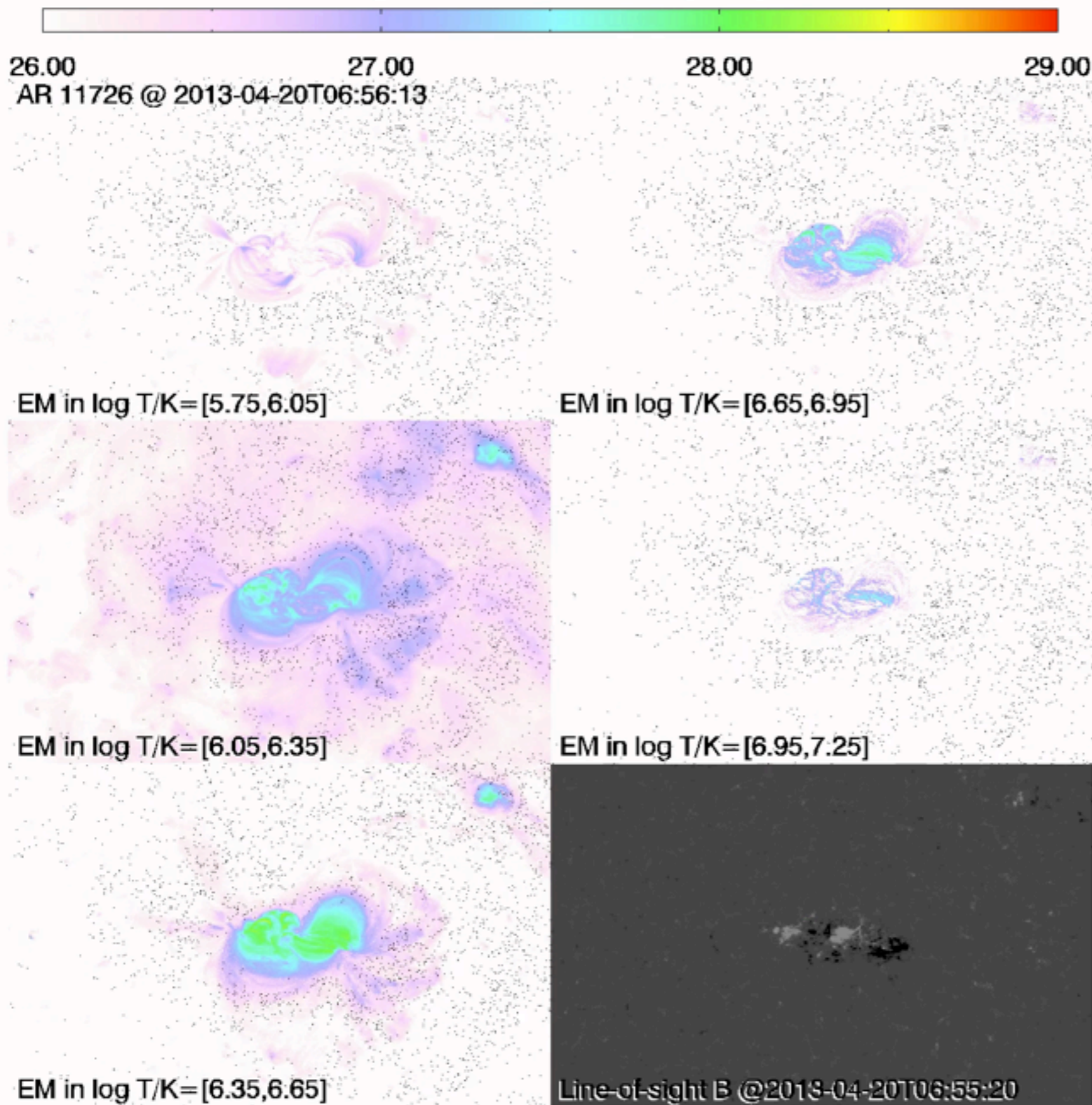
- Joint AIA-XRT DEM inversions
- Download `aiaxrt.pro` from <http://tinyurl.com/aiadem>
 - `.compile aia_sparse_em_init`
 - `.r aixrt`
- This script solves uses sample AIA data to solve for a DEM cube. Then it synthesizes AIA and XRT images. Then it uses AIA+XRT for DEM inversion. Key line is
- `aia_sparse_em_init, timedepend = s.oindex[0].date_obs, /
evenorm, use_lgtaxis=findgen(nlgT)*dlgT+lgTmin, xrt=['Be-med']`

Science Cases

- Thermal evolution of active regions from emergence to decay
- Thermodynamic structure of reconnection outflows
- From chromospheric evaporation to catastrophic condensation

Science Case 1) Emerging Flux

Log Emission Measure [cm^{-5}]

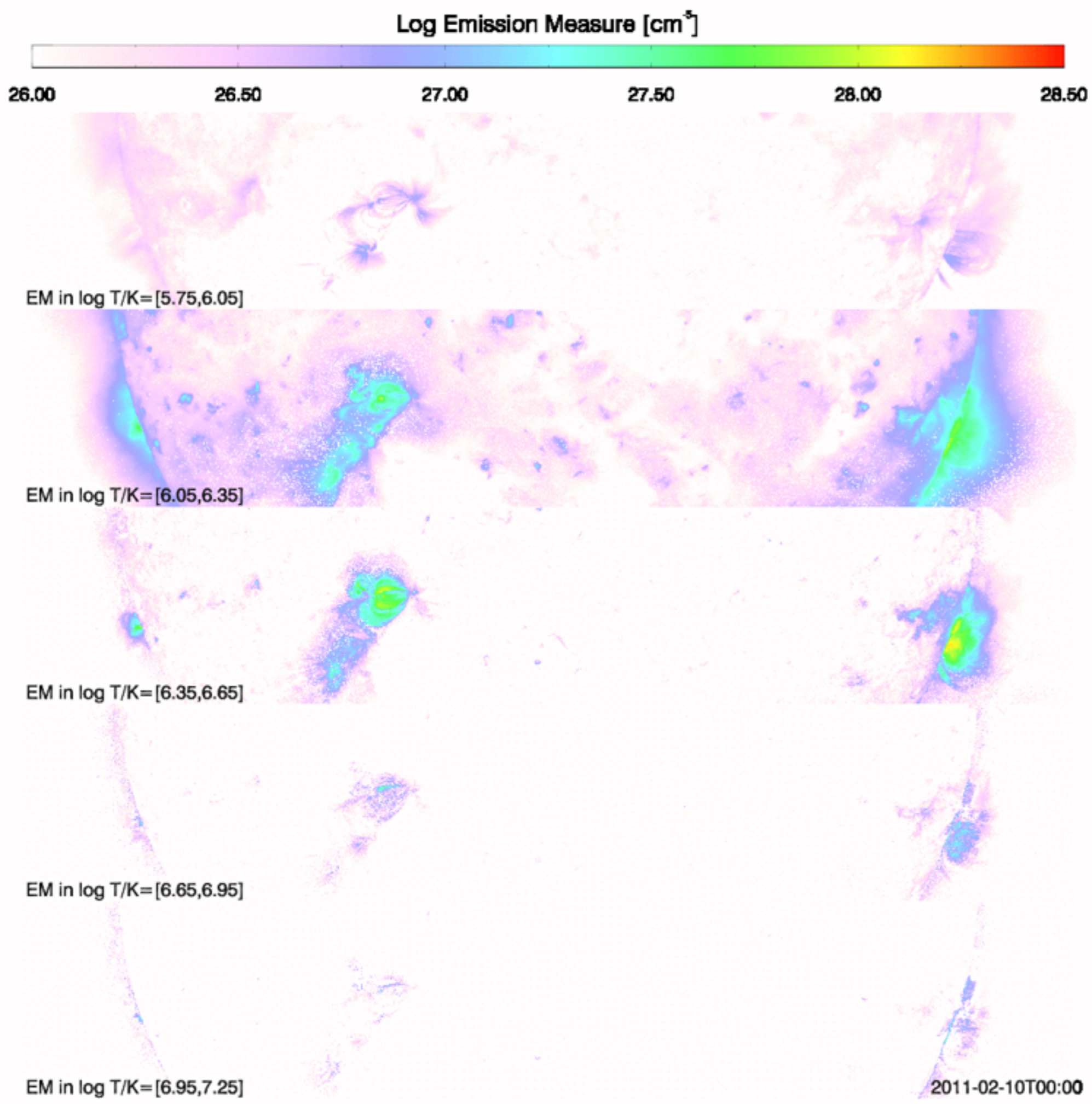


DEM movie
of the emergence
of AR 11726

Other panels:
EM in various $\log T$ bins

Lower right panel only
Greyscale:
 B_{los} from HMI
Green: 6MK EM
Yellow/Red: 10 MK EM

1. Emerging Flux Regions

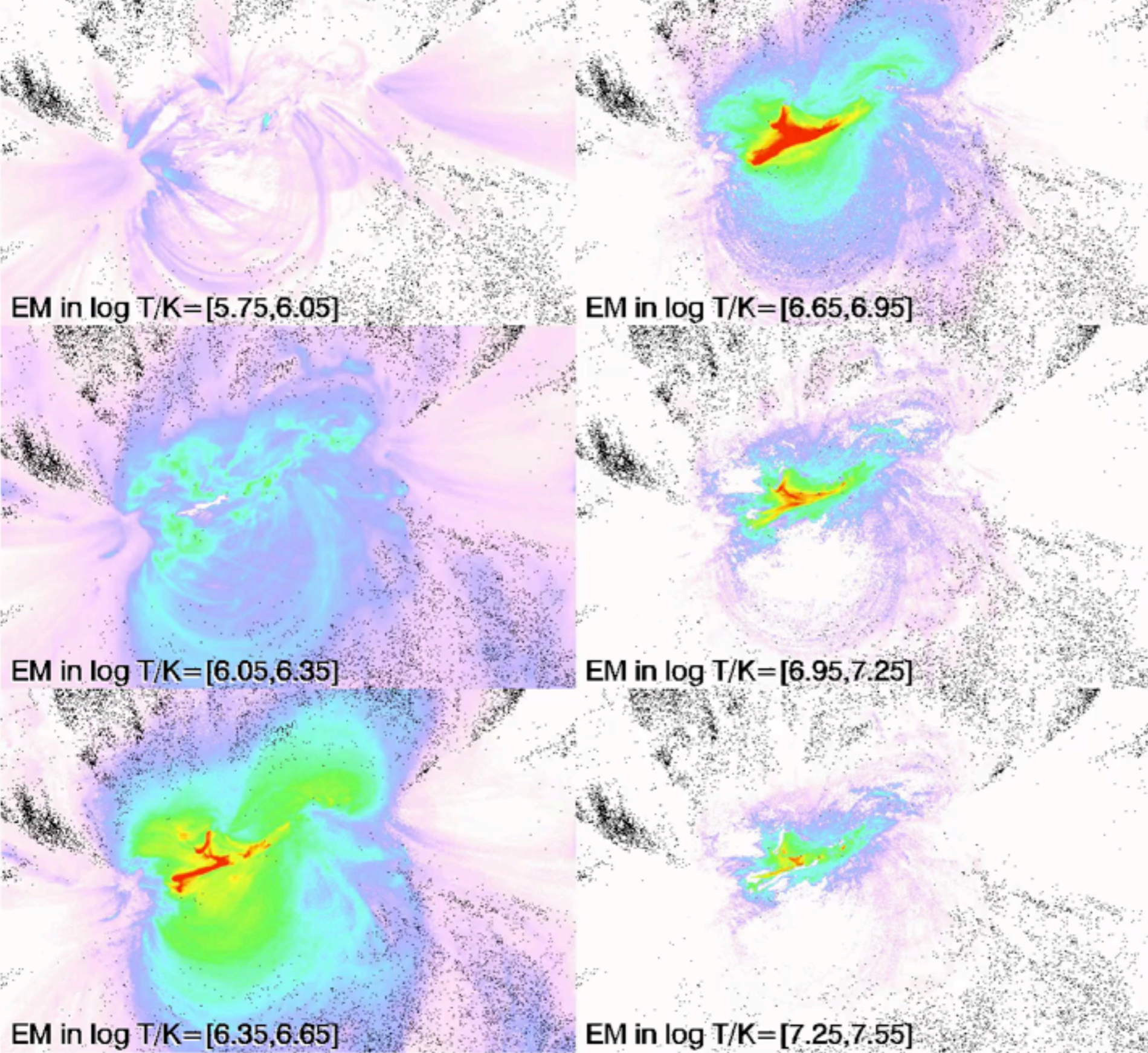


Log Emission Measure [cm^{-5}]

Science Case 1) Emerging Flux

26.00 27.00 28.00 29.00

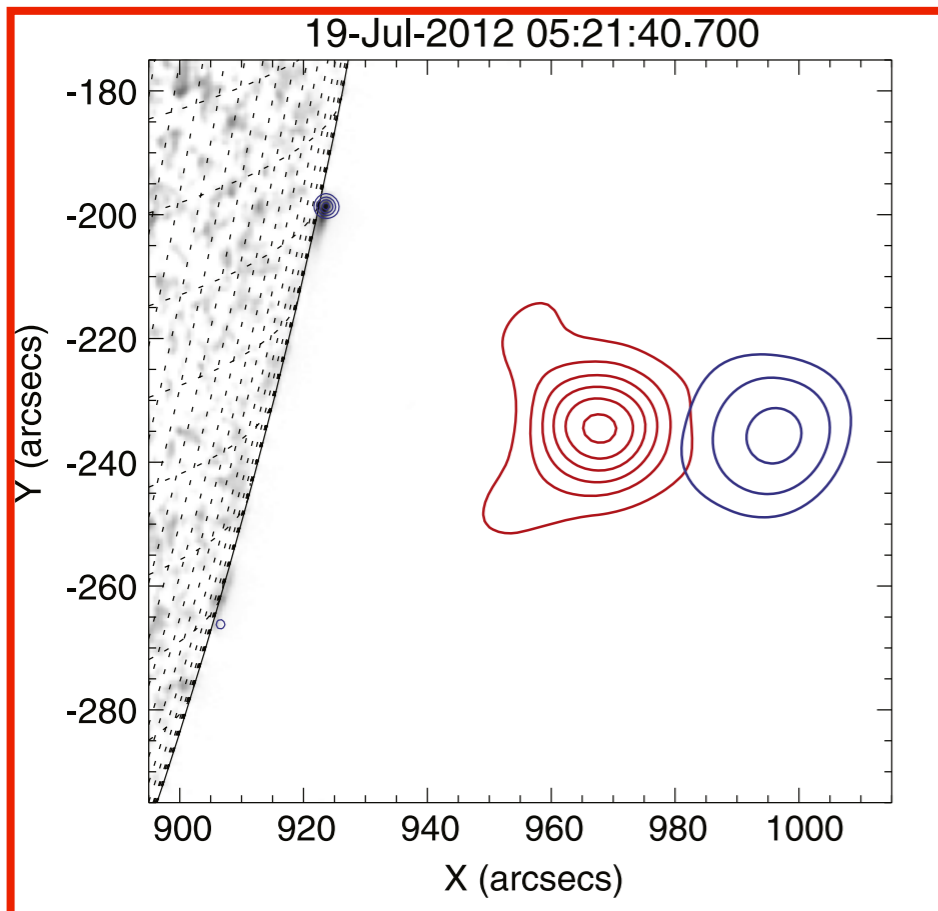
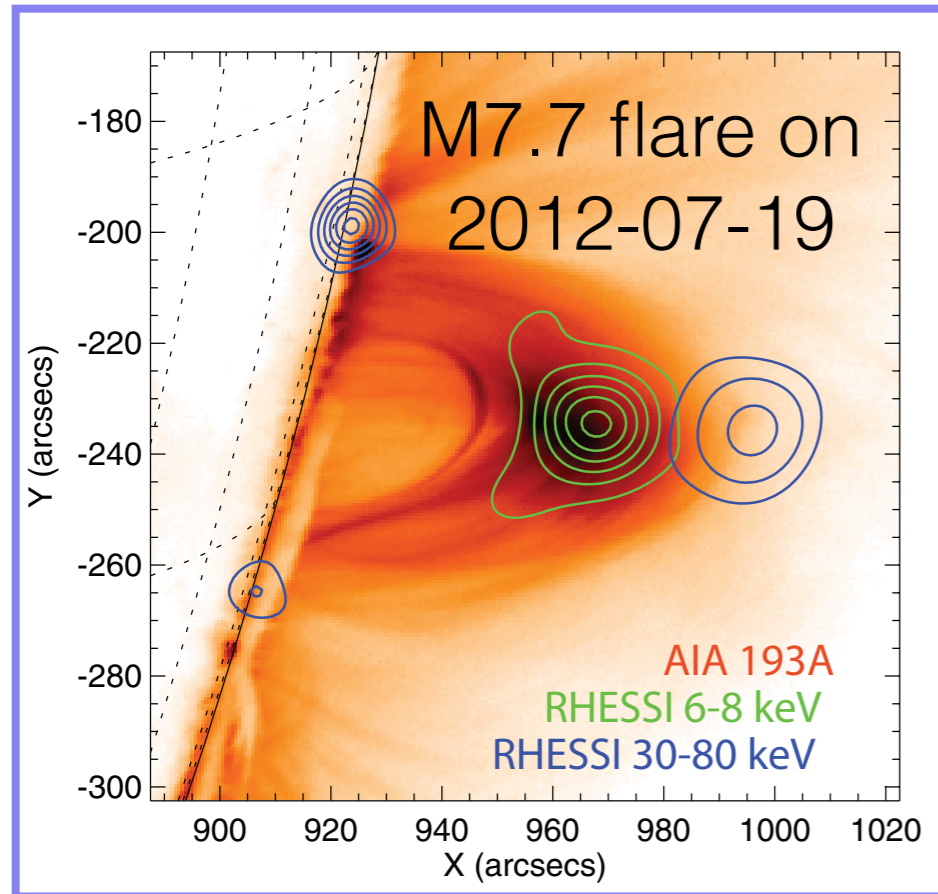
AR 11158 @ 2011-02-16T01:12:14



DEM
of the emergence
of AR 11158

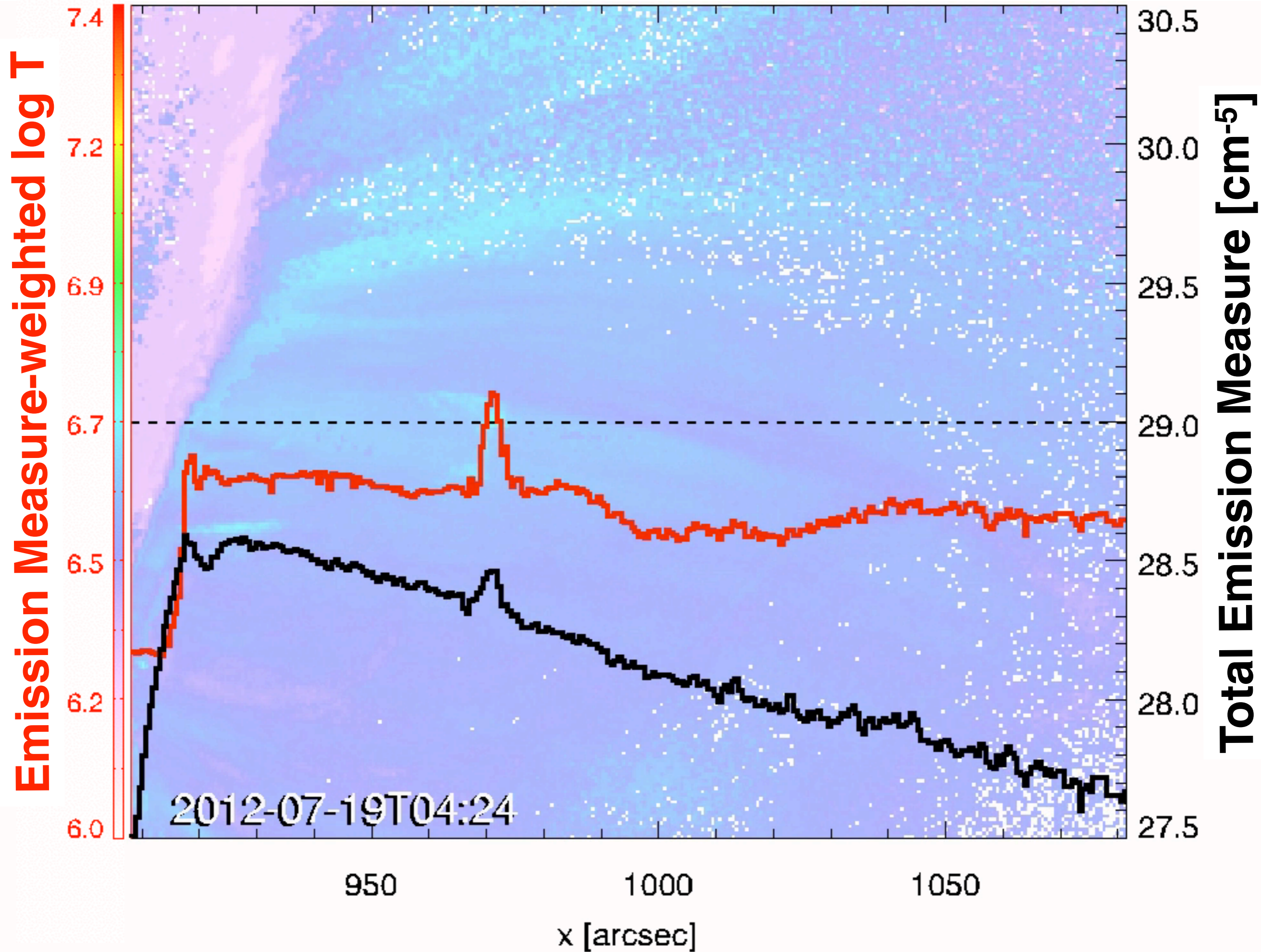
Black pixels are
where no solutions
were found

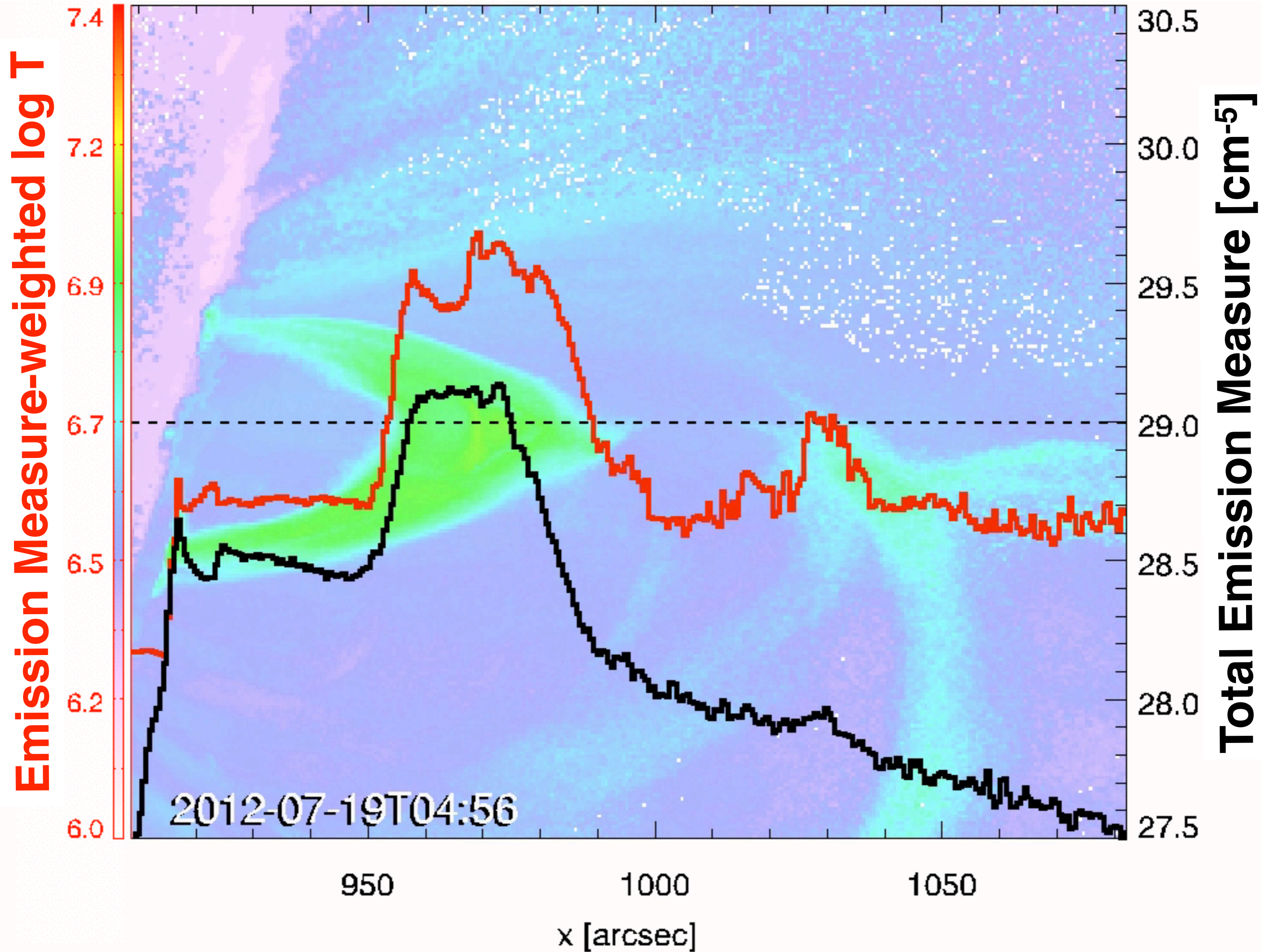
Science Case 2) Reconnection Outflows

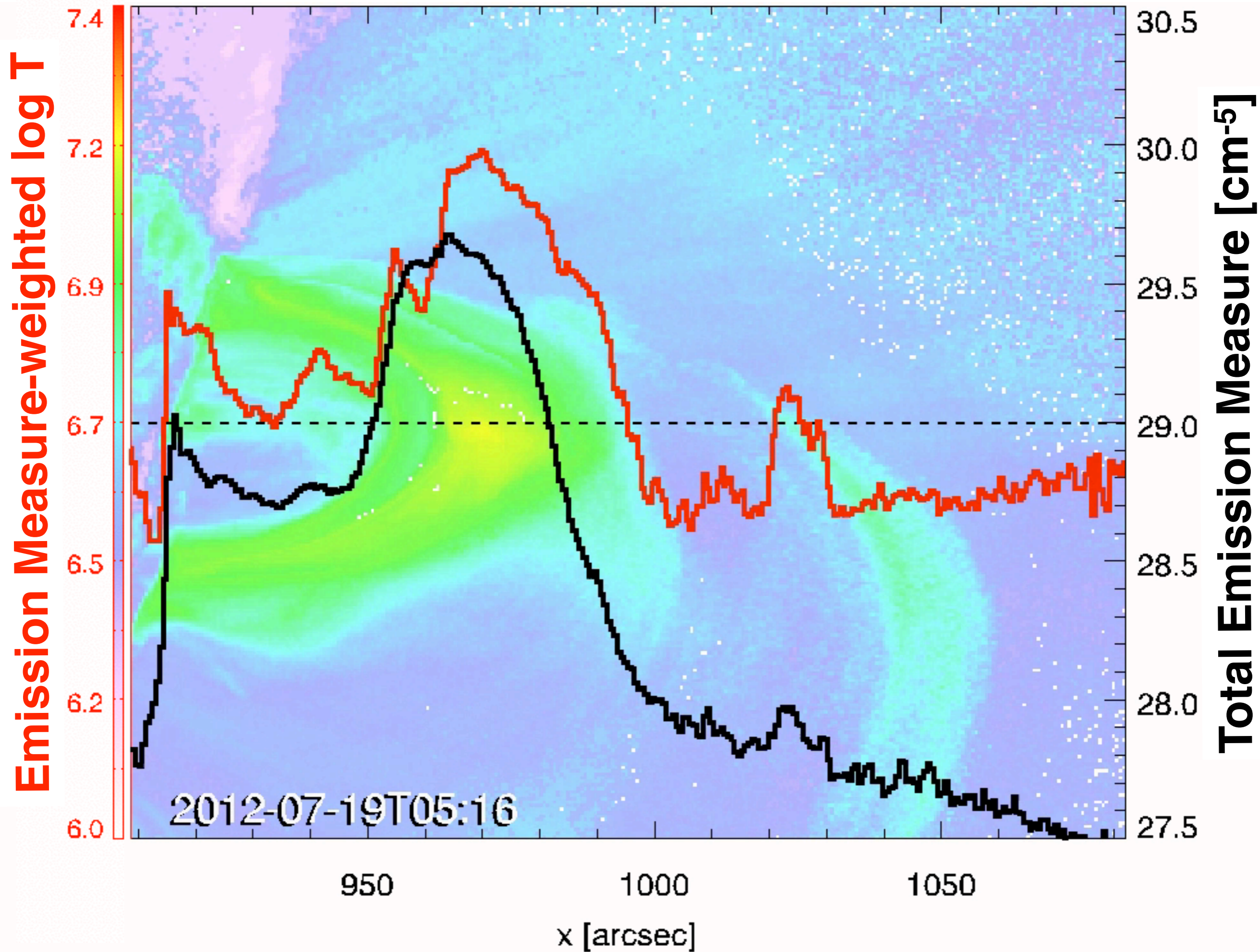


Selected scientific studies of this flare:

- [Patsourakos, Vourlidas & Stenborg, 2013, ApJ, 764, 125](#): Prior confined eruption produced a pre-existing coronal flux rope, which then erupted to give the M7.7 flare.
- [Wei Liu, Chen & Petrosian, 2013, ApJ, 767, 168](#): Detailed timeline of sequence of events including timing and propagation of EUV and X-ray sources.
- [Rui Liu, 2013, MNRAS, 434, 1309](#): Same onset time for HXR and microwave (Nobeyama RH data) bursts.
- [Krücker & Battaglia, 2014, ApJ, 780, 107](#): Ratio of thermal protons (from AIA) to non-thermal electrons (from RHESSI HXR) in loop-top source is of order 1.
- [Sun, Cheng & Ding, 2014, ApJ, 786, 73](#): Performed a very detailed DEM (imaging) analysis of this flare. They used `xrt_iterative_dem2.pro` (code by M. Weber, non-linear least square inversion with splines).
- [Krücker et al., 2015, ApJ, 802, 19](#): HMI white light (WL) enhancement at footprint co-incident with HXR footpoint source. Interpretation: energy deposition by non-thermal electrons is radiated away and does not cause chromospheric evaporation.

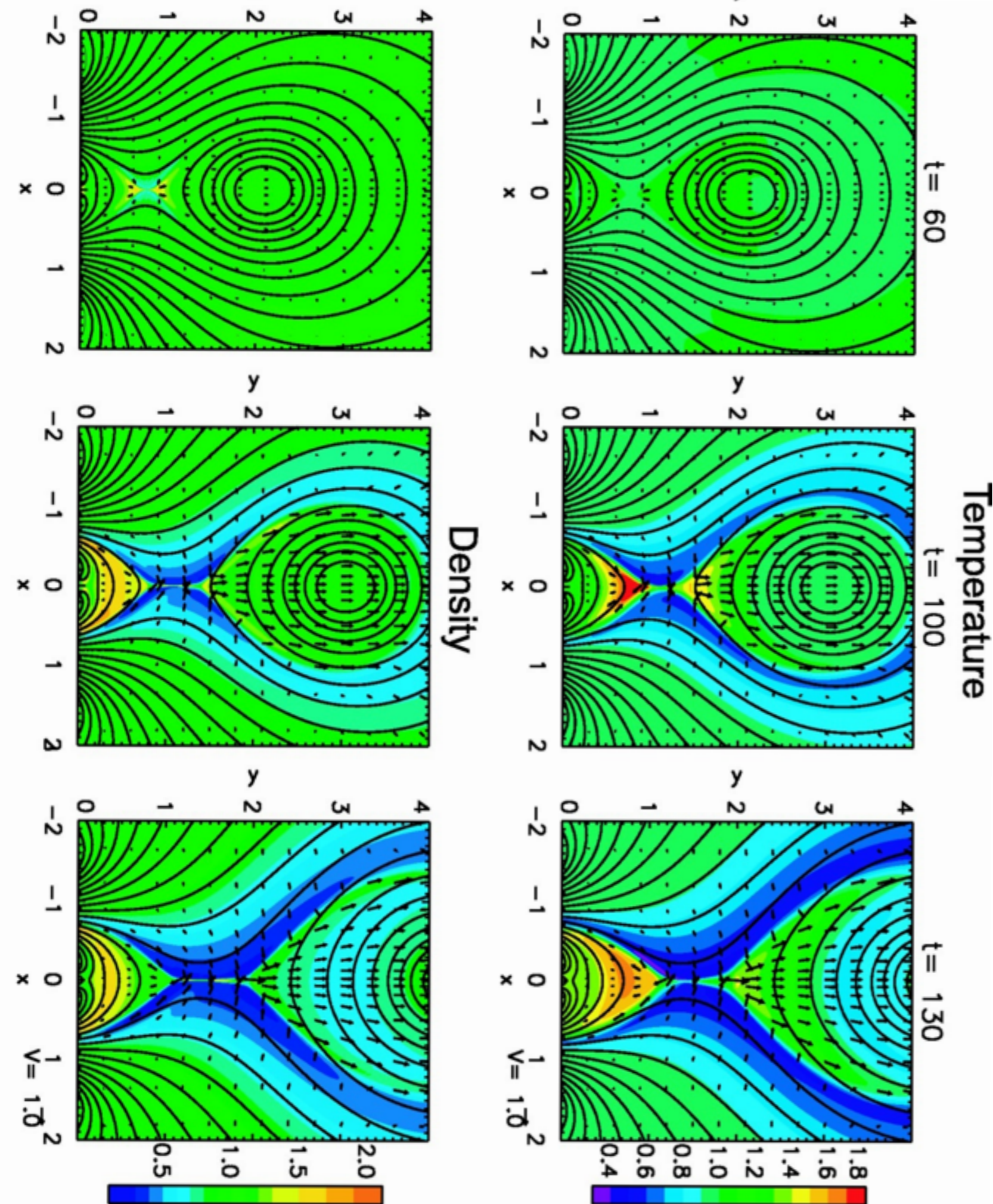






Shiota et al. (2005, ApJ, 634, 663):

- 2.5D MHD simulation of the eruption of a pre-existing flux rope triggered by flux emergence.
- Similar scenario as modeled by Chen & Shibata (2000, ApJ, 545, 524) but with field-aligned thermal conduction.
- Both temperature and density are initially uniform (dimensionless value of unity).



Dashed contours: Total EM = 10^{29} cm^{-5}
Solid contours: Total EM = 10^{30} cm^{-5}

Chromospheric evaporation



**Downward mass pumping from
reconnection outflow**



2012-07-19T05:02

Science Case 3) Chromospheric Evaporation & Condensation

Observations

Spectra covering temperatures from 4,500 K to 10 MK

Images covering temperatures from 4,500 K to 65,000 K

Baseline: 5s for slit-jaw images, 1s for 6 spectral windows, rapid rastering

Predicted Count Rates

Ion Spectrum	λ	$\Delta\lambda$	Log T K	Estimated Count Rate (counts/s/line/spatial pixel)			Detector
	Å	mÅ		Quiet Sun	Active Region	Flare	
UV Spectra (effective area of 2.8 cm ² for far-UV, 0.3 cm ² for Mg passband, continuum is 1 Å)							
†: Count rates for Mg II wing, h and k are in counts/s/spectral pixel/spatial pixel							
Si I (3P) Cont	1335	12.5	3.7	40	80	---	1
Mg II wing	2820	25	3.7-3.9	2100†	7500†	7500†	3
O I	1356	12.5	3.8	50	100	250	1
Mg II h	2803	25	4.0	870†	3400†	13000†	3
Mg II k	2796	25	4.0	1100†	4500†	10000†	3
C II	1335	12.5	4.3	540	1970	22000	1
C II	1336	12.5	4.3	500	1780	20000	1
Si IV	1403	12.5	4.8	400	1000	1e6	2
Si IV	1394	12.5	4.8	640	2200	3e6	2
O IV	1401	12.5	5.2	65	116	2e5	2
O IV	1400	12.5	5.2	25	60	1e5	2
Fe XII	1349	12.5	6.2	30	50	500	1
Fe XXI	1354	12.5	7.0	10	40	4e4	1
UV Slit-Jaw Images				Estimated Count Rate (counts/s/pixel)			
Effective area 0.005 cm ² with 4 Å FWHM filter for Mg II; 0.7 cm ² with 40 Å FWHM for far-UV.							
Mg II wing	2831		3.7-3.9	2300	5300	5300	4
Mg II k	2796		4.0	750	3500	8500	4
C II	1335		4.3	400	1300	13000	4
Si IV	1400		4.8	300	1200	2e5	4

IRIS is designed to probe the chromosphere and transition region, but it also sees flare plasma (**Fe XXI @10 MK**).

What about the temperature range in between?

Joint observations between IRIS and AIA to fill the temperature gap.

From the IRIS poster @ iris.lmsal.com

At <http://www.lmsal.com/data.html>,
go to 'List of Flares Observed with IRIS'
compiled by Kathy Reeves.

20140917 -
19:26 C7.5 flare - behind
the limb, nice big loop of Fe
XXI visible, red shift in
Fe XXI

IRIS SJI 1330: Diffuse, long-lived loops reaching into the
corona are generally attributed to Fe XXI 1354 Å emission.

2014/09/17 19:49:54.930

Log Emission Measure [cm^{-5}]



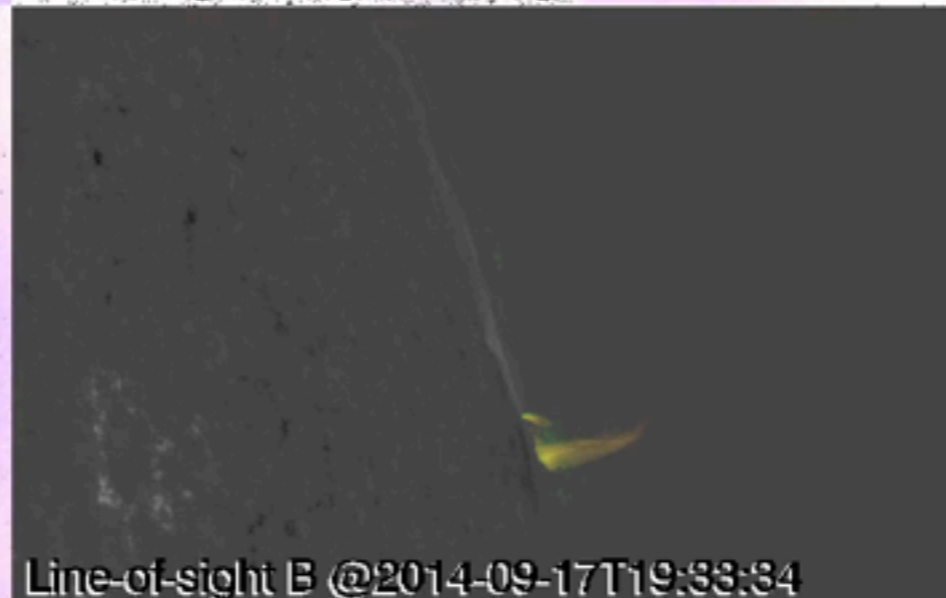
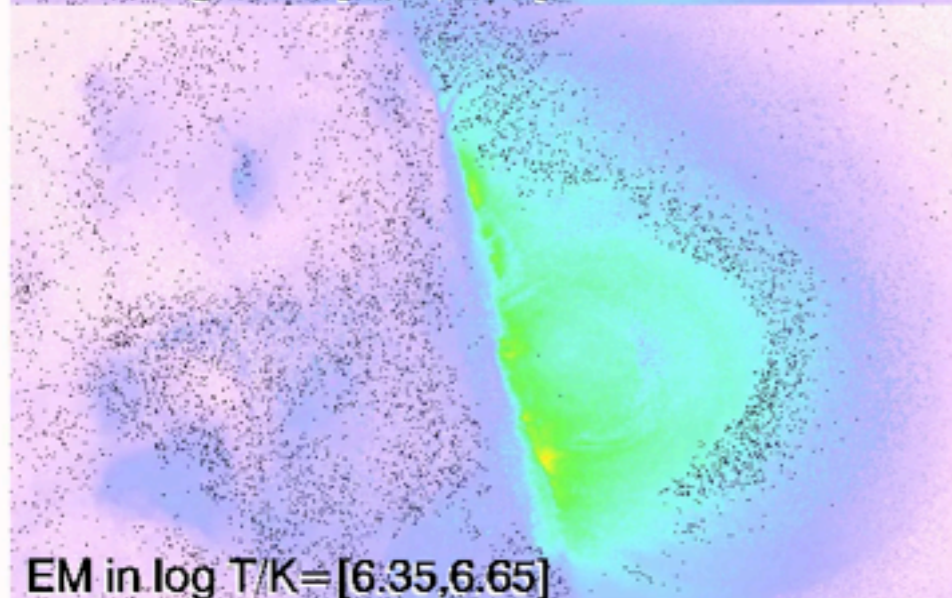
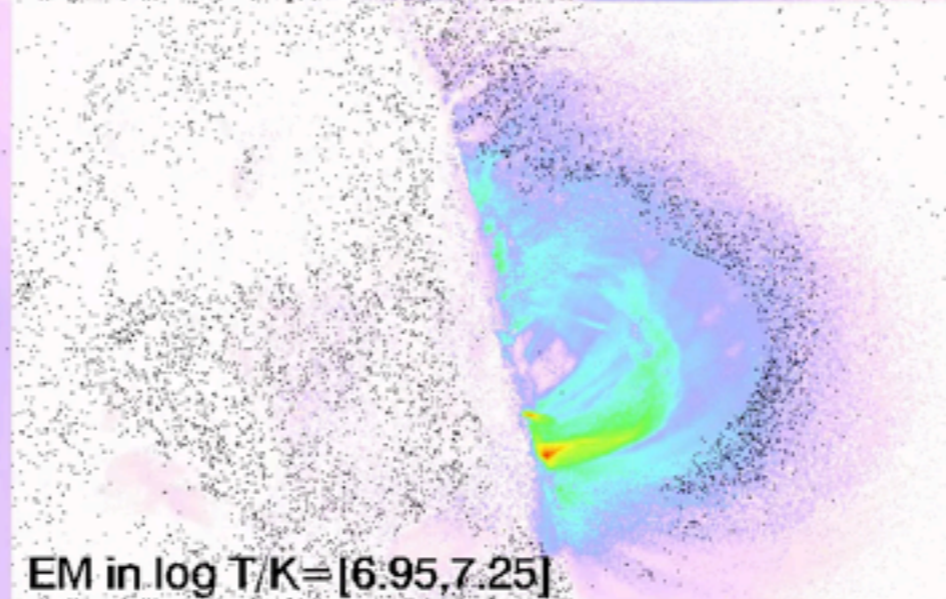
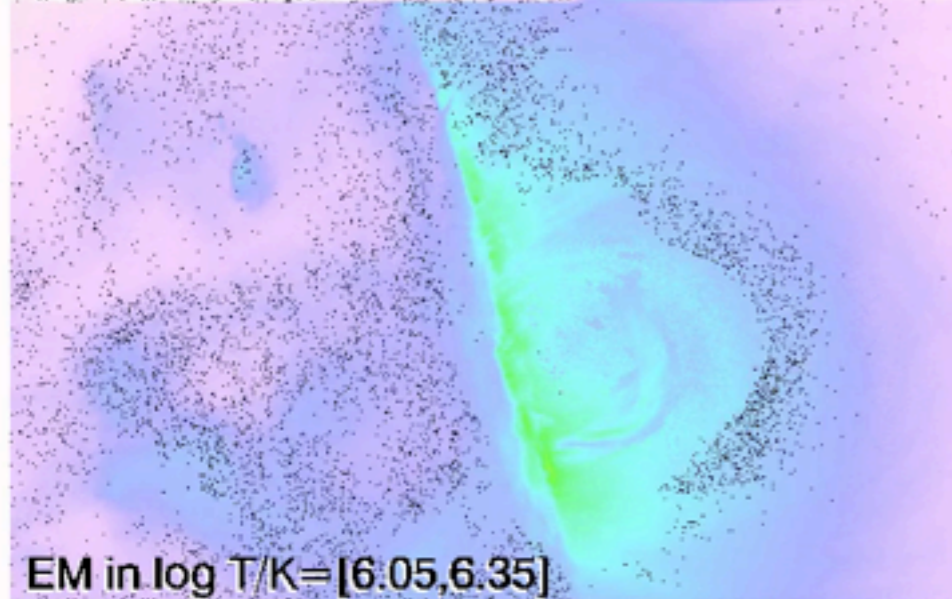
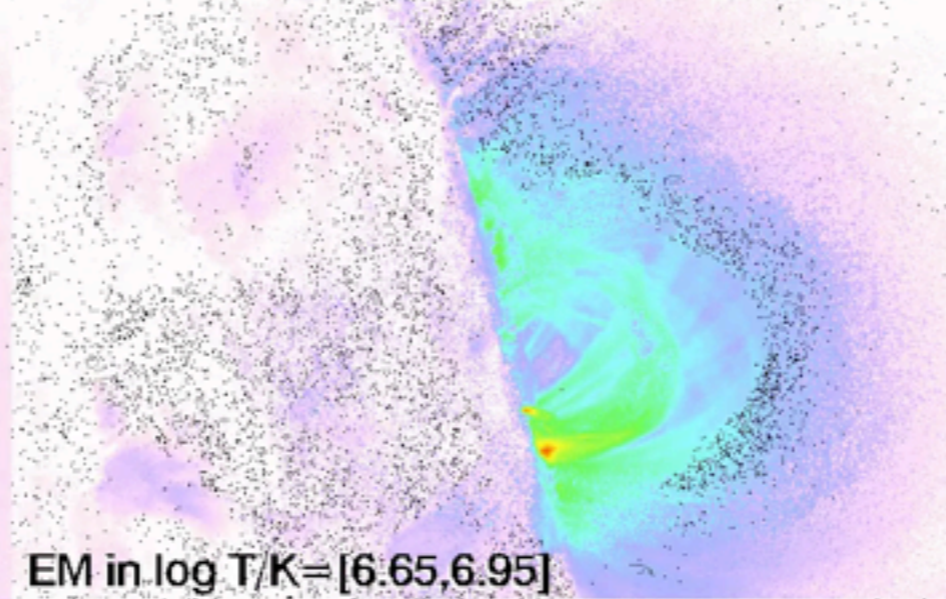
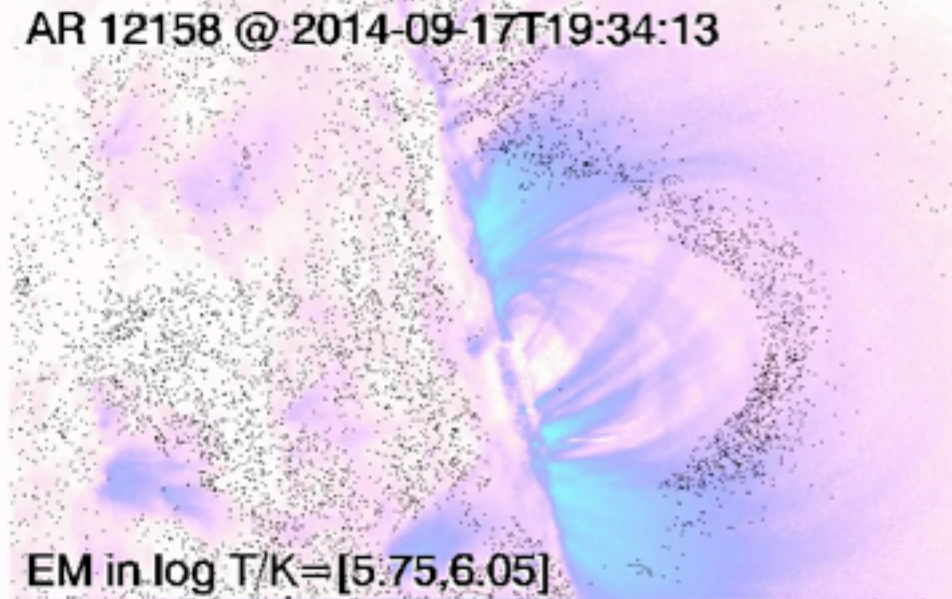
Other panels:

EM in various log T bins

26.00 27.00
AR 12158 @ 2014-09-17T19:34:13

28.00

29.00



- **Tell-tale signs of chromospheric evaporation**
- **Loops filled with plasma at 10 MK and above**
- **Loops cool to lower log T bins**
- **At time (~20:29 UT) when plasma cools down to log T/K ~ 5.8, coronal condensations in SJI 1330 begin to appear.**

Lower right panel only

Greyscale:

B_{los} from HMI

Green: 6MK EM

Yellow/Red: 10 MK EM

Log Emission Measure [cm^{-5}]



Other panels:

EM in various log T bins

26.00 27.00
AR 12158 @ 2014-09-17T19:55:25

28.00 29.00

EM in log T/K=[5.75,6.05]

EM in log T/K=[6.65,6.95]

EM in log T/K=[6.05,6.35]

EM in log T/K=[6.95,7.25]

EM in log T/K=[6.35,6.65]

Line-of-sight B @2014-09-17T19:54:34

- Tell-tale signs of chromospheric evaporation
- Loops filled with plasma at 10 MK and above
- **Loops cool to lower log T bins**
- At time (~20:29 UT) when plasma cools down to log T/K ~ 5.8, coronal condensations in SJI 1330 begin to appear.

Lower right panel only

Greyscale:

B_{los} from HMI

Yellow/Green: 6MK EM

Red: 10 MK EM

Log Emission Measure [cm^{-5}]



Other panels:

EM in various log T bins

26.00 27.00
AR 12158 @ 2014-09-17T20:29:01

28.00 29.00



EM in log T/K=[5.75,6.05]

EM in log T/K=[6.65,6.95]

- Tell-tale signs of chromospheric evaporation
- Loops filled with plasma at 10 MK and above
- Loops cool to lower log T bins
- **At time (~20:29 UT) when plasma cools down to log T/K ~ 5.8, coronal condensations in SJI 1330 begin to appear.**

EM in log T/K=[6.05,6.35]

EM in log T/K=[6.95,7.25]

EM in log T/K=[6.35,6.65]

Line-of-sight B @2014-09-17T20:27:34

Lower right panel only

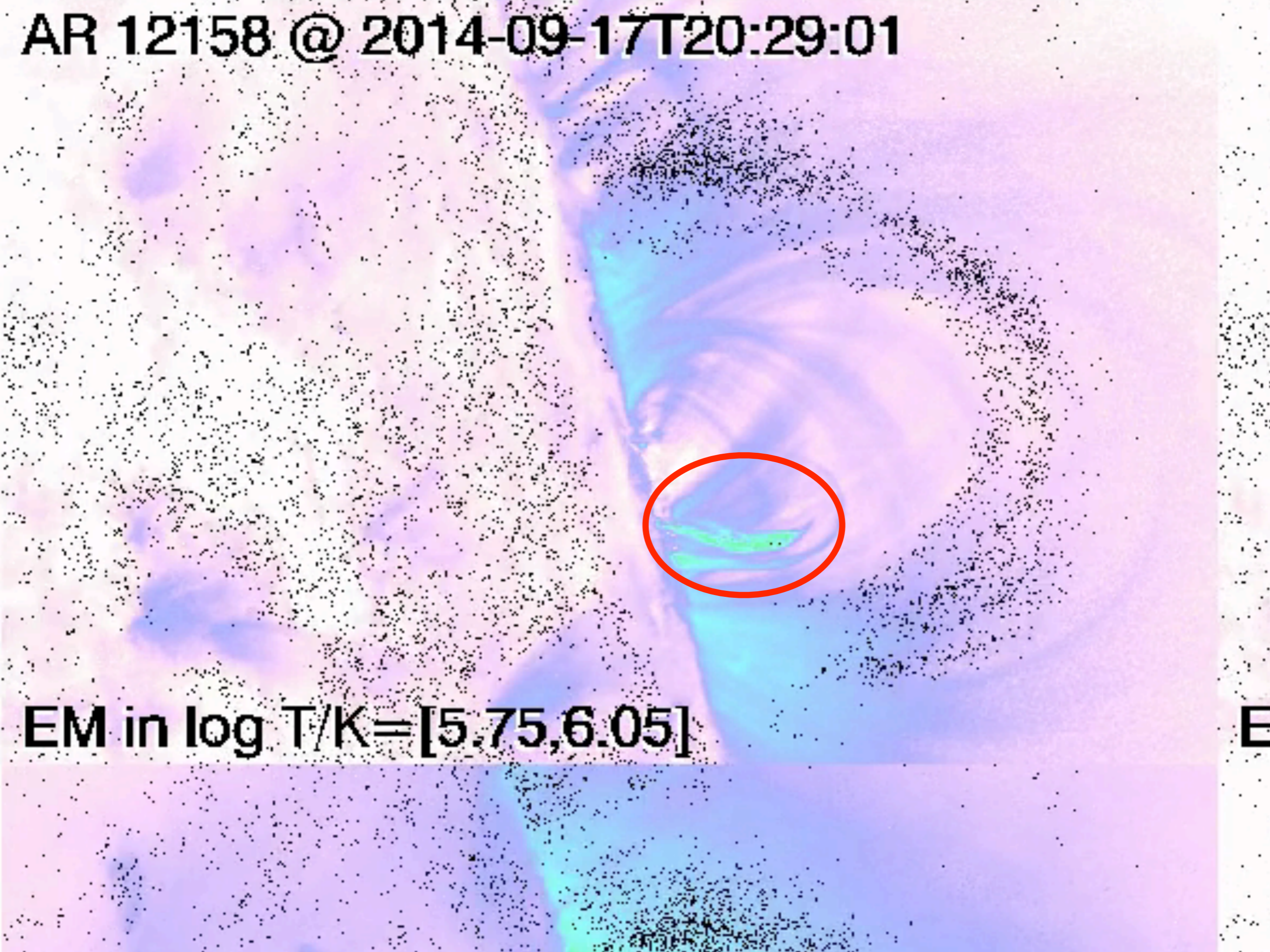
Greyscale:

B_{los} from HMI

Yellow/Green: 6MK EM

Red: 10 MK EM

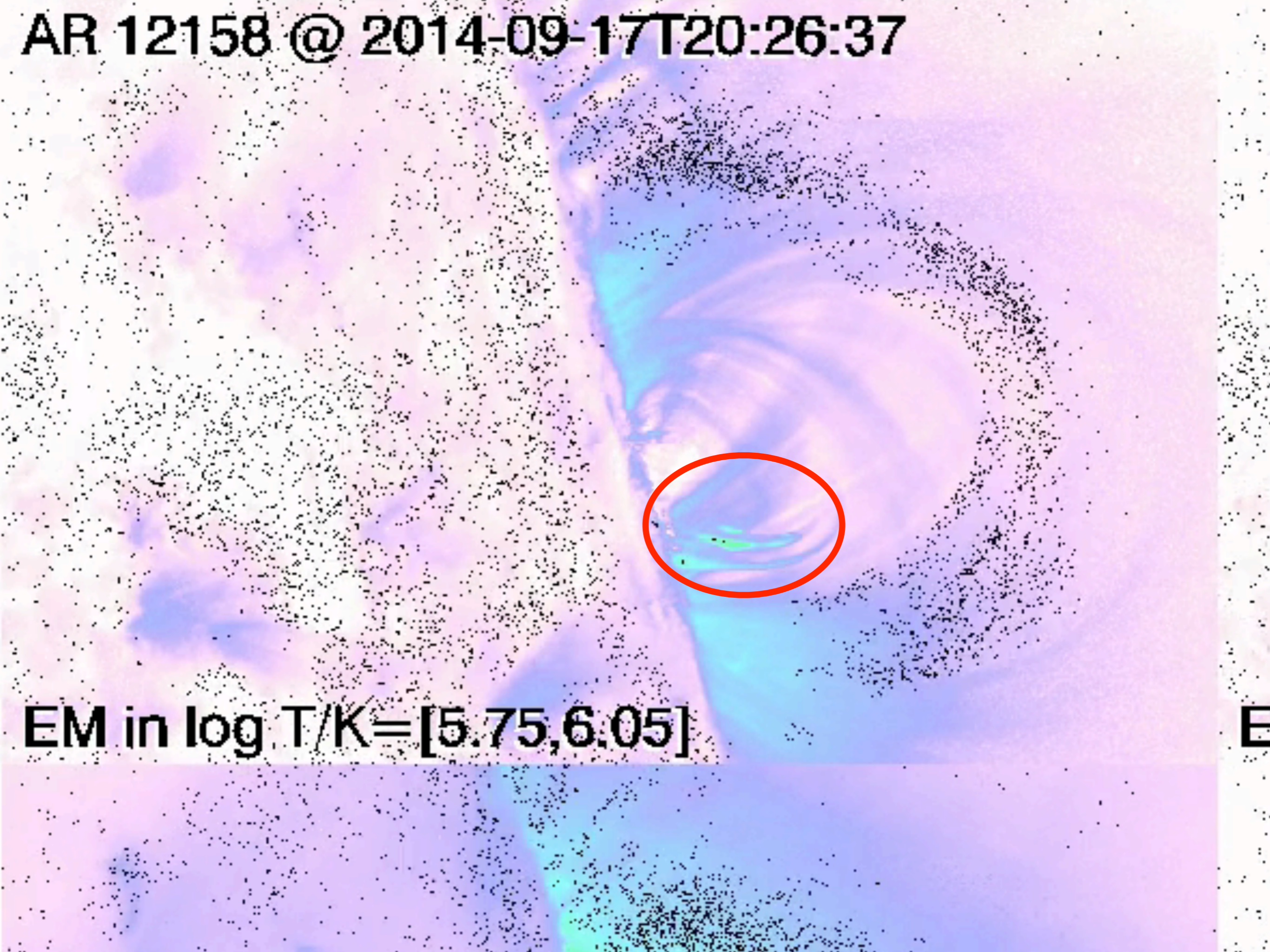
AR 12158 @ 2014-09-17T20:29:01



EM in $\log T/K = [5.75, 6.05]$

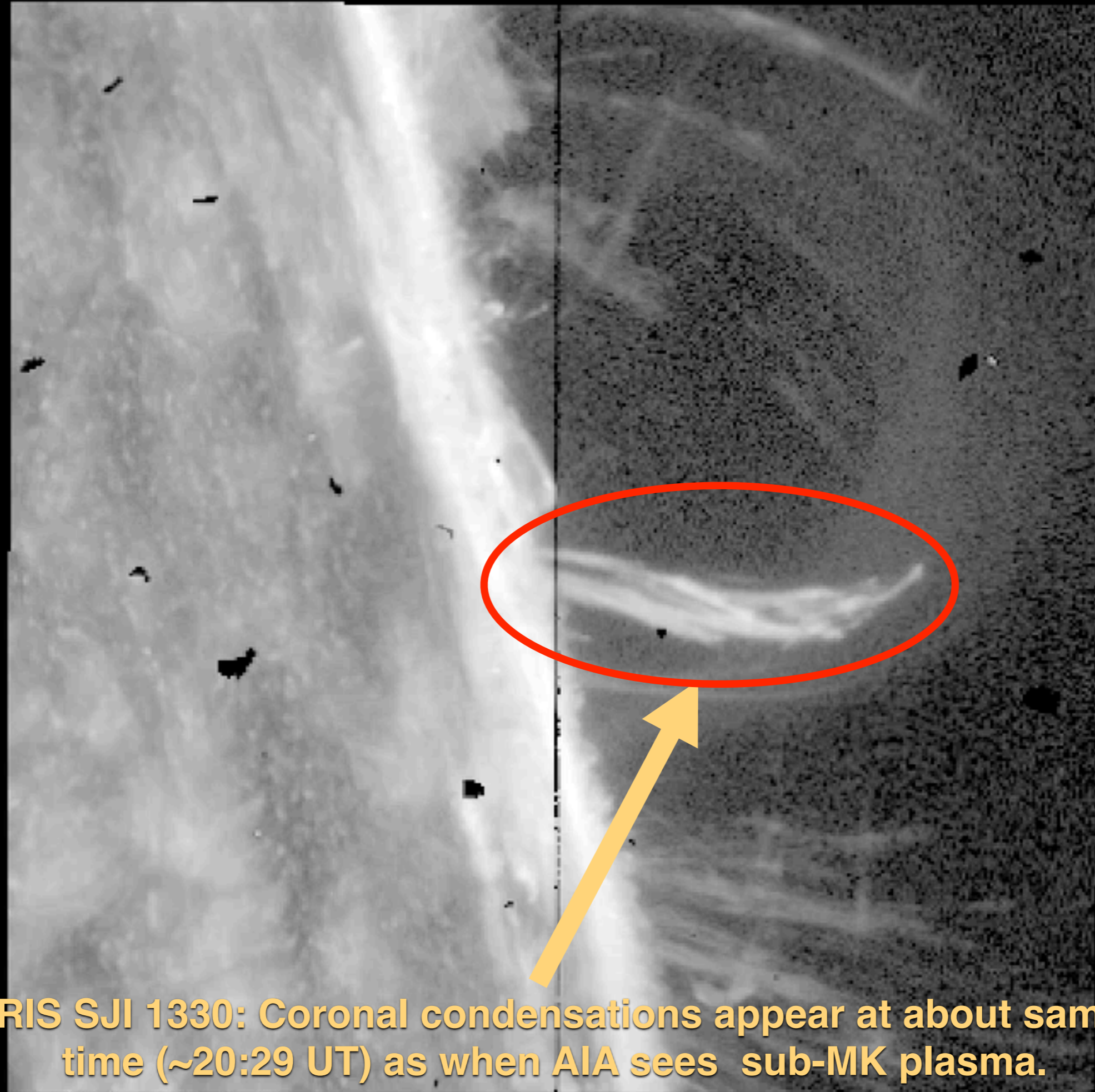
E

AR 12158 @ 2014-09-17T20:26:37



EM in $\log T/K = [5.75, 6.05]$

E



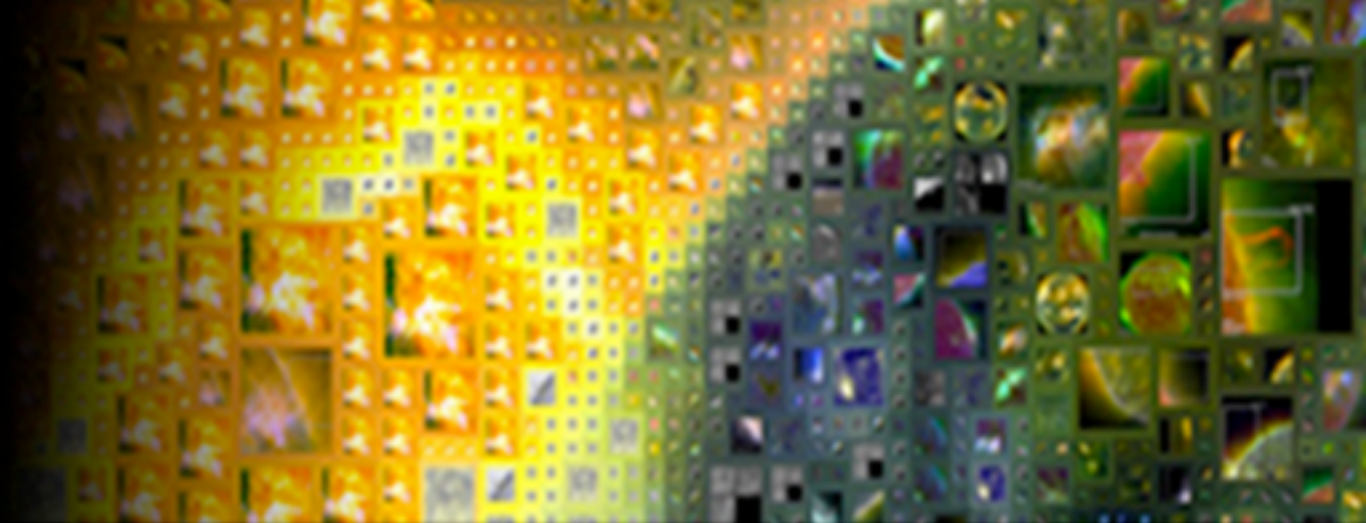
IRIS SJI 1330: Coronal condensations appear at about same time (~20:29 UT) as when AIA sees sub-MK plasma.

Summary

- Thermal diagnostics with SDO/AIA using a new, validated DEM inversion method (Cheung et al., 2015, ApJ)
 - Provides positive definite solutions.
 - Speed: $O(10^4)$ solutions / sec with a single IDL thread.
 - Method tested against various thermal models: (1) Log-normal (Gaussian) distributions, (2) 3D models of quasi-steady loop atmospheres in a non-linear force-free field reconstruction of AR 11158, (3) MHD simulation of AR corona formation and (4) AIA-XRT cross comparison.
- Science applications
 - 1) Emerging Flux Regions
 - 2) Reconnection Outflows
 - 3) Chromospheric Evaporation & Condensation
- AIA and IRIS together give temperature coverage from the quiet chromosphere to the flaring corona.

SDO 2016: Unraveling the Sun's Complexity

October 17 - 21, 2016 | Burlington, Vermont



Mini Workshop on Friday Oct 21st @ SDO 2016

<p>Thermal Diagnostics with SDO/AIA (Part I)</p>	<p>The first part of this workshop is a tutorial on how to perform differential emission measure (DEM) inversions on EUV imaging observations of the solar corona taken by the SDO/AIA. We will describe the method (see Cheung et al., 2015, ApJ, 807, 2), show some validation tests and walk through some examples on how to use the AIA team's DEM inversion code.</p>
<p>Thermal Diagnostics with SDO/AIA (Part II)</p>	<p>For the second part of the workshop, we solicit contributions that use SDO/AIA data for thermal mapping of the solar corona. Example of science topics that can be addressed with AIA-derived DEM maps include: (1) the thermal evolution of active regions and emerging flux regions, (2) the thermodynamic structure of magnetic reconnection outflows, and (3) chromospheric evaporation in solar flares. We encourage contributions that complement AIA data with data from other space instruments (e.g. SDO/EVE, IRIS, Hinode/XRT, Hinode/EIS, RHESSI etc.) and ground-based observatories (e.g. radio observations).</p>